University of Alberta

Refinement Study of the Alberta Environment Dry Deposition Inference Model

By

Mary Joy Wesley
Mary Joy Wesley

A thesis submitted to the Faculty of Graduate Studies and Research in partial fulfillment of the requirements for the degree of Master of Science

In

Environmental Engineering

Department of Civil and Environmental Engineering

Edmonton, Alberta

Fall 2007

Your file Votre référence
ISBN: 978-0-494-33369-3
Our file Notre référence
ISBN: 978-0-494-33369-3

Abstract

The Alberta Environment inference model for predicting dry deposition (including gaseous and particle deposition) in Alberta is a simplification of the Environment Canada model requiring fewer input variables. Since it is very difficult to take direct measurements to test the validity of the models, the performance of the Alberta Environment model was evaluated by comparing its results with those of the Environment Canada model. The objective was to improve the performance of the Alberta Environment model by examining the operation of the models and the impacts of the assumptions and boundary conditions used in the two models using data from 2003 at Fort Mackay, Alberta. It was found that changes in most of the boundary conditions had little effect on the model performance. Step changes in the magnitude of R_c were found to be much more important in influencing total deposition than step changes in R_a or R_b.

Dedication

This work is dedicated to my father-in-law, Allister Everett Wesley, who believes that every generation is responsible for providing the shoulders upon which the next generation may stand.

Acknowledgements

I would first like to thank my children for their patience with their mother's addiction to University. I would like especially to thank my daughter, Megan, for all her computer technical assistance. I would like to thank my spouse for all his encouragement throughout the years. As well, I would like to thank my mother, my mother-in-law, and my father-in-law for their support over the years.

I would like to thank Dr. Gamal El-Din who always managed to motivate me. He earned my respect both as an individual and a professor.

I would also like to thank Dr. Kindzierski for his advice and insight that led to the improvement of my technical writing ability.

I would like to thank Drs. Buchanan and Clark for the time that they invested in reading my thesis and their resultant and insightful comments.

Finally, I would like to thank my environmental science and engineering peers, especially Helen, Laurie, Garrett, Johnny, and Mehrdad, who made our time together into the great adventure that it was.

Table of Contents

List of Tables

List of Figures

List of Symbols

C	concentration ($\mu g/m^3$)
$Cos\ \alpha$	cosine of sun/leaf angle, set as 0.5
$Cos\ \theta$	sine of solar zenith angle
D_{AENV}	diffusion coefficient of the substance of interest (cm^2/s) (AENV)
D_{ENVC}	water-vapour-pressure deficit (ENVC)
D_i	molecular diffusivity
D_v	water diffusivity
$E^*(T)$	saturation water vapour pressure (kPa) at air temperature T (K)
E	ambient water vapour pressure (kPa)
F	dry deposition flux ($\mu g/m^2/s$)
$f(D)$	conductance-reducing effects of water-vapour-pressure deficit D
$f(T)$	conductance-reducing effects of air temperature T (°C)
f_{snow}	snow cover fraction
$f(\psi)$	conductance-reducing effects of water stress ψ
$FCLD$	fraction of cloud covering (%)
g	gravitational acceleration (9.81 m/s^2)
$G_s(PAR)$	unstressed leaf stomatal conductance
H	sensible heat flux (w/m^2)
k	von Karman constant (0.4)
L	Monin-Obukhov length scale
LAI	Leaf Area Index
LUC	Land Use Category (26 *LUCs* in gas model)
MW	Molecular Weight, $MW_{air} = 29$
P	surface pressure (kPa)
PAI	Potential Acid Input (kg H^+/ha/yr)
PAR	Photosynthetic Active Radiation

Pr	Prandtl number for air (0.72)
$Prec$	precipitation (mm/hour)
R_a	aerodynamic resistance (s/m)
R_b	boundary-layer resistance (s/m)
R_c	surface resistance (s/m)
R_B	Bulk Richardson number
R_{ac}	in-canopy aerodynamic resistance (not chemical species-dependent)
R_{cut}	cuticle uptake resistance (scaled from SO_2 and O_3's R_{cut})
R_g	ground resistance (scaled from SO_2 and O_3's R_g)
R_m	mesophyll resistance (dependent only on chemical species)
R_{st}	stomatal resistance
R_{cutd0}	reference values of dry cuticle resistance
R_{cutw0}	reference values of wet cuticle resistance
$R_{cutw0(SO_2)}$	50 s/m or 100 s/m for rain or dew conditions, respectively
RH	relative humidity (%)
Sc	Schmidt number
SC	Seasonal Category (5 in particulate model)
Sd	snow depth (cm)
Sd_{max}	maximum snow depth (cm)
SR	solar radiation (W/m^2)
SW	soil wetness
T_{avg}	temperature average, $T_{avg} = (T_{2p} + T_s)/2$ (°K)
T_d	temperature difference between 10 and 2 m (T_{10} - $T_{2\,AENV}$)
$T_{2\,AENV}$	temperature at 2 m (Kelvin) AENV
$T_{2\,ENVC}$	temperature at reference height (10 m) (°K) ENVC
T_{2p}	potential temperature at reference height (°K)
T_s	surface temperature (°K)

u	wind speed (m/s)
u^*	friction velocity (m/s)
V_d	deposition velocity (m/s)
V_i	thermal diffusivity
W_{st}	fraction of stomatal blocking under wet conditions
$[X]$	concentration of X chemical species deposited (kg/ha/yr)
z	reference height (10 m)
z_0	surface roughness length (m)
η	dynamic viscosity of air (18.0×10^{-6} N-s/m^2 at 1 atm and 25°C)
ρ	density of air (1.18 kg/m^3 at 1 atm and 25°C)
σ_θ	standard deviation of wind direction (rad)
ψ_{AENV}	integrated stability correction term (AENV model)
ψ_{ENVC}	water stress (ENVC model)
ψ_{c1} and ψ_{c2}	leaf-water-potential dependency
ψ_H	stability function

1 Introduction

1.1 Background

Environment Canada (ENVC) developed a dry deposition inference model to predict deposition of gaseous and particulate species onto land or water in Canada (Zhang *et al.*, 2003a, 2003b, 2002a, 2001a, 2001b; Brook *et al.*, 1999). Environment Canada's model is referred to as "A Unified Regional Air Quality Modeling System" (AURAMS) (Zhang *et al.*, 2002a). AURAMS uses pollutant and meteorological data collected from the Canadian Air and Precipitation Monitoring Network (CAPMoN) (Brook *et al.*, 1999). Alberta Environment (AENV) has been working over the past several years to develop a dry deposition inference model (Cheng *et al.*, 2001) to similarly predict deposition of gaseous and particulate species onto land and water in Alberta. Both approaches are a form of dry deposition inference modeling.

Dry deposition inferential models have evolved from methods used by meteorologists and foresters to characterize H_2O, CO_2, heat, and momentum exchange between the atmosphere and plant canopies. While numerous dry deposition inference models are used in practice in North America, uncertainty exists in results from these models because of an inability to take direct measurements to test their validity (Lovett, 1994). Dry deposition inference models should have the capability to represent dry deposition of atmospheric pollutants in a manner that reflects current scientific understanding. Also important is that results from any one approach should compare reasonably well with other approaches used to represent dry deposition.

Alberta Environment is interested in developing their dry deposition inference model for wider use in Alberta. WBK & Associates Inc. (WBK, 2006) undertook initial testing of the ENVC and AENV models using a common set of meteorological and pollutant data to examine how they compared for predicting dry deposition of eleven gaseous and particulate species. Initial findings of this work indicated both models gave similar results for amounts of dry deposition for gaseous and inorganic species on a monthly and annual basis. One of the recommendations from the initial study was to

undertake further comparative testing of these two models to better understand reasons why model results departed from each other.

1.2 Objectives

Further investigation of the AENV and ENVC dry deposition inference models was undertaken as a follow-up to recommendations of WBK (2006). The objectives of this study were as follows:

i) to examine the performance of the Alberta Environment inference model relative to the ENVC model for predicting dry deposition in Alberta,

ii) to identify and recommend changes for assumptions and boundary conditions in the AENV inference model to improve its performance relative to the ENVC inference model, and

iii) to gain insight in the application of inferential modeling to dry deposition.

The ENVC inference model does not necessarily represent the best set of assumptions and conditions to characterize dry deposition; however, results from any one approach should compare reasonably well with other approaches used to characterize dry deposition.

1.3 Thesis Organization

Dry deposition is initially discussed and general modeling approaches of acid deposition are presented based upon current scientific literature. The ENVC modeling approach is presented in detail along with the AENV model and a comparison of the theory of the two models including the gaseous and the particulate portions. The discussion is split into gaseous and particulate deposition.

The AENV model was run using different boundary conditions and the results were compared with the model run under original conditions for similar inputs. A number of the different boundary conditions were based on conditions set in the ENVC model. A summary of conditions evaluated is presented in Table 1. Finally, the AENV model was run using different boundary conditions and compared with the ENVC model

run using similar inputs. Based upon comparisons of results for these sets of model runs, recommendations were made about how best to proceed with using assumptions and boundary conditions for operating the AENV model in the future.

Table 1 Boundary conditions evaluated during study.

Parameter	Units	Original Default	Revised Default Evaluated	Basis for Revision
R_a	s/m	upper limit undefined	upper limit capped at 1000 s/m (at 2000 s/m for water)	limit set in ENVC model
R_a	s/m	lower limit undefined	lower limit capped at 5 s/m	limit set in ENVC model
Monin-Obukhov length	m	undefined limit	upper limit of -5 m on negative side and lower limit of +5 m on positive side	limit set in ENVC model
wind speed	m/s	set to 0 m/s if less than 0.09 m/s	set to 1 m/s if less than 1 m/s	limit set in ENVC model

2 Acid Deposition Background

2.1 Introduction to Dry Deposition

Acid rain may contribute to acidification of terrestrial and aquatic systems (AENV, 1999). Acid rain involves three processes including transport, transformation, and deposition (Wesely and Hicks, 1977). Acid deposition can occur by wet and dry processes. Dry deposition is reported to represent about 40% of total deposition (Smith *et al.*, 2000).

Increased industrialization in Alberta, particularly oil sands extraction and processing in north eastern Alberta and petroleum upgrading and refining activities in central Alberta, is raising awareness about potential acid deposition due to industrial activities. A critical load approach is used in Alberta as a receptor-based approach for managing acid deposition (AENV, 1999). Since it is very difficult to directly measure dry deposition, models are essential for the estimation of the amount of dry deposition that a particular land type will experience given an atmospheric concentration of a depositing species. Because these values are used to regulate the amount of these chemicals that industry would be allowed to emit, over estimating the amount of acid deposition occurring is a more conservative approach than under estimating the amount of acid deposited.

Dry depositing species can be divided into sulfur compounds, nitrogen compounds, and base cations. Sulfur compounds of interest include gaseous sulfur dioxide (SO_2) and particulate sulfate (SO_4^{2-}). Nitrogen compounds include several gases including nitrogen dioxide (NO_2), nitrous acid (HNO_2), nitric acid (HNO_3), and ammonia (NH_3). Particulate forms of nitrogen include nitrate (NO_3^-) and ammonium (NH_4^+). Base cations include particulate calcium (Ca^{2+}), sodium (Na^+), potassium (K^+), and magnesium (Mg^{2+}).

2.2 *Inferential Methods*

The inferential method refers to a method of approximating deposition processes with a resistance analogy. It is distinguished from the previous method of concentration monitoring (Hicks *et al.*, 1987). The inferential method reflects the concept that different surfaces will experience different amounts of deposition. Early inference models approximated the entire canopy as one large surface and were referred to as a "big-leaf" method (Hicks *et al.*, 1987). Two big leaf models have evolved to emphasize separate treatment of sunlit and shaded portions of a canopy (Zhang *et al.*, 2001a, 2001b).

Multi-layer models (MLMs) or second generation models have evolved that include integration of deposition along the canopy height of vegetation (Meyers *et al.*, 1998). Peters *et al.* (1995) reported that third generation models will include interactions among chemistry, deposition processes, and meteorology, and may include physiological phenomena such as photosynthesis and CO_2 production (Niyogi *et al.*, 2003). Consequently, third generation models will be highly complex. A schematic of possible interrelations showing this complexity is included in Figure 1.

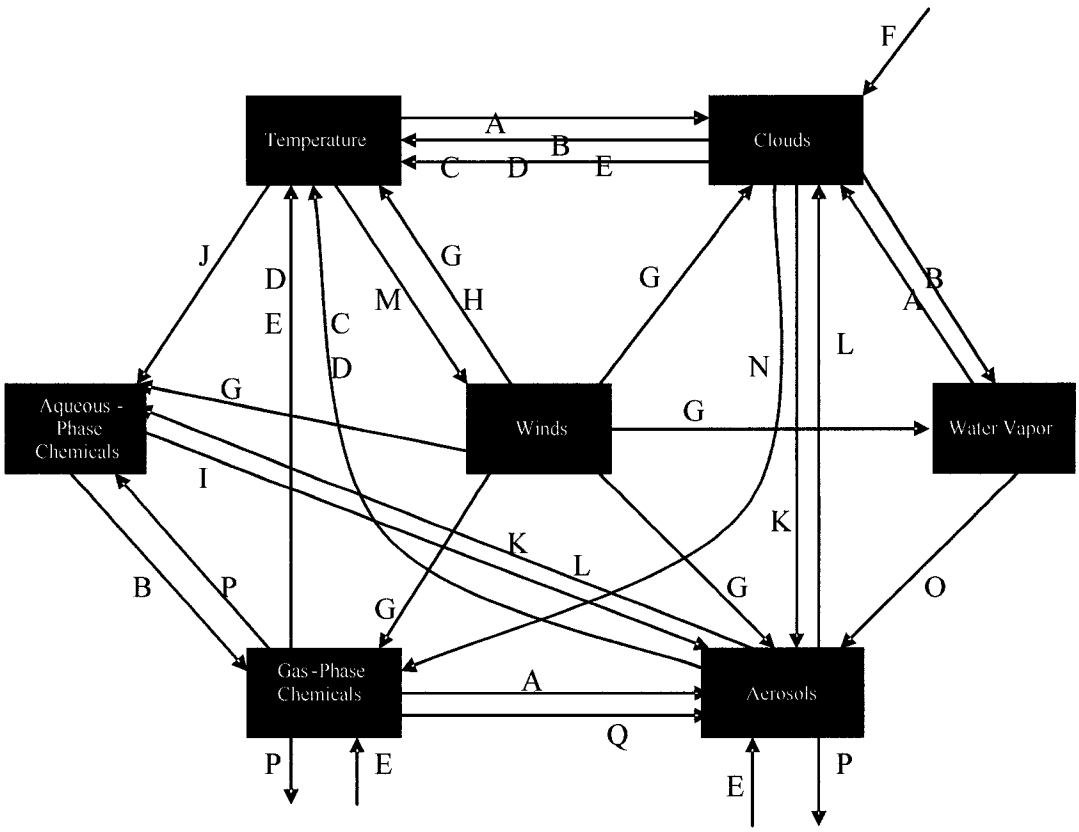

A: Condensation
B: Evaporation
C: Scattering
D: Absorption
E: Emission
F: Sunlight
G: Transport
H: Expansion
I: Resuspension
J: Solubility
K: Activation
L: Collection
M: Pressure Gradient Force
N: Photochemistry
O: Deliquescence
P: Deposition
Q: Nucleation

Figure 1 Possible interrelationships for potential inclusion in third-generation dry deposition inference models (adapted from Peters *et al.*, 1995).

2.3 *Deposition Velocity*

Deposition velocity is an engineering factor which is multiplied by the concentration of a chemical in air in order to calculate mass flux density (Wesely and Hicks, 2000). Values for deposition velocities are reported to range from close to 0 cm/s for inert substances to about 2 cm/s for reactive substances such as nitric oxide (HNO_3) (Wesely and Hicks, 2000). Deposition velocities are quoted in several units including m/s, mm/s, or cm/s, the latter being the most commonly used. The behavior of the flux of gaseous ammonia near a canopy surface is bidirectional, meaning that both deposition to and emission from the surface occurs (Wyers and Erisman, 1998). The concept of deposition velocity should not be used for substances such as ammonia because it violates an assumption that the flux is unidirectional (towards the surface) (Hicks *et al.*, 1987; Wesely and Hicks, 2000).

2.3.1 Gaseous Deposition

Deposition velocity is commonly modeled as three resistances in series (Hicks *et al.*, 1987). These resistances include aerodynamic resistance (R_a) associated with turbulent transfer, boundary layer resistance across the near-surface layer (R_b), and surface resistance involving the pollutant-surface interaction (R_c) (Voldner *et al.*, 1986). Parameterization methods for representing these resistances in the Environment Canada and Alberta Environment inference methods are presented in detail in Appendices A and B, respectively.

Aerodynamic Resistance (R_a)

Parameters used for modeling aerodynamic resistance are meteorological-specific, including wind speed, wind direction, and air temperature at two heights above the ground (usually 2 and 10 m). Modeled R_a values vary depending upon stability and surface roughness conditions, which are determined using these parameter inputs. Most inference methods represent surface roughness by using default values for different sets of surface roughness conditions (e.g., Voldner *et al.*, 1986). Because the input parameters are meteorological and not chemical specific, the aerodynamic resistance term is independent of chemical species.

Boundary Layer Resistance (R_b)

The boundary layer is a thin layer next to the surface (refer to Figure 2). Molecular diffusion determines gas transfer while Brownian diffusion and inertial impact determine particle transfer (WBK, 2006). Parameters needed for this resistance term include wind speed, roughness length, and temperature. R_b is usually smaller than aerodynamic resistance, which means it is usually less important for deposition velocity calculations (Walcek *et al*, 1986).

Total Surface Resistance (R_c)

R_c includes all the processes involving the actual surface and the particular chemical of interest (Hicks *et al.*, 1987). Most of the difference between models is in the modeling of the surface resistance. As models evolve to include more and more physiological phenomena, variables such as soil pH, surface wetness, and photo synthetically active radiation are required (Wesely and Hicks, 2000). Data for these variables can be difficult or expensive to obtain.

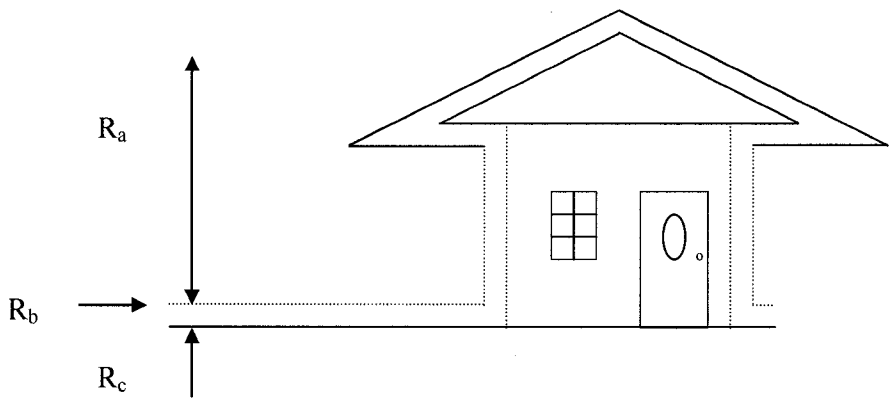

Figure 2 Relative locations where dry deposition resistance factors R_a, R_b, and R_c apply (adapted from WBK, 2006).

In more sophisticated models, such as the ENVC model, R_c is more finely divided into component resistances including stomatal resistance, mesophyll resistance, in-

canopy aerodynamic resistance, ground resistance, and canopy cuticle resistance (Zhang *et al.*, 2003). Stomatal resistance involves gas molecules entering the leaf through the stomata. Mesophyll resistance involves resistance to gas molecules dissolving in the mesophyll cells in the interior of the leaf. In-canopy aerodynamic resistance refers to meteorological issues within the canopy such as temperature gradients. Ground resistance includes resistance of soil, ground litter, and any water surface under the canopy. Finally, canopy cuticle resistance includes interaction with the cuticular surface of the plant which is important for more reactive chemicals such as nitric oxide. Alternatively, simpler parameterizations of R_c have represented it as a series of default values for different surface conditions represented by season, time of day, and surface wetness condition (Voldner *et al.*, 1986).

2.3.2 Particles

Particles in the atmosphere containing chemical species or elements tend to have a range of sizes that can be represented a by log-normal distribution having a mass median diameter and a geometric standard deviation (Ruijgrok *et al.*, 1995). A mass median diameter is the diameter of the particle having the median mass of the distribution. Larger sized (mass median diameter) elements tend to have a unimodal distribution while smaller sized elements (≤2 μm) tend to have a bimodal distribution (Milford and Davidson, 1985). The general size distribution of a particle typically depends upon its origin. Particles can be divided into three size modes (Holsen and Noll, 1992):

- The largest size mode (≥2.5μm) results from mechanical abrasion and wind erosion.
- Fine size mode particles (0.1 to 2.5 μm) originate through coagulation processes and are primary aerosol emissions.
- The smallest particles (<0.1 μm) are secondary products of emissions.

Gases may also react with larger particles and be present in larger particles (Ruijgrok *et al.*, 1995). This second origin for smaller sized elements may explain the bimodal shape of the size distribution (emissions related particles). Atmospheric

chemical reactions involving gaseous precursors to particulates can be affected by the presence of other chemicals (Ruijgrok *et al.*, 1995). Nitrate may reside on large particles as a result of reactions of nitric oxide with alkaline species of crustal origin (Ruijgrok *et al.*, 1995; Wolff, 1984). If ammonia gas is present such as in areas having animal feedlots, nitric oxide may react with the ammonia gas, resulting in nitrate (and ammonium) on small particles (Ruijgrok *et al.*, 1995; Wolff, 1984).

The size distributions used in particulate deposition modeling must be reasonable representations of the conditions for the area and the time being modeled. Particle size distributions may be different for different areas or different times of the year (Ruijgrok *et al.*, 1997; Wiman and Agren, 1985; Whitby, 1978; Milford and Davidson, 1985; Hoff *et al.*, 1983). Neighboring salt water bodies (as found in coastal areas), animal feedlots, and soil types can all strongly influence the size distribution of particulate matter. In terms of time, Arimoto *et al.* (1997) stated that particle size distributions may never reach equilibrium. In addition, Hedin *et al.* (1994) stated that the amount of atmospheric cations may have been declining in regions of Europe and North America as indicated by records from 1965 - 1990. It is speculated that the sources of the decline may be related to a reduction in unpaved roads, changing agricultural tillage practices, and a reduction in forest fires.

Models that represent deposition based on particle size are considered as process-oriented models, as opposed to bulk resistance-oriented models that do not distinguish between particle size (Ruijgrok *et al.*, 1995). Particle deposition mechanisms include (Slinn, 1982) diffusion, interception, impaction, gravitational settling, and phoretic mechanisms. Brownian diffusion dominates small particle (<0.1 μm) deposition; whereas gravitational sedimentation dominates large particle (≥ 2.5 μm) deposition (Ruijgrok *et al.*, 1995). Deposition velocities are highest for large particles for which the controlling mechanism is sedimentation (Ruijgrok *et al.*, 1995). Deposition velocities reach a minimum for particles from 0.1 to 1 μm in size where the particles are too large to be dominated by Brownian diffusion, but too small to be dominated by impaction and interception (Ruijgrok *et al.*, 1995).

Process-oriented models can be further increased in complexity by the inclusion of phoretic effects including electrophoresis, thermophoresis, and diffusiophoresis

(Ruijgrok *et al.*, 1995). Hygroscopic growth of particles can be an issue for high relative humidities (greater than 80%) (Draaijers *et al.*, 1997; Ruijgrok *et al.*, 1995). For example, an inference model used by Erisman *et al.* (1997) includes cases for wet and dry surface conditions as well as for relative humidities above and below 80%. Another complication that is not commonly addressed in particle deposition models is that Brownian diffusion will decrease if a gas molecule becomes attached to a particle (Sehmel, 1980). Finally, atmospheric stability issues may be a concern if a model was only designed for neutral stability conditions (Ruijgrok *et al.*, 1995). Deposition velocities may be overestimated for stable conditions and underestimated for unstable conditions (Ruijgrok *et al.*, 1995).

High deposition velocities related to sedimentation of large particles result in models that can be extremely sensitive to the method used to represent the large size end of the size distribution (Holsen and Noll, 1992). Solely using the mass median diameter (MMD) to represent particle size without integrating across the whole size distribution can cause large differences in model results (Ruijgrok *et al.*, 1995). It is very important to represent the distribution as divided into sufficiently small portions so that the full effects of the large particle end of the distribution are sufficiently represented. For example, Dulac *et al.* (1987) calculated mean dry deposition fluxes for sodium-bound particulates as 915, 700, and 30,000 $\mu g/m^2$/day when dividing the same distribution into 1, 6, and 100 different size step intervals or sections, respectively, for the same distribution (mean MMD of 6.5 μm).

Large particles, while rarer, can be responsible for more than 90% of the flux of a chemical because of large deposition velocities (Holsen and Noll, 1992). For large particles, process-oriented models using numerous size distributions are highly sensitive to the selection of the largest particle size as well as to the representativeness of the lognormal distribution (Holsen and Noll, 1992). Particles originating from crustal material tend to be large (≥60 to 100 μm) (Ruijgrok *et al.*, 1995). Given that larger particles are the base cations which act to reduce the impact of acidic components, underestimating the amount of deposition of these larger particles will result in higher total acid deposition or potential acid input (*PAI*) values which may act as a safety factor in setting more conservative limits on the levels of emissions tolerated.

2.4 *Dry Deposition Model Issues*

Dry deposition can be difficult to model because of scientific complexities and the limitations in approaches used to represent these complexities. Others have reported that it is not possible to incorporate all relevant physiological and atmospheric processes into an acid deposition model for the following three reasons (Venkatram *et al.*, 1988; Lovett, 1994):

- incomplete understanding of the processes involved,
- limitations in computational capacity, and
- limitations in model validation, including limitations of measuring equipment.

Wesely and Hicks (2000) state that there is an extremely large number of processes involved in the transfer of a chemical from air to a surface. Phenomena that are currently difficult to represent in a deposition model include surface wetness, surface roughness, edge effects, in-canopy chemical reactions, and bi-directional chemical gradients (Wesely and Hicks, 2000; Lovett, 1994; Venkatram *et al.*, 1988).

Computational capacity is always an issue in modeling and models are usually designed up to the limits of the applicable computer processing speed and capacity (Venkatram *et al.*, 1988). Modeling natural processes always involves approximating complicated relationships including interactions, thresholds, and feedback loops. In this study, Alberta Environment's ultimate objective is to be able to provide industry with a simple, easy to use model. This objective further limits the amount of computer sophistication that is permitted.

Model validation is of particular concern in acid deposition. Current measuring equipment is not able to detect the small concentrations of species rapidly enough to detect or to measure deposition phenomena. Eddy correlation techniques are reported to be the most sophisticated approaches for measuring dry deposition (Meyers *et al.*, 1996; Lovett, 1994); however, this method requires sensitive anemometry and rapid-response pollutant monitoring equipment (Lovett, 1994). In addition, errors in measurement techniques are reported to frequently be higher than 40% (Businger, 1986). Finally, it is uncertain as to whether deposition information gathered at one location in one time period can be applied to represent different locations or at different times.

Wesely and Hicks (2000) reported that comparisons of model results with deposition measurements have shown differences as large as +/-30%. In addition, they state that it is likely that the current methods for representing deposition velocity are an oversimplification and that the role of plant physiological processes are not sufficiently incorporated into models. For modeling gaseous deposition, possible modeling limitations can be due to a failure to adequately represent edge effects, heterogeneity of landscape, and terrain complexity (Hicks *et al.*, 1987). Difficulties associated with modeling particle deposition mechanisms may result in underestimating particle deposition by as much as an order of magnitude (Holsen and Noll, 1992).

3 Model Descriptions

3.1 Environment Canada (ENVC) Model

Details of the Environment Canada (ENVC) Model are provided in Appendix A. The following discussion summarizes the major aspects of the ENVC model.

3.1.1 Gases

The gas module of the ENVC model calculates deposition velocity (V_d) as the inverse of the sum of the three resistances (R_a, R_b, and R_c) as follows (Zhang *et al.* 2003):

$$V_d = \frac{1}{R_a + R_b + R_c} \tag{1}$$

Aerodynamic resistance (R_a) is calculated as:

$$R_a = \frac{1}{ku_*}\left[0.74\ln(z/z_0) - \psi_H\right] \tag{2}$$

using von Karman's constant (k), friction velocity (u^*), reference height (z), roughness length (z_0), and the stability function (ψ_H) (Brook *et al.*, 1999). In the ENVC model, values for the roughness lengths are taken from tabular values. Further details regarding calculation of these parameters can be found in Appendix A.

Sublayer or boundary layer resistance (R_b) is calculated as:

$$R_b = \frac{5}{u_*}\left(\frac{V_i}{D_i}\right)^{2/3} \tag{3}$$

using friction velocity (u^*), thermal diffusivity (V_i), and molecular diffusivity (D_i) (Brook *et al.*, 1999).

Total surface resistance (R_c) of the ENVC model is represented by stomatal and non-stomatal resistances (Zhang *et al.*, 2003). The stomatal resistance components include stomatal (R_{st}) and mesophyll (R_m) resistance, adjusted for stomatal blocking caused by wet conditions (W_{st}) (Zhang *et al.*, 2003). Non-stomatal resistance components include in-canopy aerodynamic resistance (R_{ac}), ground resistance (R_g), and cuticle resistance (R_{cut}) (Zhang *et al.*, 2003).

Mathematically, the R_c portion of the model can be stated as follows (adapted from Zhang *et al.*, 2003):

$$\frac{1}{R_c} = \frac{1 - W_{st}}{R_{st} + R_m} + \frac{1}{R_{ac} + R_g} + \frac{1}{R_{cut}} \tag{4}$$

Stomatal resistance (R_{st}) includes (Zhang *et al.*, 2003) unstressed leaf stomatal conductance ($Gs(PAR)$), conductance reducing effects of air temperature ($f(T)$), water-vapor pressure deficit ($f(D)$), leaf water potential ($f(\psi)$), molecular diffusivity (D_i), and water diffusivity (D_v). Mathematically, stomatal resistance can be stated as (Zhang *et al.*, 2003):

$$R_{st} = \frac{1}{G_s(PAR) f(T) f(D) f(\psi) D_i / D_v} \tag{5}$$

Mesophyll resistance (R_m) is species dependent and Environment Canada represents this term as a series of default values for different chemical species which can be found in Table A.3 (Zhang *et al.*, 2003).

Non stomatal resistances include in-canopy aerodynamic resistance (R_{ac}), ground resistance (R_g), and canopy cuticle resistance (R_{cut}) (Zhang *et al.*, 2003). In-canopy aerodynamic resistance is represented as a series of default values adjusted for leaf area indices (LAIs) for different seasons. Ground resistance is represented as a series of default values adjusted for temperature, rain or dew conditions, and snow cover fraction (Zhang *et al.*, 2003). Cuticle resistance is represented as a series of default values according to land use category and adjusted for temperature, rain or dew conditions, leaf area indices, and snow cover fraction (Zhang *et al.*, 2003).

3.1.2 Particulates

The ENVC model uses a separate module for modeling particle deposition velocity (V_d) which includes components of gravitational settling (V_g), aerodynamic resistance (R_a), and surface resistance (R_s) in the following relationship (Zhang *et al.*, 2001):

$$V_d = V_g + \frac{1}{R_a + R_s} \tag{6}$$

Gravitational settling velocity (V_g) includes particle density (ρ), particle diameter (d_p), gravitational acceleration (g), viscosity (μ), and the Cunningham slip correction factor (C) in the following relationship (Zhang *et al.*, 2001):

$$V_g = \frac{\rho d_p^2 g C}{18\mu} \tag{7}$$

Aerodynamic resistance (R_a) is calculated the same way as for gaseous deposition in the ENVC model (Zhang *et al.*, 2001). Surface resistance (R_s) includes collection efficiency of Brownian diffusion (E_B), impaction (E_{IM}), interception (E_{IN}), a stickiness factor (R_1), friction velocity (u^*), and a constant (ε_0) as illustrated in the following relationship (Zhang *et al.*, 2001):

$$R_s = \frac{1}{\varepsilon_0 u_* (E_B + E_{IM} + E_{IN}) R_1} \tag{8}$$

As previously stated in Section 2.3.2, the sizes of particles of a particular chemical can be represented by log-normal distribution (Ruijgrok *et al.*, 1995). In the ENVC model, smaller particles (SO_4^{2-} and NH_4^+) are modeled as a log-normal distribution having a mean of 0.35 μm and a standard deviation of 2.0 μm as was used by Wesely *et al.* (1985). The larger particles (NO_3^-, Na^+, K^+, Ca^{2+}, and Mg^{2+}) are all modeled using the log-normal distribution for Na^+ having a mean of 5.12 μm and a standard deviation of 2.64 μm as used by Ruijgrok *et al.* (1997).

It is not possible to represent the log-normal distribution merely using the mean of the distribution because the deposition velocity of particles is different for different size particles as was shown in Figure 3 (Section 2.3.2). It is necessary to divide the distribution into small enough pieces so that the variation in the deposition velocity for the different sizes is accurately represented and not distorted by averaging effects.

The ENVC model uses 40 incremental ranges (or bins), such that the maximum size represented in each of the 40 bins is defined by the following formula (Zhang *et al.* 2001):

$$size\_increment\ (\mu m) = 0.0010 * I^{2.5} \quad \text{where I is from 1 to 40} \tag{9}$$

For example, the first bin would include all particles of the size range from 0 to 0.0010 μm and the second bin would include all particles of the size range from 0.0010 to 0.0057 μm. The 40th bin would include particles from 9.5 to 10.1 μm. The deposition velocity is

calculated for each bin using the largest particle size in the particular bin. The deposition velocity for a particular chemical is calculated by summing the individual deposition velocities for each of the 40 bins, weighted based on the proportion of the mass in the bin. The proportion of particles in the bin is merely the area under the particle distribution curve for that size range. A similar process is used for the distribution of larger particles.

3.2 Alberta Environment (AENV) Model

Details of the Alberta Environment (AENV) Model are provided in Appendix B. The following discussion summarizes the AENV model and compares it with the ENVC model.

3.2.1 Gases

A description of the AENV model is provided by Cheng *et al.* (2001) and WBK (2006) and briefly described here. The AENV model uses the same resistance analogy approach for calculation of deposition velocity (V_d) as the ENVC model, but calculates each of the three components differently (Appendix B) (WBK, 2006; Cheng *et al.* 2001). The AENV calculation for R_a involves initially calculating a value for the surface roughness length (z_0) as a monthly average only using hourly data where the wind speed (u) is greater than 6 m/s:

$$z_0 = z\, e^{-\left(\frac{0.4u}{u^*}\right)} \tag{10}$$

Since the calculation of the friction velocity (u^*) normally requires the roughness length (z_0), the friction velocity for each hour is initially estimated using the wind speed and the standard deviation of wind direction (σ_θ) with the formula:

$$u^* = \frac{u\sigma_\theta}{1.9} \tag{11}$$

Once the roughness length is determined for each month, hourly values for R_a are calculated using the formula:

$$R_a = \frac{1}{ku^*}\left\{\ln\frac{z}{z_0} - \psi\right\},\ \psi = f\left(\frac{z}{L}\right) \tag{12}$$

which is slightly different than the formula used in the ENVC model.

The AENV model calculates R_b based upon von Karman's constant (k), the friction velocity (u^*), the Schmidt number (Sc) for a chemical, and the Prandtl number (Pr) for air in the following relationship (Cheng *et al.*, 2001):

$$R_b = \frac{2}{ku^*}\left(Sc \times \frac{1}{\mathrm{Pr}}\right)^{2/3} \tag{13}$$

Again, this formula is slightly different than that used in ENVC model.

For the gases SO_2 and NO_2, the AENV model represents R_c as default values as shown in Table B1 that are different for different land use covers, seasons, and wetness; while for HNO_2 and HNO_3, R_c is always set at 10 s/m. The default values for SO_2 and NO_2 are calculated (for each season, land use cover, and wetness) from literature values which are adjusted for incident radiation for each season based on the latitude of the area being modeled. Varying the R_c value for the three parameters of land cover, season, wetness, and latitude functionally addresses the variation in R_c caused by stomatal and non-stomatal resistances as calculated in the ENVC model.

In the AENV model, if surface wetness is unavailable then relative humidity is used as a surrogate for surface wetness. The model allows a minimum relative humidity (RH) measurement cut-off of 87% to be used as an approximation for representing a surface as being wet.

3.2.2 Particulates

The AENV model uses the same deposition velocity relationship for particulates as used by the gaseous model. Initially, use of this approach may appear to be quite different from that of the ENVC model; however, the two models are actually quite similar as the gravitational settling velocity component of the ENVC model is considered to be quite small.

For particulates, R_c is considered negligible and this resistance is assigned a value of 0. R_a is determined independent of chemical species. R_b is represented with default values for different species and is derived from scientific literature and adjusted for

dry/wet and seasonal conditions (as a function of surface type) and weighted according to average day length for each month at a mid-Alberta latitude location (54°N latitude).

4 Dry Deposition Modeling for ENVC and AENV Models

4.1 Model Methods for Coniferous Forest (Base Case)

The model results can be reported and evaluated for each chemical in terms of either monthly deposition velocities or monthly deposition fluxes. Reporting in terms of monthly deposition velocities is more common in the scientific literature because it allows the comparison of results for a given land cover from different areas around the globe. Evaluating the models in terms of monthly deposition fluxes is more practical because fluxes also address the concentrations of the chemicals in the atmosphere. For example, it is possible for deposition velocity results to be quite different between the two models without affecting the difference between total monthly deposition fluxes. From the point of view of Alberta Environment regulating acceptable emissions levels, it is the accuracy of the total monthly deposition fluxes that is important.

The two dry deposition inference models in their original forms as described in Appendices A and B were run to establish a starting point from which to evaluate the effects of changes made to the AENV model. These results were initially shown for monthly deposition fluxes to permit a comparison of the overall performance of the two models for a coniferous forest land use category (*LUC*) and considering 11 species (SO_2, SO_4^{2-}, NO_2, HNO_3, HNO_2, NO_3^-, NH_4^+, Ca^{2+}, Na^+, K^+, and Mg^{2+}).

Secondly, results were examined using deposition velocities (V_d) for each species involved in the calculation of monthly deposition flux. Since deposition velocities should be relatively constant for all chemical species for a given land use and set of meteorological conditions, comparisons with deposition velocity literature values were made for individual species. The behavior of the three most important individual species making up the largest difference in monthly deposition flux between the two models was further examined to better understand the importance of these species. These species included SO_2, NO_2, and HNO_3. Using the "contribution to total deposition flux" rather than "deposition velocity" of an individual species allowed an understanding of how important each species was in contributing to change in total deposition flux when modifications to the AENV model were made.

The original model form for the AENV model was also used to generate results for seven other *LUCs* for which the AENV model was designed. These results were compared with original results for a coniferous forest *LUC*. These comparisons were done for monthly deposition flux, as well as for surface resistance (R_c) values for gases and deposition velocity (V_d) values for particles. It is important to note that inputs for meteorological parameters used in comparing the two dry deposition inference models were obtained from a geographical setting consistent with a coniferous forest *LUC*.

These parameter inputs were used to make comparisons for the seven *LUCs* to better understand their general behavior for the AENV model. These parameter inputs are not necessarily representative of the settings for the seven *LUCs* because some meteorological parameters (such as roughness length and relative humidity) are affected by the respective surface conditions. As such, deposition velocities and surface resistance values cannot be fairly compared with literature values for these seven *LUCs*.

4.1.1 Input Parameters for Modeling

All of the modeling in this study were performed using measurements of hourly pollutant concentrations for 11 species and hourly values for meteorological parameters made at the Wood Buffalo Environmental Association Fort MacKay air monitoring station for the year 2003. Gaseous species measured included SO_2, NO_2, HNO_3, and HNO_2. Particulate ions included SO_4^{2-}, NO_3^-, and NH_4^+. Base cations included K^+, Na^+, Ca^{2+}, and Mg^{2+}. Measured meteorological values included wind speed, standard deviation of wind direction, air temperature at 2 m and 10 m heights, and relative humidity. Inputs for solar zenith angle and solar radiation values used in the ENVC model were computed using a Visual Basic program developed during a previous study (WBK, 2006). The forms and units of the inputs used in the model and any conversions performed in the ENVC and the AENV models are summarized at the ends of Appendices A and B, respectively.

Quality assurance and quality control were performed on the data. Unusual input values were found to be very uncommon and were left in the input data set. Including unusual values allows the performance of the models to be evaluated using typical data

which is representative of real world data. Missing hourly data were replaced with the average of the value for the hours before and after the hour of the missing value if only one hour's value was missing. If two or more consecutive hours were missing, then the month's median value for each of those hours was used to represent the missing data for those hours. For species measured intermittently (24 hours every 6 days), the hourly average was used for all of the 144 hours (6 days) in that time period. These procedures were used in the previous study and complete details of data collection, processing, and assumptions are described in WBK (2006).

4.1.2 Atmospheric Concentrations of Chemical Species

Deposition of a particular species is the product of species concentration and deposition velocity. From a practical point of view, it is important to understand those species having the greatest influence on acid deposition in terms of hydrogen ion equivalents. Monthly average species concentrations are provided in Appendix C.

Concentrations for nitrogen compounds (NO_2, HNO_3, HNO_2, NO_3^-, and NH_4^+) tend to be higher in winter than summer months. Deposition velocities for NO_2, HNO_3, and HNO_2 tend to be lower in winter months. Species and respective concentration ranges were as follows for the 2003 data set:

- NO_2 was the species with the highest recorded hourly concentration (range 3.7 to 21.7 $\mu g/m^3$).
- SO_2 was the second most important species although hourly levels observed were much lower (range 1.0 to 4.9 $\mu g/m^3$).
- Calcium ion (Ca^{2+}) levels ranged from 0.2 to 1.9 $\mu g/m^3$. Calcium concentration maxima occurred in April, July, and November.
- Sulphate (SO_4^{2-}) ions ranged from 0.5 to 2.4 $\mu g/m^3$.
- HNO_3 concentration ranged from 0.2 to 1.5 $\mu g/m^3$.
- Levels of all other species were less than 1.0 $\mu g/m^3$ for all months of the year.

4.2 Model Results – Coniferous Forest

4.2.1 Deposition Flux

The first modeling was done using AENV and ENVC models in their original forms. Total monthly deposition flux values ranged from less than 0.0005 to 0.016 kg hydrogen ion per hectare (kg H^+/ha) for the AENV model and from 0.004 to 0.018 kg H^+/ha for the ENVC model (Table 2). Total deposition flux for the year was 0.141 kg H^+/ha for the AENV model and 0.153 kg H^+/ha for the ENVC model. For total annual deposition, the difference between the two models was small at 0.012 kg H^+/ha, representing a difference of about 8%. As shown in Figure 3, months having the largest differences were November, July, and September, all of which showed the AENV model to underestimate the ENVC model. May, October, April, and December showed moderate differences. Total deposition for the months of January, February, March, June, and August were similar for both models.

Table 2 Comparison of monthly summed deposition flux (kg H^+/ha) for 11 species to a coniferous forest cover using the AENV and ENVC models.

Month	AENV	ENVC	Difference
Month 1	0.016	0.016	0.000
Month 2	0.011	0.011	-0.001
Month 3	0.016	0.016	0.000
Month 4	0.016	0.017	-0.001
Month 5	0.014	0.012	0.002
Month 6	0.007	0.006	0.001
Month 7	0.007	0.011	-0.003
Month 8	0.013	0.013	0.000
Month 9	0.010	0.012	-0.003
Month 10	0.016	0.018	-0.002
Month 11	0.000	0.004	-0.004
Month 12	0.016	0.017	-0.001
Total	0.141	0.153	-0.012
Total % difference			8

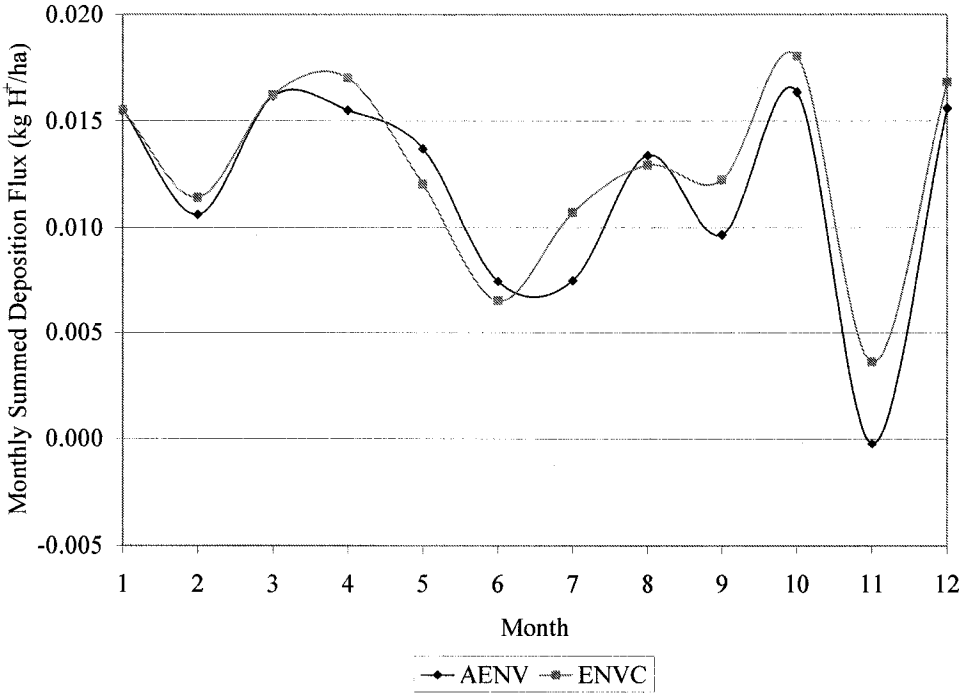

Figure 3 Comparison of monthly summed deposition flux for 11 species to a coniferous forest cover using the AENV and ENVC models.

4.2.2 Deposition Velocities – Coniferous Forest

The initial model results were separated out to show monthly average deposition velocities for each species in Figures 4 to 9. Tabular values associated with Figures 4 to 9 can be found in Appendix D.

4.2.2.1 Deposition Behavior of Gases (SO_2, NO_2, HNO_3, HNO_2)

SO_2

Resulting average deposition velocities (V_d) for SO_2 for the two models indicate that SO_2 deposition ranges from 0.09 to 0.49 cm/s across the year. The AENV model under represents the ENVC model in winter and spring months, but over represents it in summer months (Figure 4).

In a study from the literature, a U.S. National Dry Deposition Network (NDDN) model (which is reported to be similar to the ENVC model) was used to simulate acid deposition at Ann Arbor, Michigan, for a land use combination of grass, water, and forest (Brook, 1996). Their model results indicated SO_2 monthly average deposition velocities ranged from 0.20 to 0.55 cm/s, with the peak in June (Brook, 1996). These values are similar to those found for the ENVC and AENV models in this study as was shown in Figure 4.

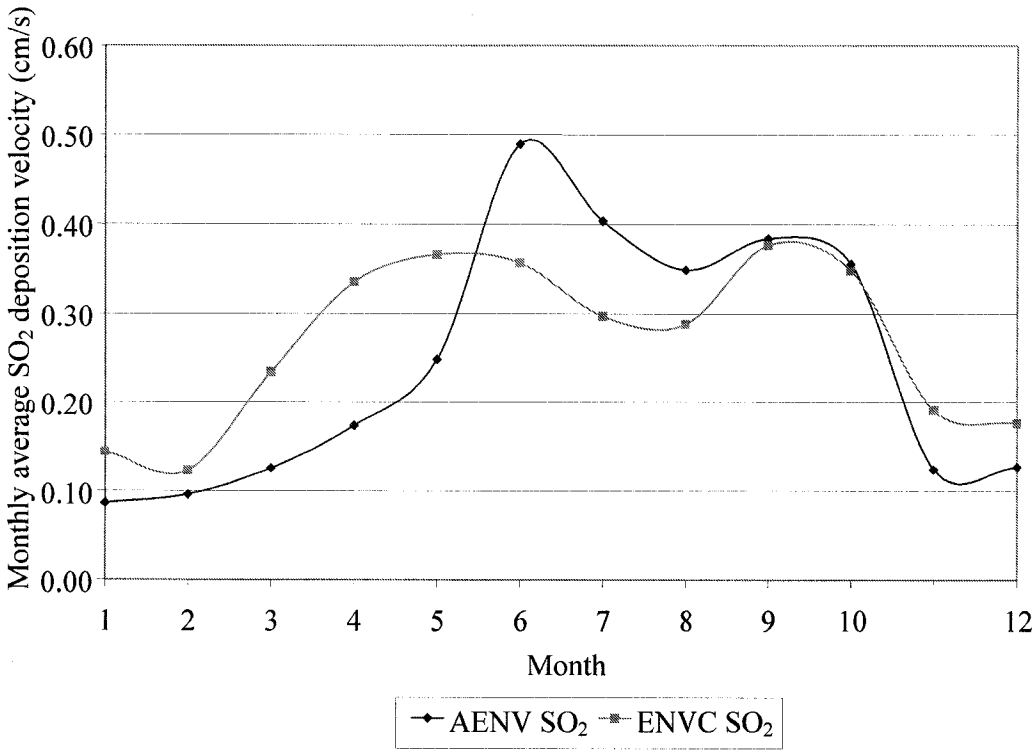

Figure 4 Comparison of monthly average SO_2 deposition velocity for a coniferous forest cover using the AENV and ENVC model.

NO_2

NO_2 monthly average deposition velocities are shown in Figure 5 and ranged from 0.04 to 0.25 cm/s with the AENV model under representing the ENVC model in

winter and spring months while over representing it in summer. Generally, ENVC results were quite similar to AENV results.

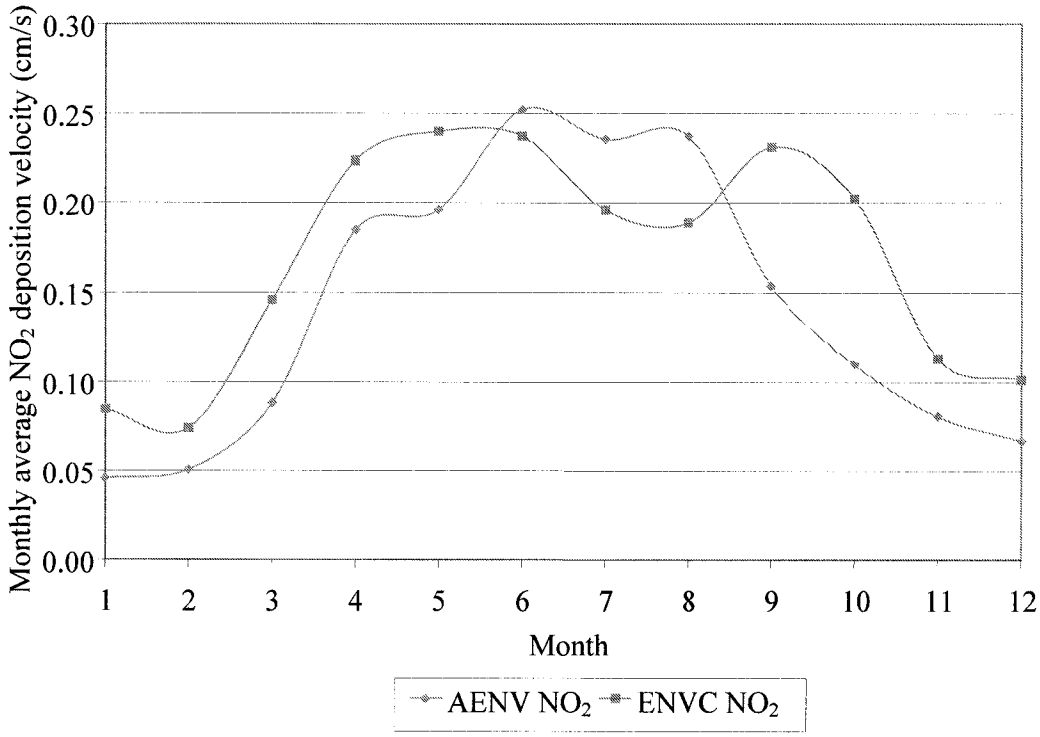

Figure 5 Comparison of monthly average NO_2 deposition velocity for a coniferous forest cover using the AENV and ENVC model.

HNO_3

Monthly average HNO_3 deposition velocities are shown in Figure 6 and they range from 0.8 to 2.1 cm/s with the AENV model over representing the ENVC model in all months except December. The two models produced similar trends with monthly average AENV deposition velocities being higher than those of the ENVC model. In the previously mentioned Ann Arbor study (Brook, 1996), the NDDN model produced HNO_3 deposition velocities ranging from 1.4 to 2.2 cm/s with peaks in April and December and troughs in August. These values are somewhat similar to those found for the ENVC and AENV models in this study as was shown in Figure 6.

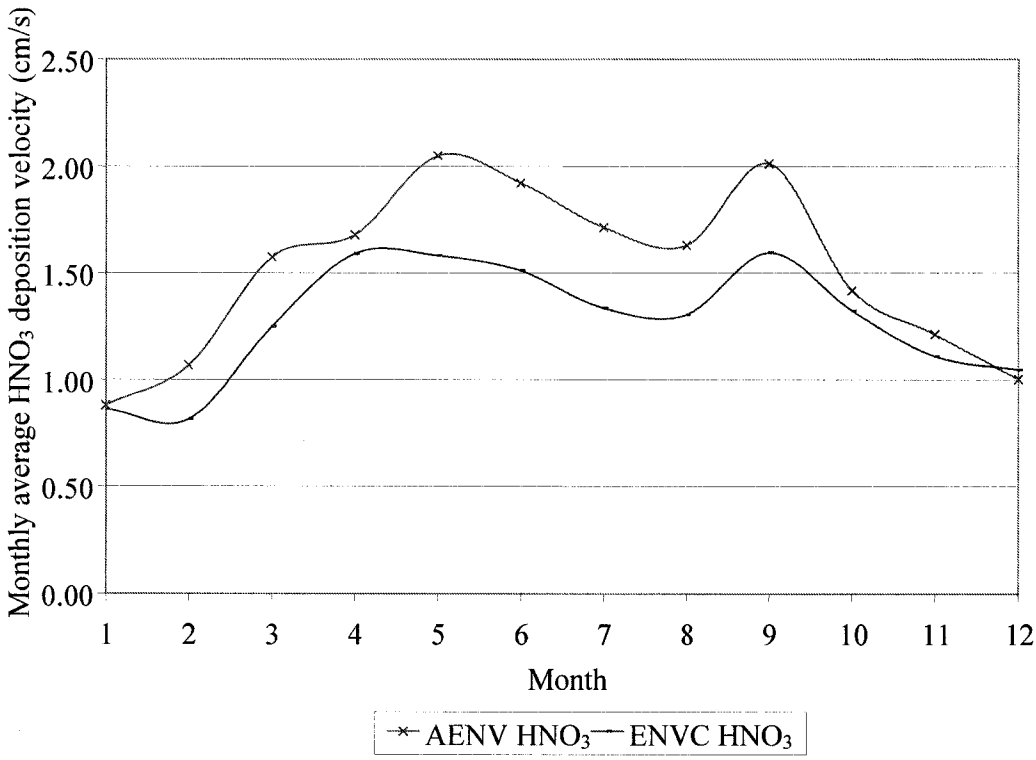

Figure 6 Comparison of monthly average HNO_3 deposition velocity for a coniferous forest cover using the AENV and ENVC model.

HNO_2

Monthly average HNO_2 deposition velocities are shown in Figure 7 and they ranged from 0.3 to 2.2 cm/s. The AENV model consistently over represented the ENVC model by two to three times. While this difference may seem substantial, the relatively low concentration of HNO_2 in the atmosphere results in a relatively small contribution to total monthly deposition flux for both of the models.

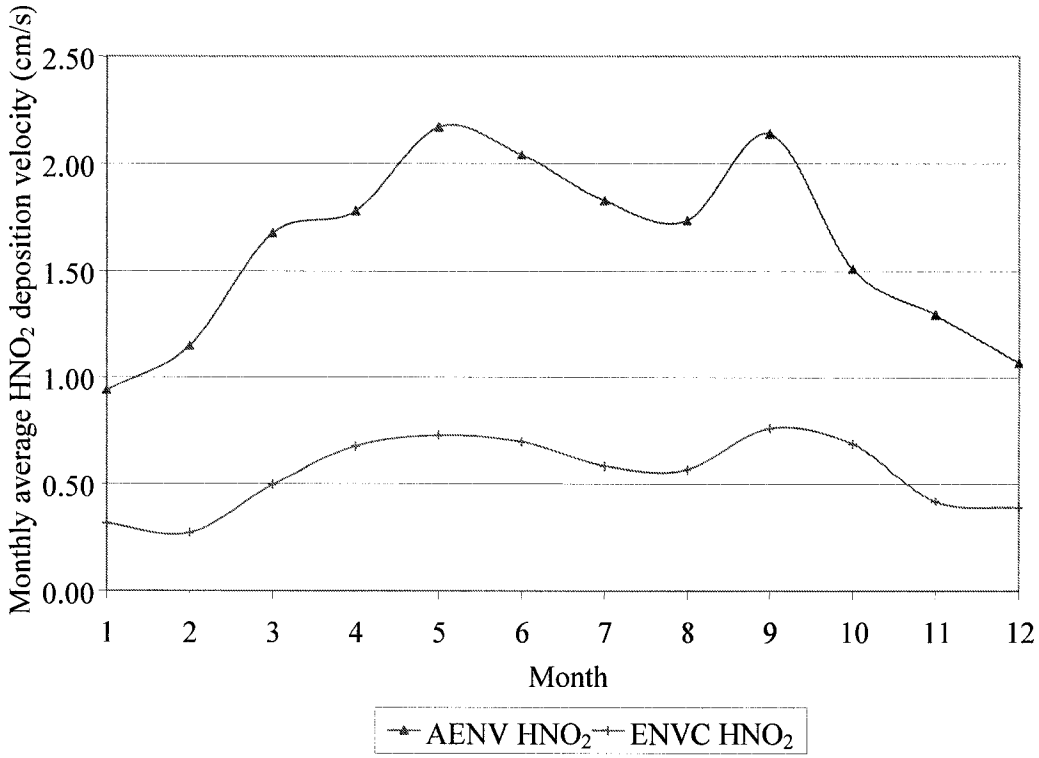

Figure 7 Comparison of monthly average HNO_2 deposition velocity for a coniferous forest cover using the AENV and ENVC model.

4.2.2.2 Fine Particle (SO_4^{2-}, NH_4^+) Deposition Behavior

Deposition velocities for smaller particles (SO_4^{2-} and NH_4^+) as represented by the log-normal distribution having a mean of 0.35 μm and a standard deviation of 2.0 μm are shown in Figure 8. The deposition velocities ranged from 0.09 to 0.35 cm/s with the AENV model over representing the ENVC model in every month. Particle deposition behavior in both models is mostly dominated by aerodynamic resistance (R_a) based on aerodynamic properties (diameter) of the particle which are independent of individual species.

The AENV results showed a peak in summer months that was absent in the ENVC model. In the literature study in Ann Arbor (Brook, 1996), the NDDN model reported small-particle monthly average deposition velocities ranging from 0.07 to 0.15 cm/s with slightly higher values in May and a minimum in winter months. These values are similar to those found for the ENVC model in this study as shown in Figure 8. The

AENV model results were somewhat higher than those of the ENVC model and the Ann Arbor study.

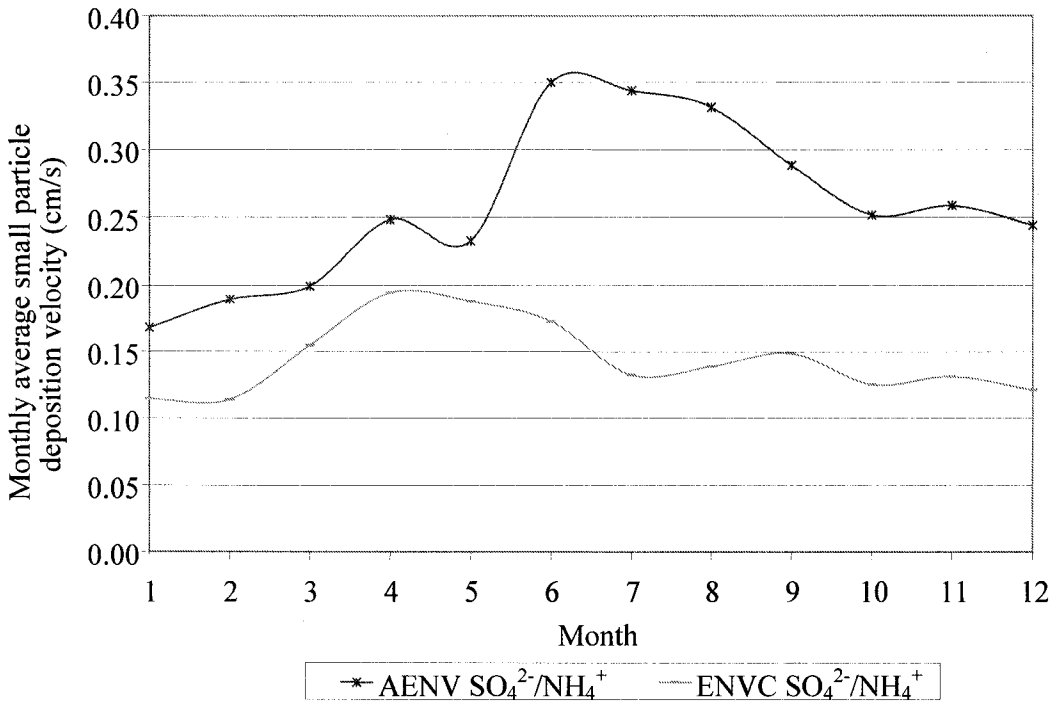

Figure 8 Comparison of monthly average small particle deposition velocity for a coniferous forest cover using the AENV and ENVC model.

4.2.2.3 Coarse Particle (NO_3^-, Na^+, K^+, Ca^{2+}, Mg^{2+}) Deposition Behavior

Deposition velocities for coarse particles (NO_3^-, Na^+, K^+, Ca^{2+}, Mg^{2+} as represented by the log-normal distribution having a mean of 5.12 μm and a standard deviation of 2.64 μm (truncated at less than or equal to 10 μm) are shown in Figure 8. Again, particle deposition behavior in both models is mostly dominated by aerodynamic resistance (R_a) based on aerodynamic properties (diameter) which are independent of individual species. Monthly average deposition velocities for larger (coarse) particles are shown in Figure 9 and they ranged from 0.29 to 0.64 cm/s. Similar to Figure 8 (small

particle deposition), monthly average deposition velocities for large particles showed a peak in summer months for the AENV model that did not occur in the ENVC model.

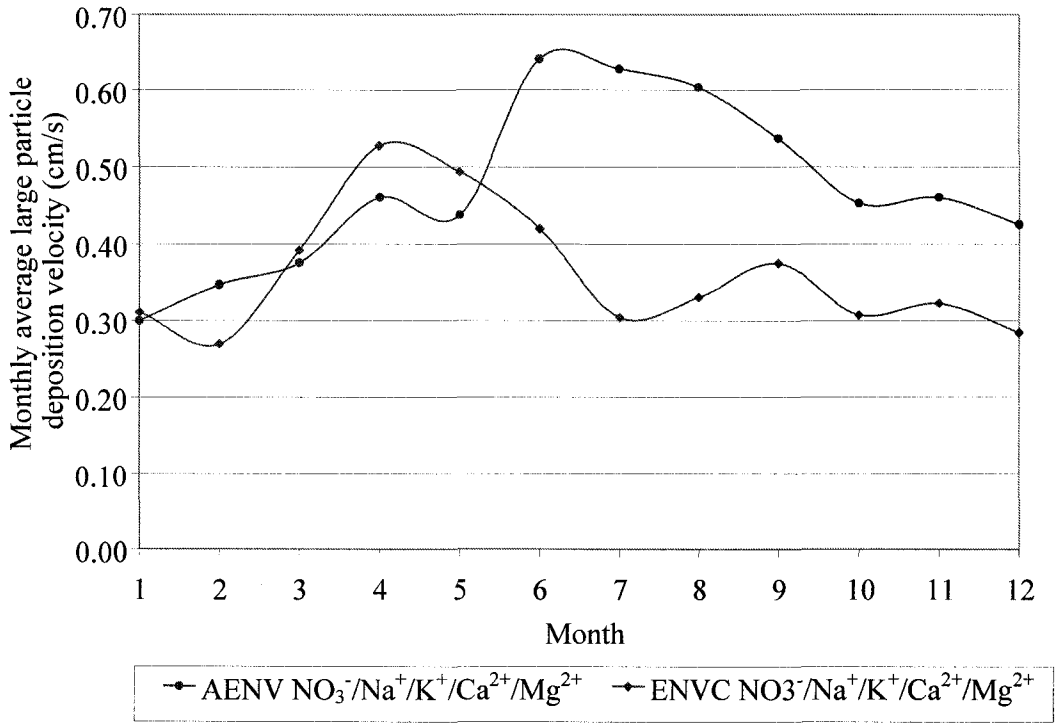

Figure 9 Comparison of monthly average large particle deposition velocity for a coniferous forest cover using the AENV and ENVC model.

4.3 Model Methods for Other Land Use Categories

The AENV model was rerun for seven land uses that represent the other land use categories (*LUCs*) for which the model was designed. Input data were the same as that used previously, the only change was the selection of the *LUC*. Because calculation of roughness length (z_0) is based on the meteorological input data, roughness lengths used for these seven *LUCs* were the same as that used for a coniferous forest *LUC*. Normally, the meteorological parameters for a different *LUC* would be such that the roughness lengths would be different than those of a coniferous forest. Nonetheless, rerunning the model for the different *LUCs* with the same meteorological data is useful in that it makes

it possible to demonstrate the impact of the different *LUCs* on the deposition fluxes without the confounding effect of different meteorological conditions.

In the AENV model, changing the *LUC* would only affect the deposition velocity through the R_b values for particulates and the R_c values for SO_2 and NO_2. The R_a values are not affected by using a different *LUC* because all the associated input meteorological input variables were kept the same. The R_b values for gases in the AENV model are also dependent only on meteorological variables (Appendix B) and are therefore not affected by the selection of the *LUC*. The R_b values for particulates are taken from a table (Appendix B) and are different for different *LUCs*, seasons, and particle sizes. The R_c values are SO_2 and NO_2 are taken from tables (Appendix B) that have different values for different *LUCs*, while the rest of the gases and the particulates are all assigned an R_c value independent of the *LUC* and season.

4.4 Model Results – Coniferous Forest

4.4.1 Deposition Flux

Monthly summed deposition flux results for all seven of the other *LUCs* are compared with a coniferous forest surface cover in Figures 10 through 16 and detailed for individual species in Tables 3 through 9. The table is done in terms of change in contribution of acidic species. A negative value for the acidic species in the tables indicates that the monthly average result for that acidic species for the alternative *LUC* is less than for a coniferous forest surface. A negative value for the basic species indicates that the monthly average result for that basic species is more than for a coniferous forest surface (so as to represent a decrease in the acid deposition total). The totals in the right hand columns therefore represent a sum of all the net acidic changes in each of the species. The negative values for flux for the month of November for several of the different *LUCs* indicates that more basic species were deposited in that month than were acidic species. This phenomenon occurs in November due to the high concentrations of calcium in the atmosphere at that time of year. Presumably, the high concentrations are the result of the lack of foliage resulting in wind erosion of the surrounding soils.

LUC 1 – Deciduous Forest Compared with Coniferous Forest

The differences in monthly summed deposition flux for a deciduous forest cover are shown in Figure 10. The differences between the two curves are further detailed for each chemical in Table 3 in which it is shown that these differences are largely a result of a difference in NO_2 and Ca^{2+} deposition in winter and a difference of Ca^{2+} deposition in summer.

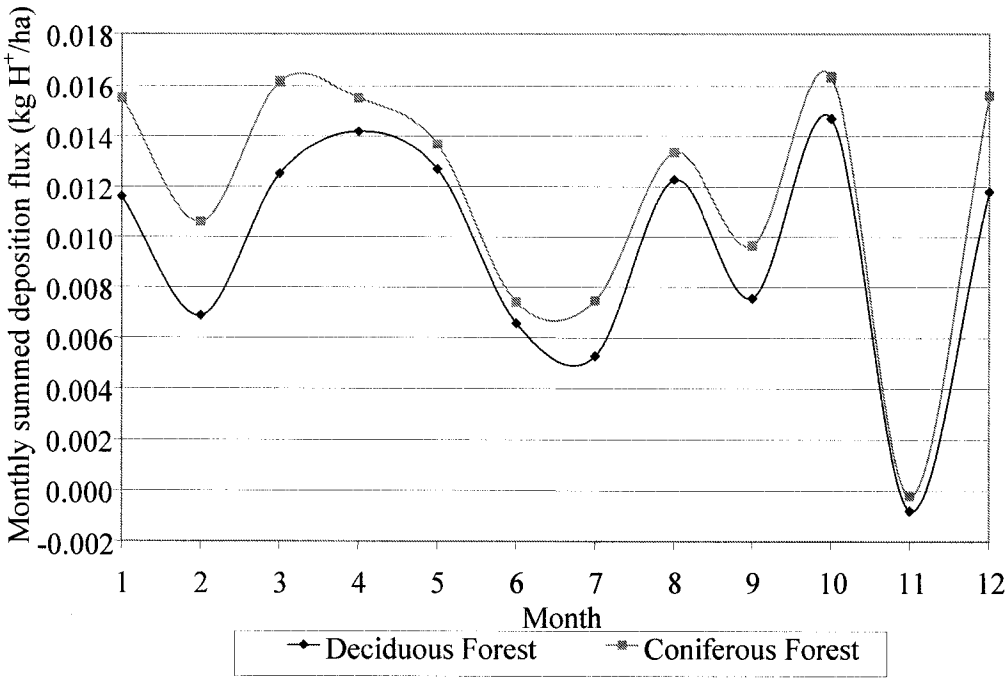

Figure 10 Comparison of monthly summed deposition flux for 11 species to a deciduous forest and coniferous forest cover using the AENV model.

Table 3 Breakdown of magnitude of differences in monthly summed deposition flux in kg H^+/ha for individual species between deciduous forest and coniferous forest cover using the AENV model.

Month	SO_2	NO_2	HNO_2	HNO_3	SO_4^{2-}	NH_4^+	NO_3^-	Na^+	K^+	Ca^{2+}	Mg^{2+}	Total
Month 1	-0.5	-2.5	0.0	0.0	-0.7	-1.2	-0.3	0.4	0.1	0.6	0.2	-3.9
Month 2	-0.7	-2.5	0.0	0.0	-0.8	-1.0	-0.2	0.3	0.0	0.9	0.2	-3.7
Month 3	-0.7	-1.8	0.0	0.0	-1.3	-1.0	-0.1	0.2	0.0	0.8	0.1	-3.6
Month 4	-0.6	-1.8	0.0	0.0	-0.6	-0.8	-0.1	0.2	0.0	2.2	0.2	-1.3
Month 5	-0.3	-1.1	0.0	0.0	-0.4	-0.5	0.0	0.1	0.0	1.0	0.2	-1.0
Month 6	0.0	0.0	0.0	0.0	0.4	0.5	0.0	-0.1	-0.1	-1.4	-0.2	-0.8
Month 7	0.0	0.0	0.0	0.0	0.4	0.4	0.1	-0.1	-0.1	-2.5	-0.3	-2.2
Month 8	0.0	0.0	0.0	0.0	0.5	0.6	0.1	-0.1	-0.1	-1.8	-0.4	-1.1
Month 9	-0.7	-1.5	0.0	0.0	-0.2	-0.3	0.0	0.1	0.0	0.4	0.1	-2.1
Month 10	-0.7	-1.7	0.0	0.0	-0.3	-0.4	0.0	0.1	0.0	1.2	0.1	-1.6
Month 11	-0.3	-2.5	0.0	0.0	-0.3	-0.6	-0.2	0.1	0.1	3.1	0.1	-0.6
Month 12	-1.2	-3.9	0.0	0.0	-0.8	-1.0	-0.6	0.4	0.2	2.6	0.4	-3.8

*highlighting indicates a difference of 2.5 kg H+/ha or more

LUC 3 – Wetland/Swamp Compared with Coniferous Forest

The differences in monthly summed deposition flux for a wetland/swamp are shown in Figure 11. The differences between the two curves are further detailed for each chemical in Table 4 in which it is shown that these differences are largely a result of NO_2 deposition being low across the year because of wet surface conditions representative of wetland/swamp and SO_2 deposition being higher in spring and summer months because of wet surface conditions representative of wetland/swamp compared to winter months.

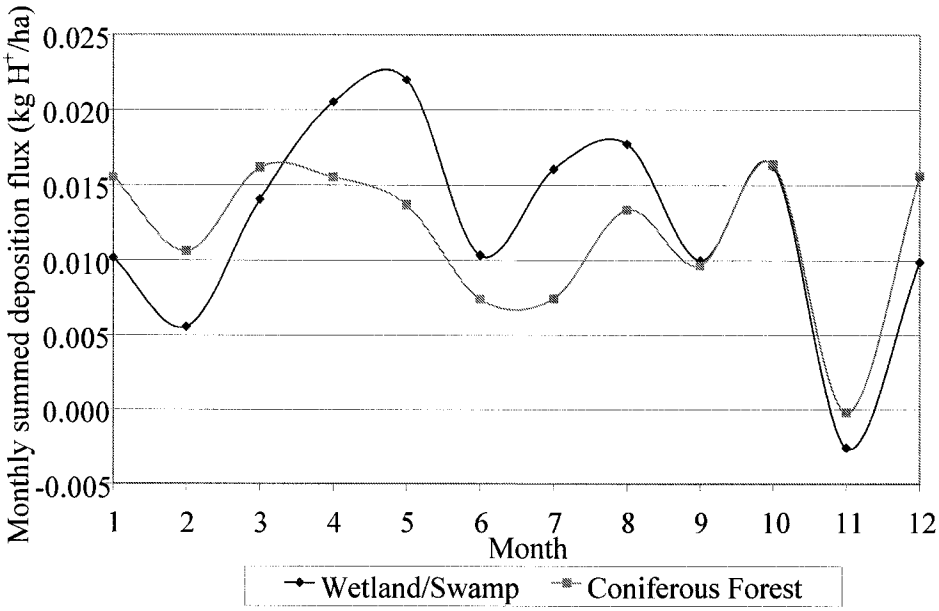

Figure 11 Comparison of monthly summed deposition flux for 11 species to wetlands/swamp and coniferous forest cover using the AENV model.

Table 4 Breakdown of magnitude of differences in monthly summed deposition flux in kg H^+/ha for individual species between wetland/swamp and coniferous forest cover using the AENV model.

Month	SO_2	NO_2	HNO_2	HNO_3	SO_4^{2-}	NH_4^+	NO_3^-	Na^+	K^+	Ca^{2+}	Mg^{2+}	Total
Month 1	-0.3	-4.2	0.0	0.0	-0.7	-1.2	-0.3	0.4	0.1	0.6	0.2	-5.4
Month 2	-0.4	-4.2	0.0	0.0	-0.8	-1.0	-0.2	0.3	0.0	1.0	0.2	-5.1
Month 3	3.8	-5.2	0.0	0.0	-0.7	-0.6	-0.1	0.1	0.0	0.5	0.1	-2.1
Month 4	11.2	-6.8	0.0	0.0	-0.3	-0.5	-0.1	0.1	0.0	1.2	0.1	5.0
Month 5	12.8	-4.7	0.0	0.0	-0.2	-0.3	0.0	0.1	0.0	0.6	0.1	8.3
Month 6	6.1	-3.8	0.0	0.0	-0.2	-0.3	0.0	0.0	0.0	0.9	0.1	2.9
Month 7	12.4	-5.3	0.0	0.0	-0.2	-0.3	-0.1	0.1	0.1	1.6	0.2	8.6
Month 8	10.5	-6.9	0.0	0.0	-0.3	-0.4	0.0	0.1	0.0	1.1	0.2	4.3
Month 9	4.1	-3.9	0.0	0.0	-0.2	-0.3	0.0	0.1	0.0	0.4	0.1	0.3
Month 10	3.7	-4.5	0.0	0.0	-0.3	-0.4	0.0	0.1	0.0	1.2	0.1	-0.1
Month 11	0.2	-4.8	0.0	0.0	-0.3	-0.6	-0.2	0.1	0.1	3.1	0.1	-2.4
Month 12	-0.7	-6.4	0.0	0.0	-0.8	-1.0	-0.6	0.4	0.2	2.7	0.4	-5.7

*highlighting indicates a difference of 2.5 kg H+/ha or more

LUC 4 – Grassland as Compared with Coniferous Forest

The differences in monthly summed deposition flux for grassland are shown in Figure 12. The trend in monthly summed deposition flux for this surface type was similar to that for a wetland/swamp cover (Figure 11). The importance of individual species and underlying conditions contributing to these differences can be understood from Table 5. Again, differences in SO_2 and NO_2 deposition accounted for most of the differences in monthly summed deposition flux.

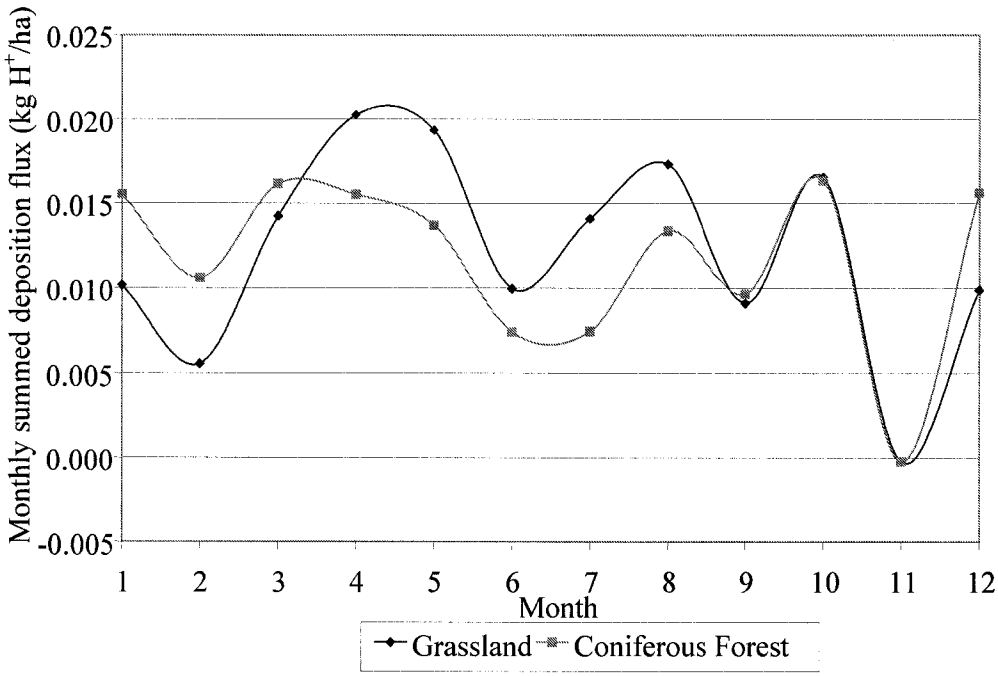

Figure 12 Comparison of monthly summed deposition flux for 11 species to grassland and coniferous forest cover using the AENV model.

Table 5 Breakdown of magnitude of differences in monthly summed deposition flux in kg H^+/ha for individual species between grassland and coniferous forest cover using the AENV model.

Month	SO_2	NO_2	HNO_2	HNO_3	SO_4^{2-}	NH_4^+	NO_3^-	Na^+	K^+	Ca^{2+}	Mg^{2+}	Total
Month 1	-0.3	-4.2	0.0	0.0	-0.7	-1.2	-0.3	0.4	0.1	0.6	0.2	-5.4
Month 2	-0.4	-4.2	0.0	0.0	-0.8	-1.0	-0.2	0.3	0.0	1.0	0.2	-5.1
Month 3	1.8	-2.5	0.0	0.0	-1.3	-1.0	-0.1	0.3	0.0	0.8	0.1	-1.9
Month 4	5.8	-2.1	0.0	0.0	-0.6	-0.8	-0.1	0.2	0.0	2.3	0.2	4.8
Month 5	6.4	-1.1	0.0	0.0	-0.4	-0.6	0.0	0.1	0.0	1.1	0.2	5.7
Month 6	2.9	-1.4	0.0	0.0	-0.5	-0.6	-0.1	0.1	0.1	1.7	0.3	2.6
Month 7	5.9	-2.0	0.0	0.0	-0.5	-0.5	-0.1	0.2	0.1	3.2	0.4	6.6
Month 8	5.1	-2.6	0.0	0.0	-0.6	-0.8	-0.1	0.2	0.1	2.2	0.4	4.0
Month 9	1.8	-2.5	0.0	0.0	-0.4	-0.6	-0.1	0.2	0.1	0.8	0.2	-0.6
Month 10	1.7	-3.0	0.0	0.0	-0.6	-0.7	-0.1	0.1	0.1	2.3	0.3	0.2
Month 11	0.0	-4.2	0.0	0.0	-0.5	-1.2	-0.4	0.3	0.1	5.8	0.3	0.0
Month 12	-0.7	-6.4	0.0	0.0	-0.8	-1.0	-0.6	0.4	0.2	2.7	0.4	-5.7

*highlighting indicates a difference of 2.5 kg H+/ha or more

LUC 5 – Cropland as Compared with Coniferous Forest

Monthly summed deposition flux for cropland has a large increase in the spring (growing) season as shown in Figure 13. It should be noted that the scale in this figure has been changed to fit the large increase associated with growing season conditions. From Table 6 which shows the differences in deposition of the individual chemicals, it can be seen that this increase is solely a result of changes (increases) in SO_2 deposition. The SO_2 deposition is very high in the spring months as a result of the use of an R_c value of 0 s/m for a dry surface wetness for the months from March through May. A low R_c value means that R_a may become the dominant resistance. Since the meteorological data used for these *LUCs* comparisons are from a coniferous forest *LUC*, the surface roughness values are far too high (around 1.0 m) whereas the typical surface roughness for a cropland would be around 0.02 to 0.1 m. Furthermore, the standard deviation of wind direction would be lower for a cropland, so using the coniferous forest meteorological data also leads to an under estimation of the surface resistance which leads to an over estimation of the deposition flux. The purpose of this comparison is to show that the AENV model does generate a higher deposition flux in the spring for a cropland *LUC* as would be expected although the actual value is amplified.

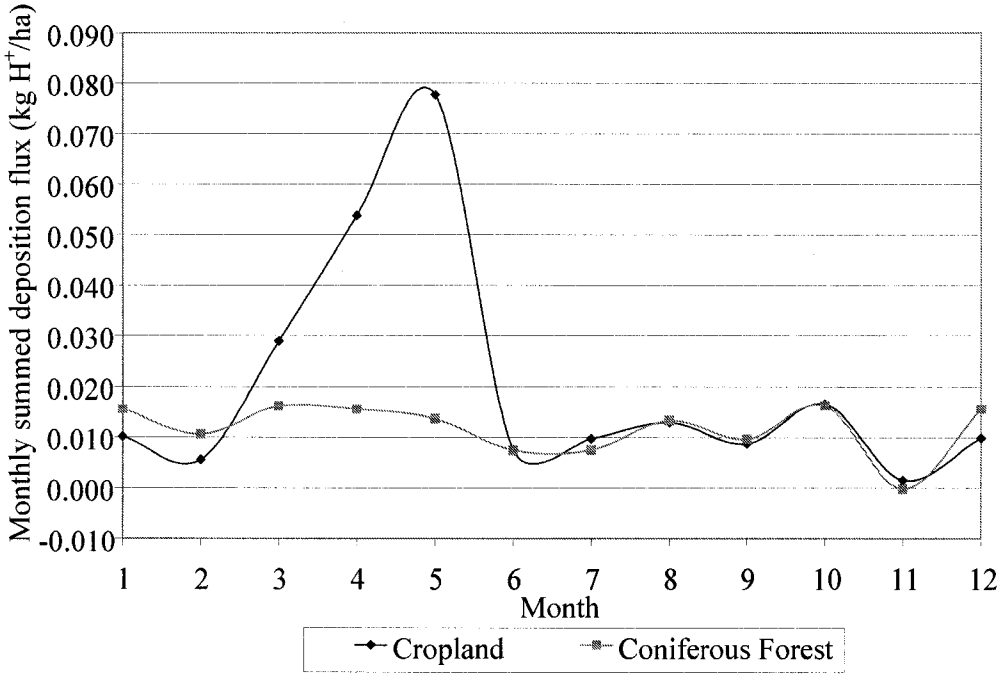

Figure 13 Comparison of monthly summed deposition flux for 11 species to cropland and coniferous forest cover using the AENV model.

Table 6 Breakdown of magnitude of differences in monthly summed deposition flux in kg H^+/ha for individual species between cropland and coniferous forest cover using the AENV model.

Month	SO_2	NO_2	HNO_2	HNO_3	SO_4^{2-}	NH_4^+	NO_3^-	Na^+	K^+	Ca^{2+}	Mg^{2+}	Total
Month 1	-0.3	-4.2	0.0	0.0	-0.7	-1.2	-0.3	0.4	0.1	0.6	0.2	-5.4
Month 2	-0.4	-4.2	0.0	0.0	-0.8	-1.0	-0.2	0.3	0.0	1.0	0.2	-5.1
Month 3	16.9	-2.5	0.0	0.0	-1.8	-1.4	-0.2	0.4	0.0	1.2	0.2	12.8
Month 4	38.8	-2.1	0.0	0.0	-0.8	-1.2	-0.2	0.3	0.1	3.1	0.2	38.2
Month 5	64.5	-1.1	0.0	0.0	-0.6	-0.8	-0.1	0.2	0.0	1.5	0.3	63.9
Month 6	1.4	-2.3	0.0	0.0	-0.5	-0.6	-0.1	0.1	0.1	1.7	0.3	0.1
Month 7	2.7	-3.3	0.0	0.0	-0.5	-0.5	-0.1	0.2	0.1	3.2	0.4	2.3
Month 8	2.4	-4.3	0.0	0.0	-0.6	-0.8	-0.1	0.2	0.1	2.2	0.4	-0.4
Month 9	1.8	-3.0	0.0	0.0	-0.6	-0.8	-0.1	0.3	0.1	1.1	0.3	-0.9
Month 10	1.7	-3.5	0.0	0.0	-0.8	-1.0	-0.1	0.2	0.1	3.3	0.4	0.3
Month 11	0.0	-4.4	0.0	0.0	-0.7	-1.7	-0.6	0.4	0.1	8.3	0.4	1.7
Month 12	-0.7	-6.4	0.0	0.0	-0.8	-1.0	-0.6	0.4	0.2	2.7	0.4	-5.7

*highlighting indicates a difference of 2.5 kg H+/ha or more

LUC 6 – Urban as Compared with Coniferous Forest

Conditions representing an urban surface resulted in similar monthly summed deposition fluxes during winter and lower values during other periods compared to a coniferous forest cover (Figure 14). The differences between the two curves are further detailed for each chemical in Table 7 in which it is shown that the differences in monthly summed deposition fluxes from March through October can be seen to be largely a result of differences in NO_2 deposition.

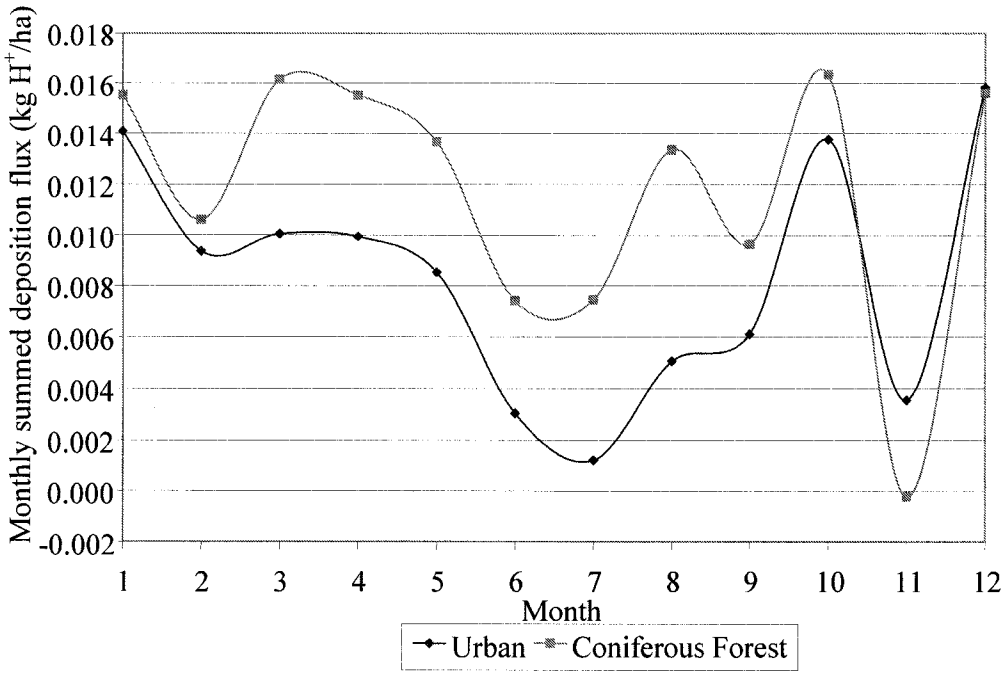

Figure 14 Comparison of monthly summed deposition flux for 11 species to urban and coniferous forest cover using the AENV model.

Table 7 Breakdown of magnitude of differences in monthly summed deposition flux in kg H^+/ha for individual species between urban and coniferous forest cover using the AENV model.

Month	SO_2	NO_2	HNO_2	HNO_3	SO_4^{2-}	NH_4^+	NO_3-	Na^+	K^+	Ca^{2+}	Mg^{2+}	Total
Month 1	-0.5	0.0	0.0	0.0	-0.8	-1.3	-0.3	0.5	0.1	0.6	0.2	-1.4
Month 2	-0.7	0.0	0.0	0.0	-0.9	-1.1	-0.2	0.3	0.0	1.0	0.2	-1.2
Month 3	-1.0	-3.3	0.0	0.0	-1.9	-1.5	-0.2	0.4	0.0	1.3	0.2	-6.1
Month 4	-1.7	-5.5	0.0	0.0	-0.9	-1.3	-0.2	0.3	0.1	3.4	0.2	-5.6
Month 5	-1.5	-4.3	0.0	0.0	-0.7	-0.8	-0.1	0.2	0.1	1.6	0.3	-5.1
Month 6	-1.3	-3.6	0.0	0.0	-0.2	-0.3	0.0	0.0	0.0	0.9	0.1	-4.4
Month 7	-2.6	-5.1	0.0	0.0	-0.2	-0.3	-0.1	0.1	0.1	1.6	0.2	-6.2
Month 8	-2.4	-6.6	0.0	0.0	-0.3	-0.4	0.0	0.1	0.0	1.1	0.2	-8.3
Month 9	-0.3	-3.5	0.0	0.0	-0.6	-0.7	-0.1	0.2	0.1	1.0	0.3	-3.5
Month 10	-0.5	-4.0	0.0	0.0	-0.7	-0.8	-0.1	0.2	0.1	2.9	0.3	-2.6
Month 11	-0.3	-1.4	0.0	0.0	-0.7	-1.5	-0.6	0.3	0.1	7.4	0.4	3.8
Month 12	-1.2	0.0	0.0	0.0	-0.8	-1.1	-0.6	0.4	0.2	2.9	0.4	0.2

*highlighting indicates a difference of 2.5 kg H+/ha or more

LUC 7 – Water as Compared with Coniferous Forest

As shown in Figure 15, water has the capacity to receive much greater acid input than a coniferous forest cover. The differences between the two curves are further detailed for each chemical in Table 8 in which it is shown that the differences are largely a result of differences in deposition of SO_2, NO_2, SO_4^{2-}, NH_4^+, NO_3^-, Na^+, Ca^{2+}, and Mg^{2+}. The peaks in March and May are the result of SO_2 and SO_4^{2-} deposition. The trough in November is the result of Ca^{2+} deposition. In general, water is far more susceptible to SO_2 deposition and less susceptible to NO_2 deposition than is a coniferous forest surface. Small particle deposition (SO_4^{2-}, NH_4^+) and large particle deposition (NO_3^-, Na^+, K^+, Ca^{2+}, and Mg^{2+}) is characteristically found to be much higher over water as compared to a coniferous forest cover. Because water has little or no resistance to SO_2 or particle deposition, total deposition is largely dependent on the atmospheric concentration of these species and the peaks are for months in when the concentrations of these chemicals are highest.

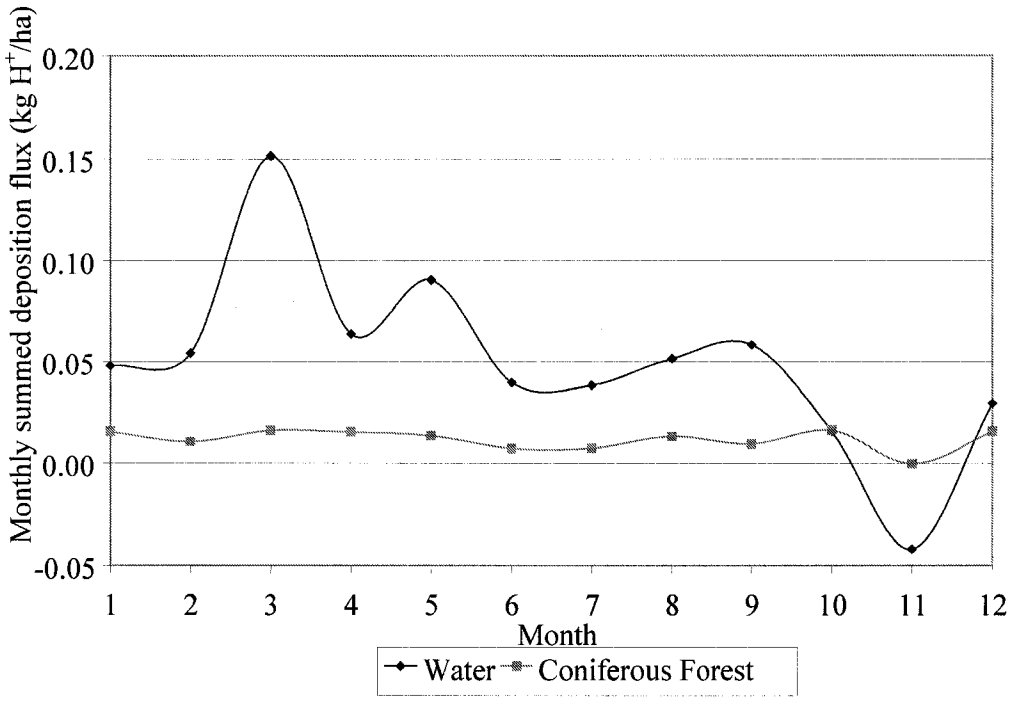

Figure 15 Comparison of monthly summed deposition flux for 11 species to water and coniferous forest cover using the AENV model.

Table 8 Breakdown of magnitude of differences in monthly summed deposition flux in kg H^+/ha for individual species between water and coniferous forest cover using the AENV model.

Month	SO_2	NO_2	HNO_2	HNO_3	SO_4^{2-}	NH_4^+	NO_3-	Na^+	K^+	Ca^{2+}	Mg^{2+}	Total
Month 1	15.1	-4.6	0.0	0.0	12.7	21.0	3.1	-5.0	-1.1	-6.6	-2.3	32.4
Month 2	25.3	-4.5	0.0	0.0	16.4	20.8	1.8	-3.3	-0.3	-10.4	-2.3	43.7
Month 3	40.6	-6.3	0.0	0.0	75.5	61.2	4.1	-8.0	-0.6	-27.1	-4.2	135.3
Month 4	52.2	-8.6	0.0	0.0	22.4	32.0	2.2	-3.8	-0.7	-44.6	-3.0	48.2
Month 5	64.6	-6.1	0.0	0.0	30.5	37.8	1.6	-4.1	-1.2	-38.9	-7.1	77.0
Month 6	42.2	-4.7	0.0	0.0	16.5	20.0	1.2	-1.4	-1.4	-34.1	-5.9	32.4
Month 7	75.8	-6.5	0.0	0.0	14.2	17.5	1.8	-2.8	-2.1	-58.9	-8.0	31.0
Month 8	52.7	-8.6	0.0	0.0	19.0	23.6	1.4	-2.7	-1.3	-38.0	-7.8	38.3
Month 9	39.5	-5.1	0.0	0.0	22.2	29.1	1.5	-5.6	-1.7	-24.6	-6.7	48.7
Month 10	19.2	-6.0	0.0	0.0	23.3	27.9	1.5	-3.0	-1.1	-56.1	-6.2	-0.5
Month 11	9.4	-5.5	0.0	0.0	12.4	30.0	6.1	-3.9	-1.4	-85.1	-3.8	-41.9
Month 12	25.5	-6.9	0.0	0.0	7.3	9.2	2.8	-2.1	-1.1	-18.5	-2.3	13.8

*highlighting indicates a difference of 2.5 kg H+/ha or more

LUC 8 – Snow/Ice as Compared with Coniferous Forest

In the AENV model, the snow and ice covers are only done for the winter months because of the seasonal categorization system. For a snow/ice-covered surface, the months of January and February are repeated at the end of the year in Figure 16 to allow for continuity of the data. Snow/ice cover results in lower monthly summed deposition fluxes compared to a coniferous forest cover. The differences between the two curves are further detailed for each chemical in Table 9 in which it is shown that these differences are largely driven by SO_2, NO_2, and small particle deposition.

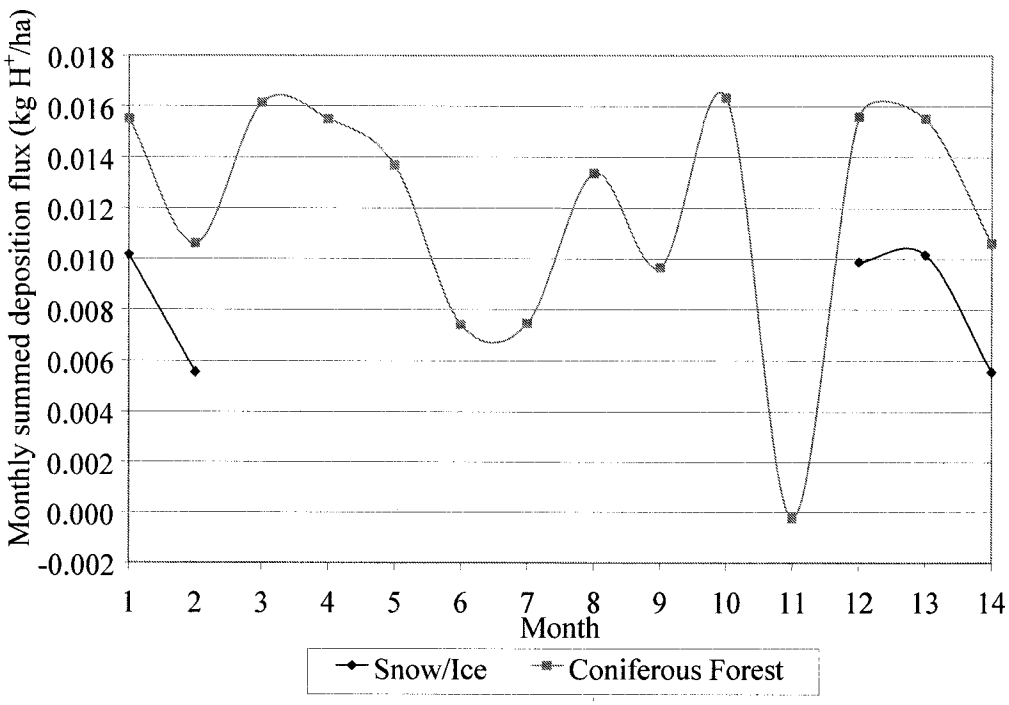

Figure 16 Comparison of monthly summed deposition flux for 11 species to snow/ice and coniferous forest cover using the AENV model.

Table 9 Breakdown of magnitude of differences in monthly summed deposition flux in kg H^+/ha for individual species between snow/ice and coniferous forest cover using the AENV model.

Month	SO_2	NO_2	HNO_2	HNO_3	SO_4^{2-}	NH_4^+	NO_3-	Na^+	K^+	Ca^{2+}	Mg^{2+}	Total
Month 1	-0.3	-4.2	0.0	0.0	-0.7	-1.2	-0.3	0.4	0.1	0.6	0.2	-5.4
Month 2	-0.4	-4.2	0.0	0.0	-0.8	-1.0	-0.2	0.3	0.0	1.0	0.2	-5.1
Month 3												
Month 4												
Month 5												
Month 6												
Month 7												
Month 8												
Month 9												
Month 10												
Month 11												
Month 12	-0.7	-6.4	0.0	0.0	-0.8	-1.0	-0.6	0.4	0.2	2.7	0.4	-5.7

*highlighting indicates a difference of 2.5 kg H+/ha or more

4.4.2 Resistance Factors and Deposition Velocities

Aerodynamic resistance (R_a) is dependent on meteorological conditions and independent of deposition species for all *LUCs* in the AENV model. Calculation of Boundary layer resistance (R_b) for gases is dependent on meteorological conditions and individual species and independent of surface (*i.e. LUC*); consequently, there are no differences in R_b values from one *LUC* to another for individual species. Finally, surface (canopy) resistance is dependent upon individual species and surface type. Given that the meteorological data is the same for all runs, the differences in the results for the different *LUCs* can all be attributed to the different R_c values that are generated for the different *LUCs*. Specifically separating out the differences between the R_c values for the three major species for the coniferous forest *LUC* and the other seven *LUCs* allows further understanding of the differences in the previous comparisons of the deposition fluxes.

4.4.2.1 Gaseous Deposition (SO_2, NO_2, HNO_3)

Surface Layer Resistance (R_c) for SO_2

The calculation of R_c for SO_2 is done from tabular values which are given in Table B3 (Appendix B) which are categorized based on *LUC*, season, and wetness conditions. The determination of whether a wetness condition is either wet or dry depends on surface wetness measurements combined with relative humidity measurements as shown in Appendix B. For the input meteorological data set used in this study, the absence of surface wetness data resulted in the wetness condition depending upon whether the relative humidity was above or below 87%. Seasons are classified as winter (December to February), spring (March to May), summer (June to August), and autumn (September to November). The exception to this season designation is that if the temperature for any hour is below 0°C during any season, then R_c for that hour is represented by the corresponding wet/dry value for winter for that species.

***LUC* 1 – Deciduous Forest**

Monthly average R_c values for a deciduous forest surface cover (shown in Figure 17) are higher in winter and early spring/late autumn than those for a coniferous forest surface cover. This would be expected due to an absence of leaves during these periods. Monthly average R_c values for both covers are similar during the leafy season (June, July, August).

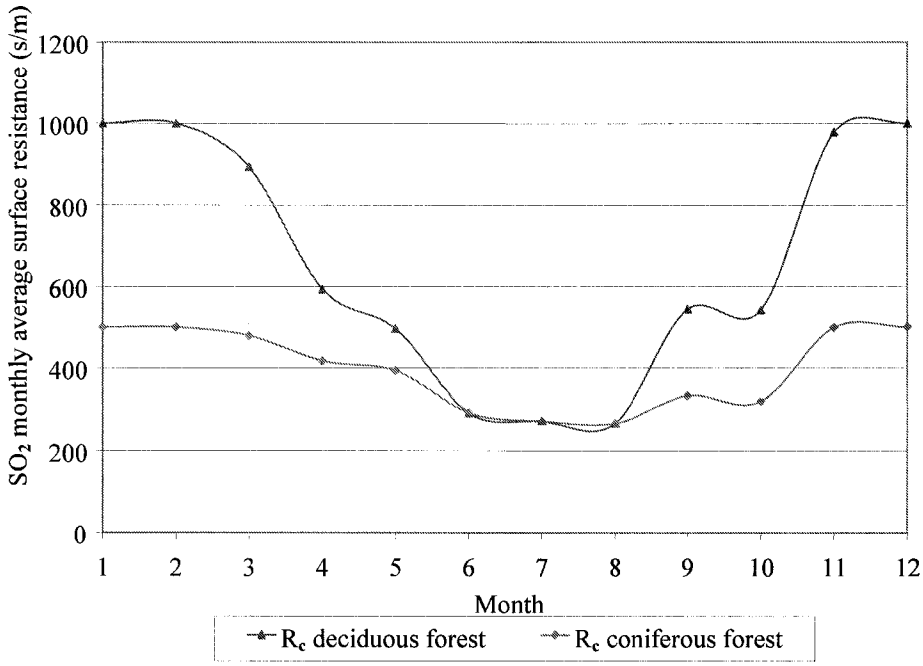

Figure 17 Comparison of SO_2 monthly average surface resistance (R_c) for a deciduous forest and coniferous forest (base case) cover using the AENV model.

LUC 3, 4, and 5 – Wetland/Swamp, Grassland, and Cropland

Monthly average R_c values for wetlands/swamp (Figure 18), grassland (Figure 19), and cropland (Figure 20) are all similar because of the nature of the growing season of vegetation representing these cover types in Alberta. Monthly average R_c values are the same for all three *LUCs* for the winter season, and they are all greater in winter compared to that for a coniferous forest cover which maintains more of its leaves (needles) during winter. During spring and summer months, monthly average R_c values for a wetland/swamp become much lower than those of the coniferous forest cover because of the growing season and the lushness of the vegetation.

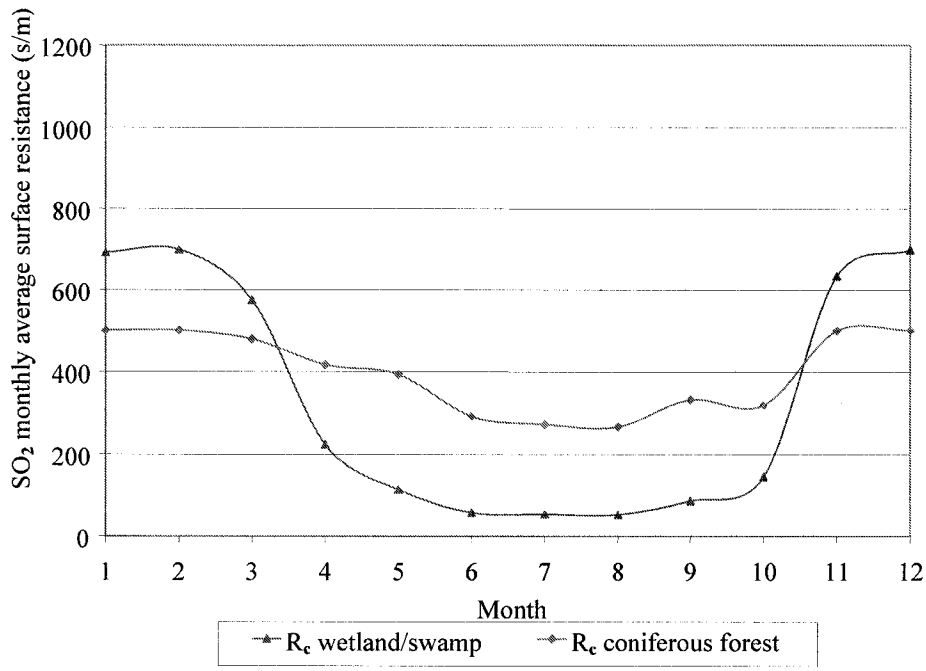

Figure 18 Comparison of SO_2 monthly average surface resistance (R_c) for wetland/swamp and coniferous forest (base case) cover using the AENV model.

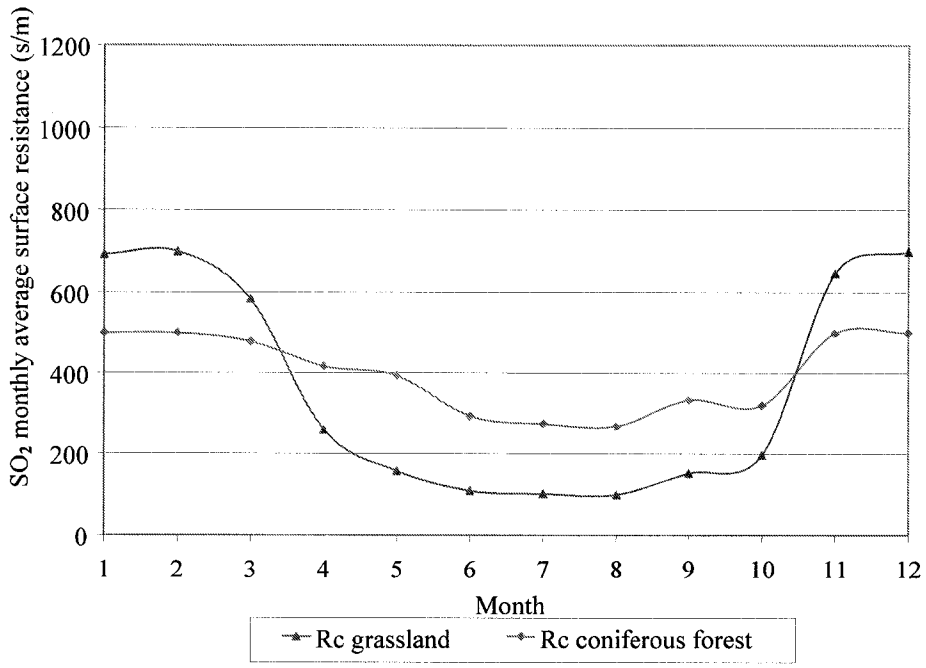

Figure 19 Comparison of SO_2 monthly average surface resistance (R_c) for a grassland and coniferous forest (base case) cover using the AENV model.

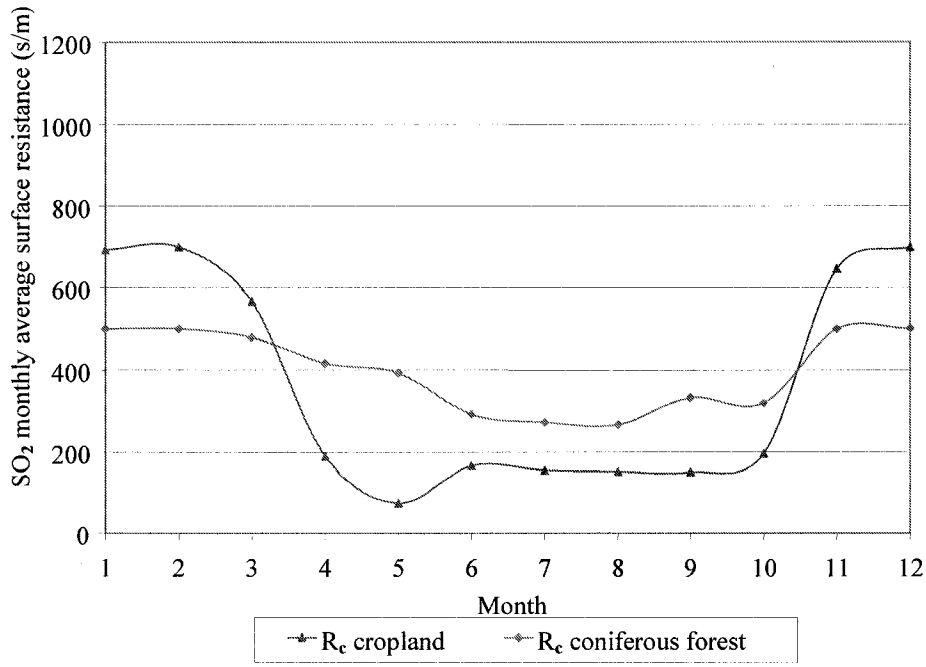

Figure 20 Comparison of SO_2 monthly average surface resistance (R_c) for a cropland and coniferous forest (base case) cover using the AENV model.

LUC 6 – Urban

Monthly average R_c values for urban land (shown in Figure 21) are higher than those for a coniferous forest cover. These higher values may be a result of the presence of building and road surfaces which are not as interactive with atmospheric SO_2 as is vegetation. The declining resistance as summer progresses to autumn is mostly attributed to the increasing relative humidity which is illustrated in Table 10. The tabular resistance values for wet conditions are lower than those for dry conditions, so a decreasing resistance can be caused by more frequent wet conditions.

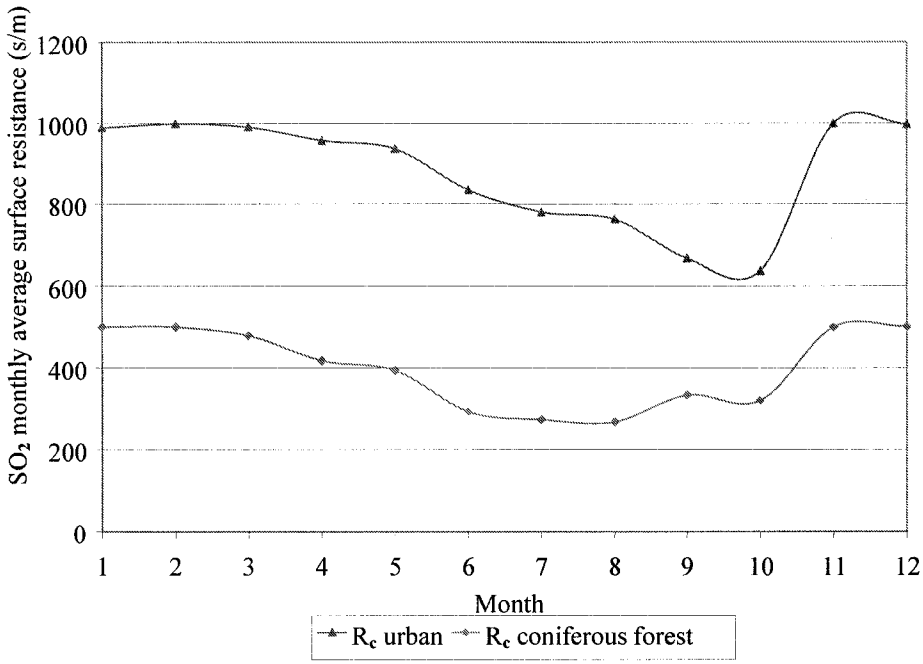

Figure 21 Comparison of SO_2 monthly average surface resistance (R_c) for urban and coniferous forest (base case) cover using the AENV model.

Table 10 Monthly average relative humidity level (%) for data used to evaluate AENV model.

month	Average
Month 1	69.2
Month 2	68.3
Month 3	63.3
Month 4	53.7
Month 5	55.5
Month 6	61.9
Month 7	67.1
Month 8	68.0
Month 9	75.4
Month 10	78.6
Month 11	73.6
Month 12	77.1

LUC 7 – Water

Monthly average R_c values for water are constant and set at zero throughout a year (Figure 24).

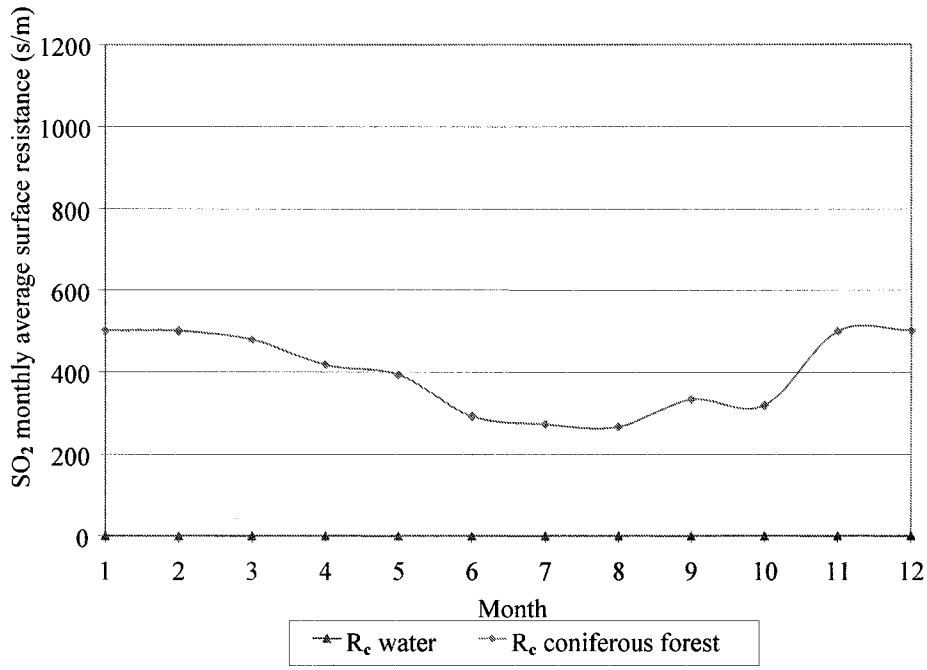

Figure 22 Comparison of SO_2 monthly average surface resistance (R_c) for a water and coniferous forest (base case) cover using the AENV model.

LUC 8 – Snow/Ice

Monthly average R_c values for a snow/ice cover are shown in Figure 23. These values are similar as those for a snow-covered grassland, cropland, or wetland/swamp surface.

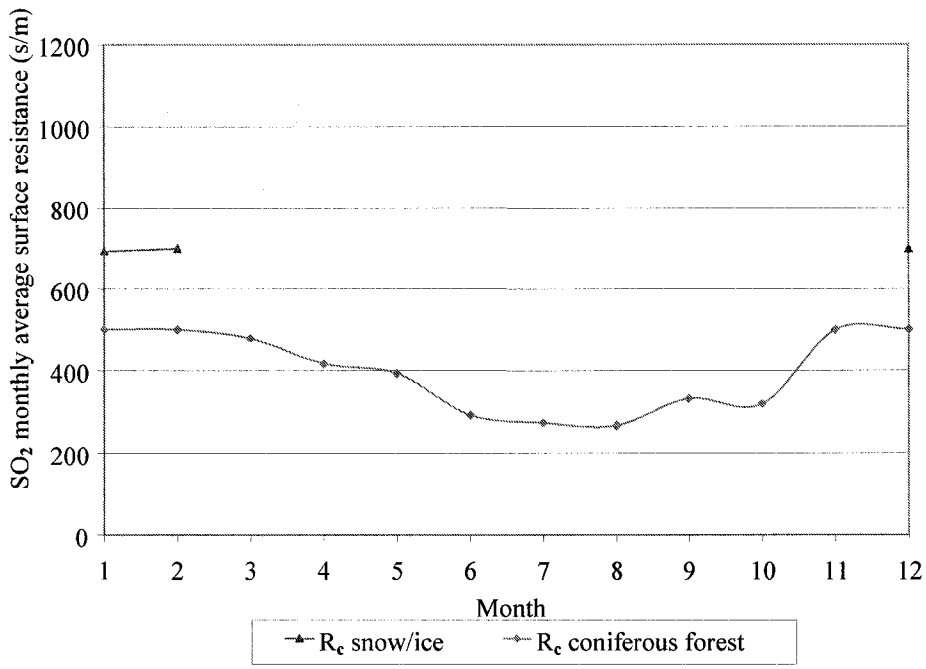

Figure 23 Comparison of SO_2 monthly average surface resistance (R_c) for snow/ice and coniferous forest (base case) cover using the AENV model.

Surface Layer Resistance (R_c) for NO_2

Similar to SO_2, R_c for NO_2 is dependent upon *LUC*, season, and wetness condition. Again, the wetness condition used in this study depended on whether relative humidity was above 87%. The relationships between monthly average R_c values for NO_2 for different land uses are shown in Figure 24 to 30. The relationships for monthly average R_c values for NO_2 were similar to those for SO_2 except that values for NO_2 were generally much higher. Monthly average R_c values for NO_2 are more sensitive to differences between wet and dry conditions as compared to SO_2. Increases in monthly average R_c values for NO_2 across spring and summer months generally observed for all surface types reflects increasing relative humidity (as shown in Table 10). Even though November is classified as an autumn month, the presence of numerous hourly temperatures less than 0°C results in November behaving as a winter month.

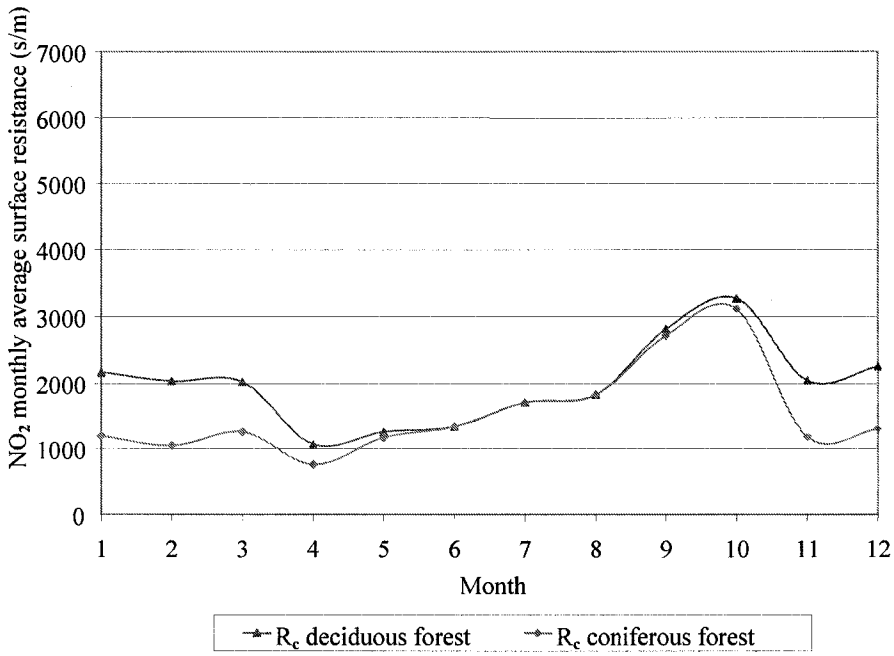

Figure 24 Comparison of NO_2 monthly average surface resistance (R_c) for deciduous forest and coniferous forest (base case) cover using the AENV model.

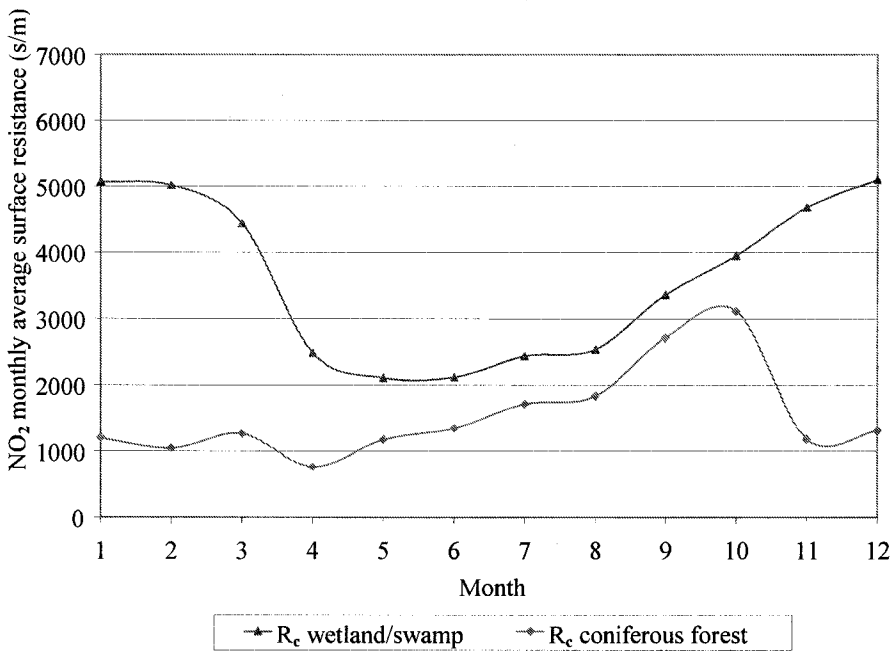

Figure 25 Comparison of NO_2 monthly average surface resistance (R_c) for wetland/swamp and coniferous forest (base case) cover using the AENV model.

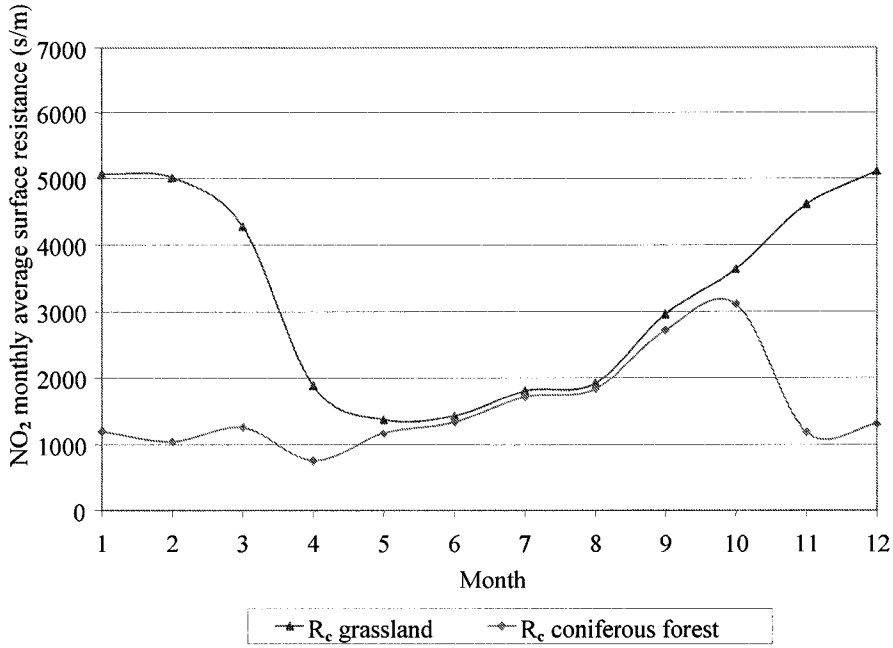

Figure 26 Comparison of NO_2 monthly average surface resistance (R_c) for grassland and coniferous forest (base case) cover using the AENV model.

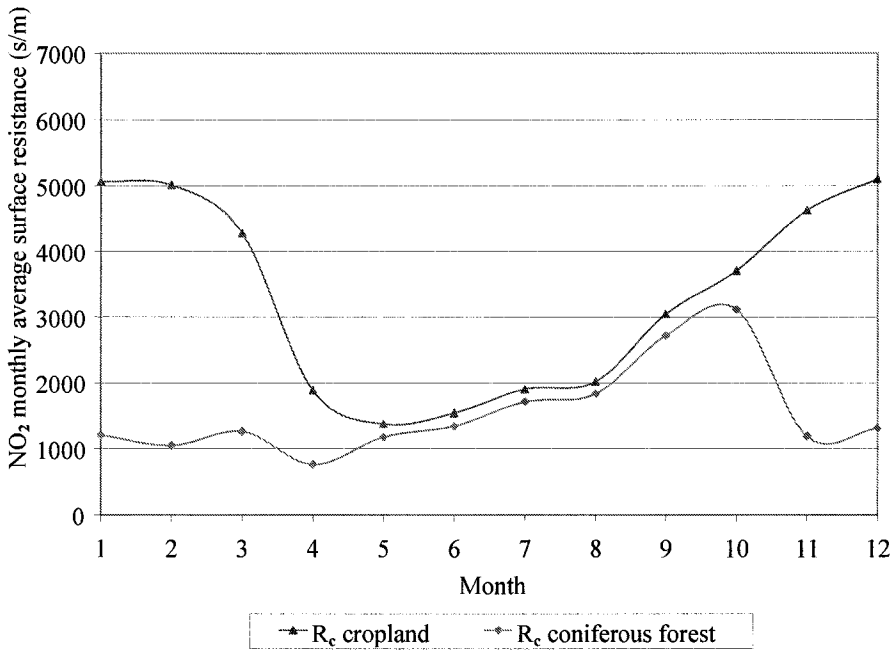

Figure 27 Comparison of NO_2 monthly average surface resistance (R_c) for cropland and coniferous forest (base case) cover using the AENV model.

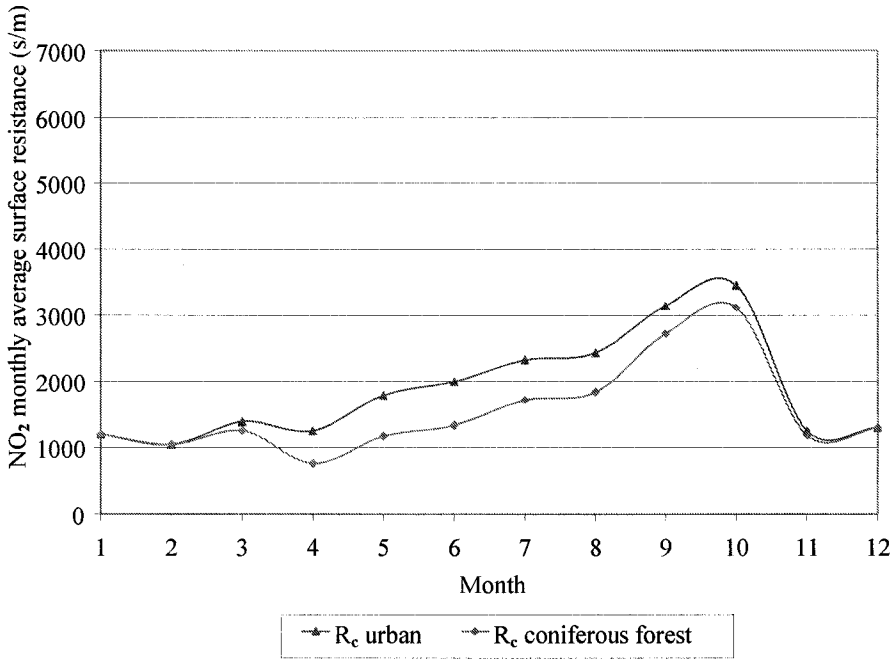

Figure 28 Comparison of NO_2 monthly average surface resistance (R_c) for urban and coniferous forest (base case) cover using the AENV model.

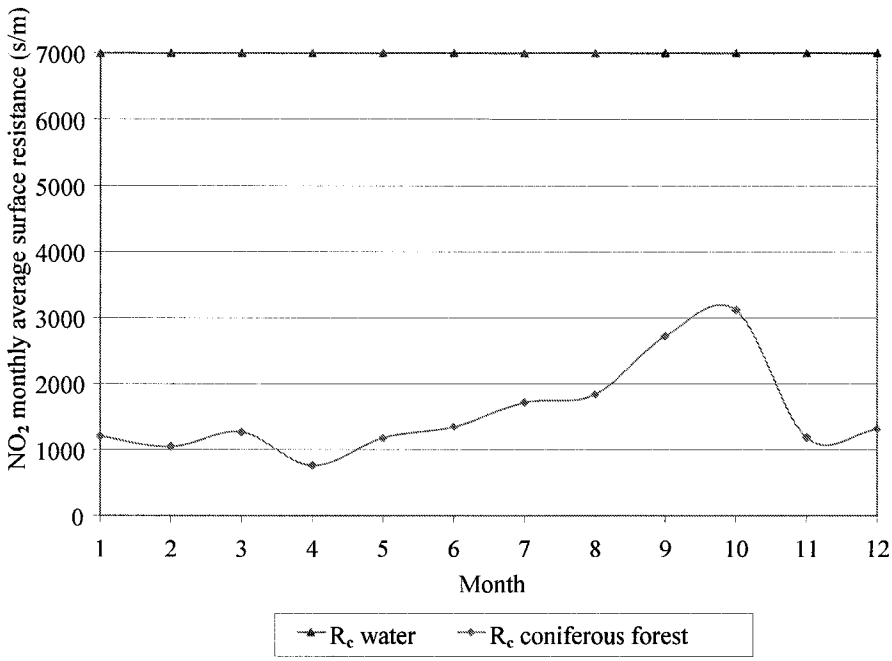

Figure 29 Comparison of NO_2 monthly average surface resistance (R_c) for water and coniferous forest (base case) cover using the AENV model.

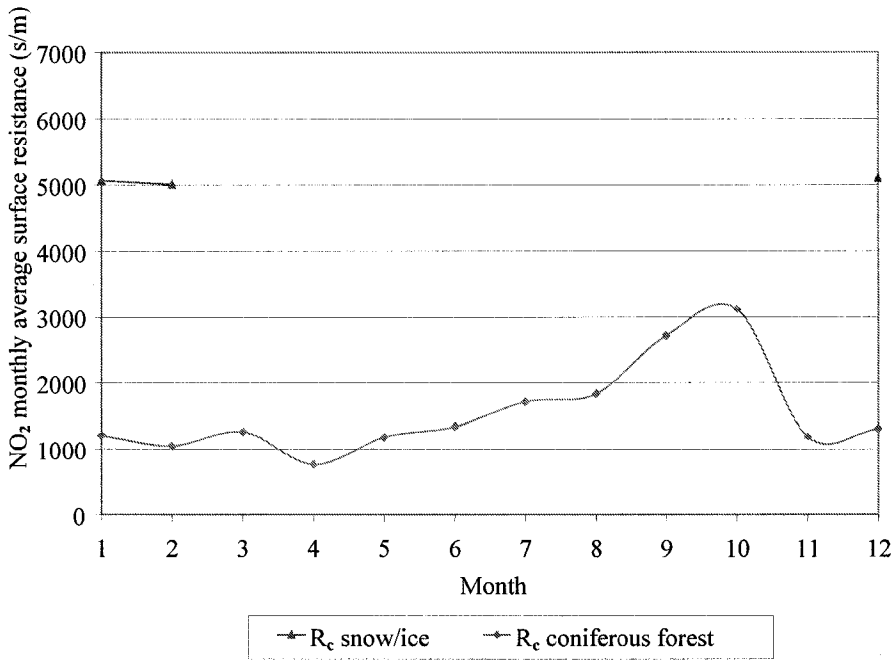

Figure 30 Comparison of NO_2 monthly average surface resistance (R_c) for snow/ice and coniferous forest (base case) cover using the AENV model.

Surface Layer Resistance (R_c) for HNO_3

Values for HNO_3 surface resistance (R_c) are treated as a constant (10 s/m) for all seasons and all surface types.

4.4.2.2 Fine and Coarse Particle Deposition (SO_4^{2-}, NH_4^+, NO_3^-, Na^+, K^+, Ca^{2+}, Mg^{2+})

The AENV model classifies fine (small) particle species as SO_4^{2-} and NH_4^+ and course (large) particle species as NO_3^-, Na^+, K^+, Ca^{2+}, and Mg^{2+}. As stated previously, particle species deposition behavior is mostly dominated by aerodynamic resistance (R_a) which is based on the aerodynamic properties (diameter) of the particles and is independent of the individual species. Boundary layer resistance (R_b) is treated as being constant within a season and within a *LUC*. Surface (canopy) resistance (R_c) is treated as being negligible for particulate ions and is always zero. Therefore, deposition velocity

for particles is modeled as the inverse of the sum of R_a and R_b (Appendix B). Since it is not informative to examine R_a or R_b independently, deposition velocity for particles for the different *LUCs* was compared.

Deciduous forest cover versus coniferous forest cover (base case)

In summer, monthly average deposition velocities for small and large particles for a deciduous forest cover are higher than those for a coniferous forest cover (base case) as shown Figure 31.

Wetland/swamp versus coniferous forest cover

In Figure 32, it can be seen that monthly average small and large particle deposition velocities are lower for wetland/swamp compared to a coniferous forest cover (base case).

Grassland versus coniferous forest cover

In Figure 33, small and large particle deposition velocities are even lower than those for wetland/swamp.

Cropland versus coniferous forest cover

In Figure 34, a summer peak remains at the same level as that for grassland, however spring and autumn deposition velocities are clearly lower.

Urban surface versus coniferous forest cover

In Figure 35, a summer peak is similar and higher compared to cropland and the spring and autumn deposition velocities are lower.

Water versus coniferous forest cover

In Figure 36, R_b and R_c values for water are 0 s/cm so deposition velocities are determined by R_a values and are very high. Values for both small and large particle deposition velocities are the same such that the small particle line is entirely hidden under the large particle line.

Snow/ice versus coniferous forest cover

In Figure 37, deposition velocities are low and similar to those of a wetland/swamp, grassland, or cropland surface.

Tables summarizing all the monthly values used for plotting Figures 31 to 37 for the eight *LUCs* are included in Appendix D.

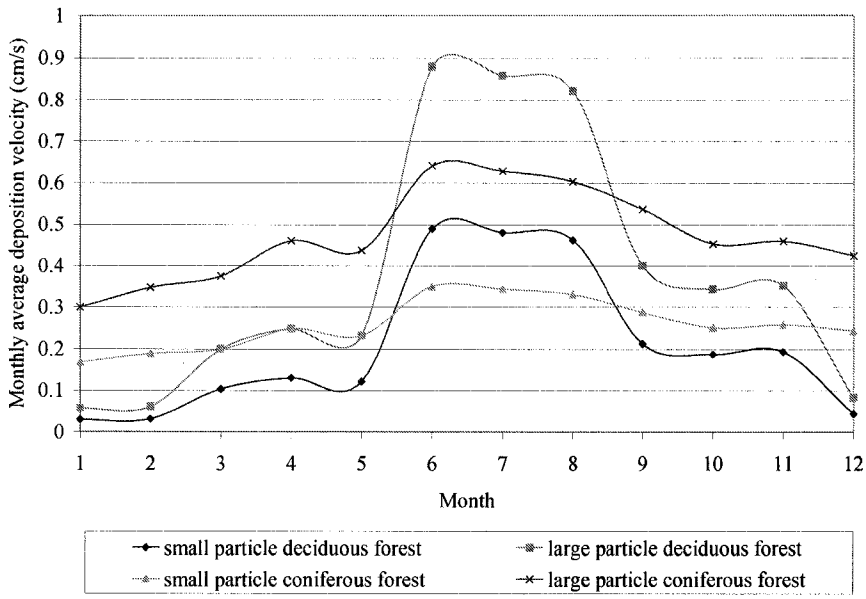

Figure 31 Comparison of monthly average deposition velocity of small and large particles for a deciduous forest and coniferous forest (base case) cover using the AENV model.

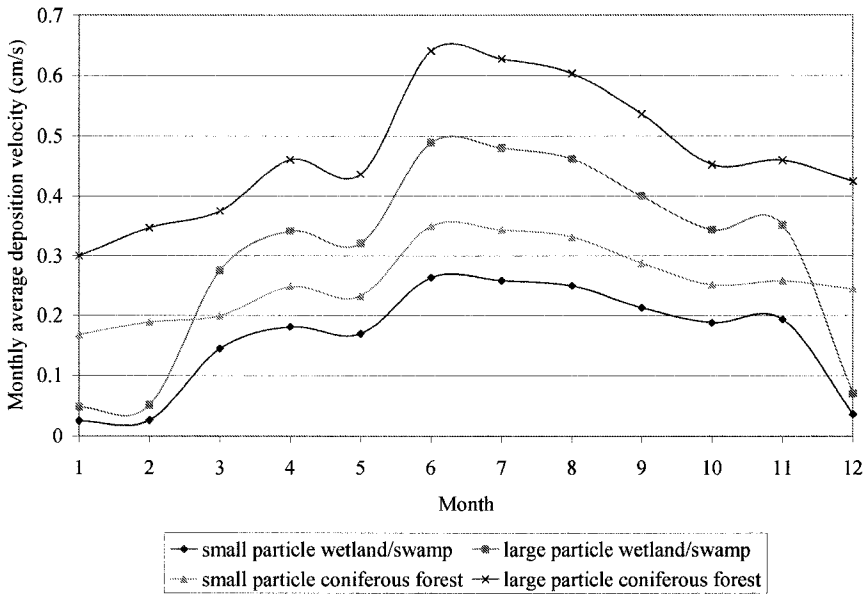

Figure 32 Comparison of monthly average deposition velocity of small and large particles for a wetland/swamp and coniferous forest (base case) cover using the AENV model.

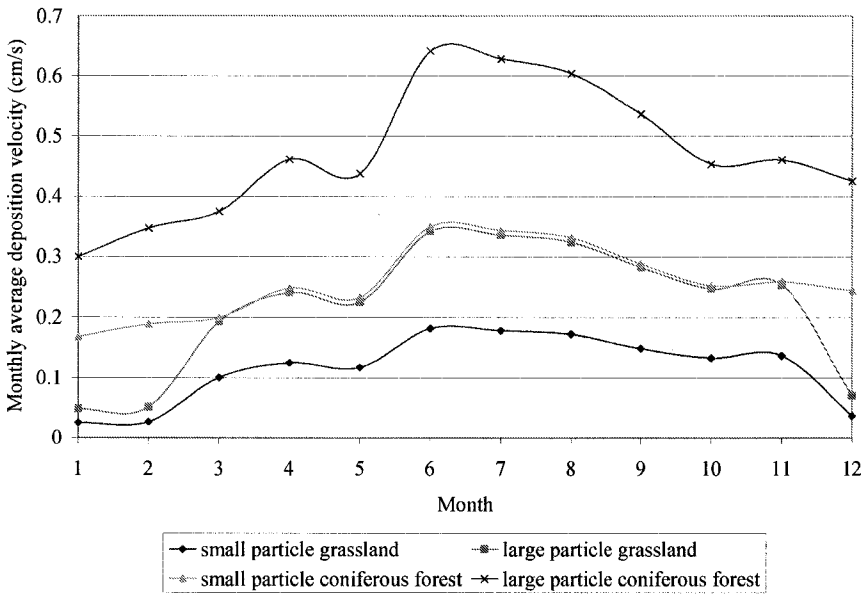

Figure 33 Comparison of monthly average deposition velocity of small and large particles for grassland and coniferous forest (base case) cover using the AENV model.

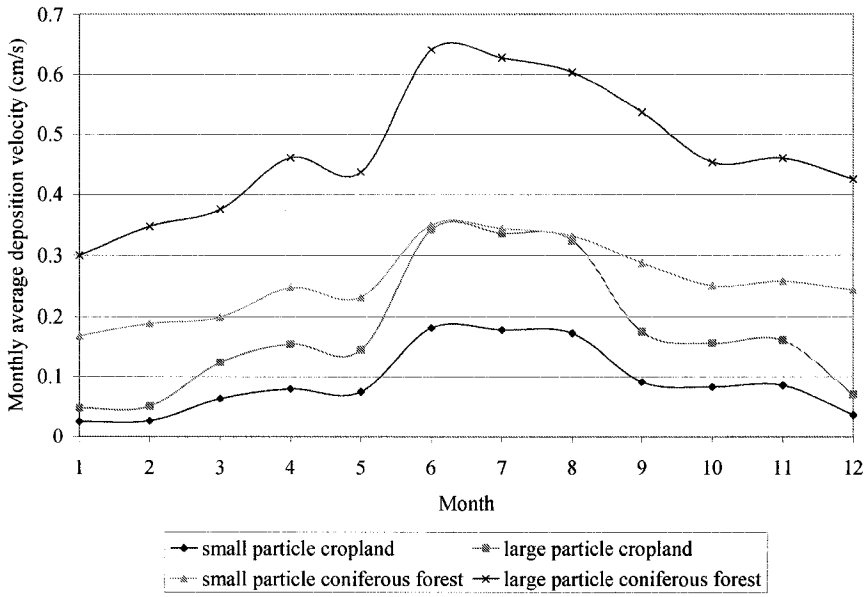

Figure 34 Comparison of monthly average deposition velocity of small and large particles for cropland and coniferous forest (base case) cover using the AENV model.

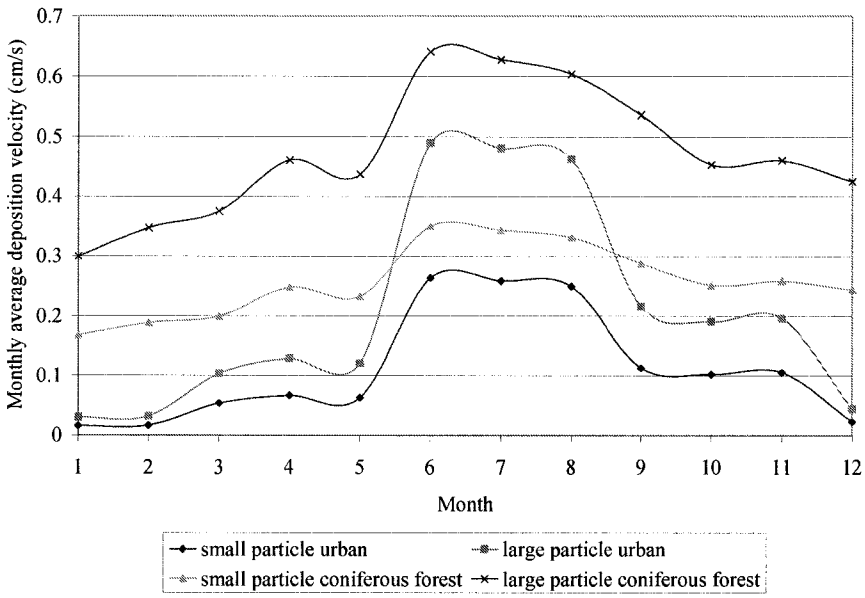

Figure 35 Comparison of monthly average deposition velocity of small and large particles for urban and coniferous forest (base case) cover using the AENV model.

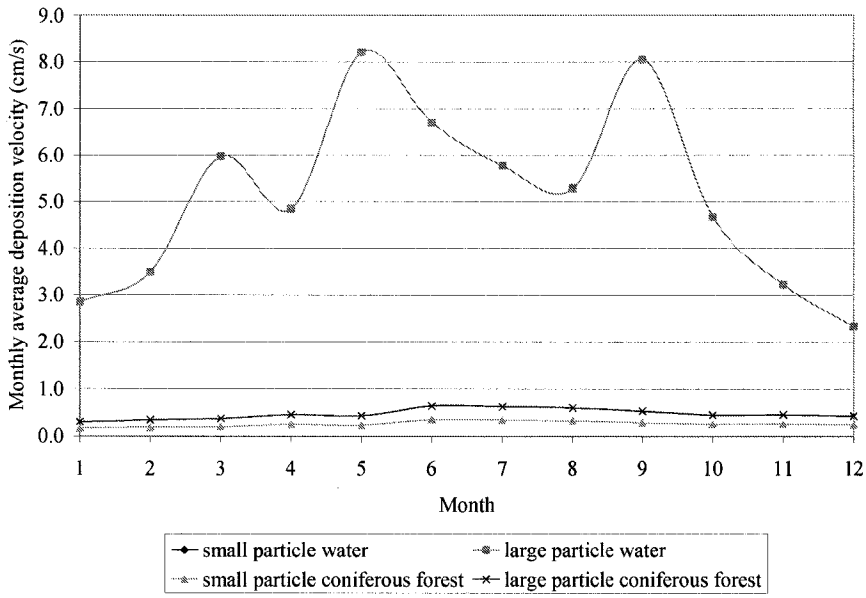

Figure 36 Comparison of monthly average deposition velocity of small and large particles for water and coniferous forest (base case) cover using the AENV model.

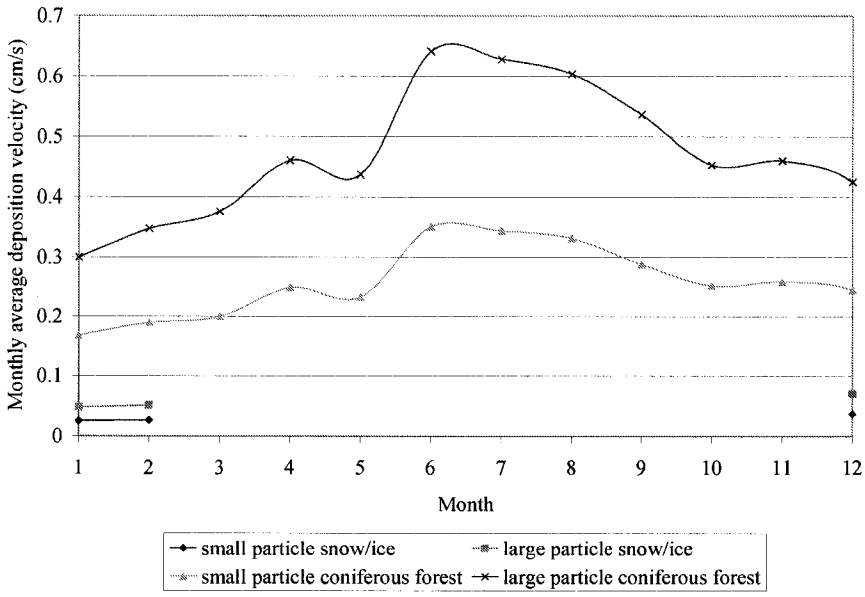

Figure 37 Comparison of monthly average deposition velocity of small and large particles for snow/ice and coniferous forest (base case) cover using the AENV model.

5 Model Evaluation

5.1 Resistance Factors

5.1.1 Evaluation Methods

Deposition velocity (V_d) is calculated on an hourly basis as the inverse of the sum of three resistances ($R_a + R_b + R_c$). Because resistances are added before the sum is inverted, the resistance with the largest magnitude of the three will dominate the determination of the deposition velocity; therefore, influence of the largest resistance factor is the most important in terms of deposition velocity.

Two methods were used to analyze the behavior of the three resistance factors derived in the AENV model. In the first method, total resistance (s/m) results for each hour for the three most important depositing acidic species (SO_2, NO_2, and HNO_3) derived from both models were divided into the following ranges:

i) less than 10 s/m,

ii) 10 to 100 s/m,

iii) 100 to 300 s/m,

iv) 300 to 1000 s/m, and

v) greater than 1000 s/m.

Within each range, the number of times that each of the three resistances was largest (or dominant) was counted. For HNO_3, size ranges less than 100 s/m were further broken down and similarly analyzed. These counts are summarized in Appendix E.

In the second method, a form of sensitivity analysis was conducted on the AENV model by separately increasing and decreasing each of the three resistances by a magnitude of 10% and 50% and observing the resulting changes in monthly summed deposition flux which included all 11 species.

5.1.2 Results

5.1.2.1 Dominant (Influential) Resistance Factors

The number of hourly occurrences in which each of the individual resistances was the dominant resistance was counted for SO_2, NO_2, and HNO_3 for each model and complete results are presented in Appendix E.

SO_2

For SO_2 in the ENVC model, R_c dominated in every instance. In the AENV model, R_c usually dominated; but, there were instances when R_a and R_b dominated. For example, in the AENV model, for SO_2 deposition in October, there were 96 occurrences in which total resistance was between 10 and 100 s/m. Of these 96, R_a was dominant 20 times, R_b was dominant in 28, and R_c was dominant in 48. In contrast, for the ENVC model for this month, there were only 12 occurrences in which total resistance was between 10 and 100 s/m and all of which were R_c dominated. This difference suggests that AENV's approach for representing R_c produces lower values than does the ENVC model. A lower dominant resistance value leads to a higher deposition velocity value that leads to a higher deposition value. The end result of these lower R_c values is therefore a higher deposition velocity predicted by the AENV model as compared with that predicted by the ENVC model. In this case, the AENV model would be a more conservative estimator of acid deposition.

In January, there were no occurrences in which total resistance was less than 300 s/m for the AENV model, but there were 71 occurrences in the ENVC in which total resistance was less than 300 s/m (three of which were between 10 s/m and 100). Again, this difference suggests that the AENV approach for representing R_c values has a tendency to predict higher deposition velocities as compared to the ENVC approach for January conditions and in the winter months (December through February). In this case, the AENV model would be a more conservative estimator of acid deposition. Unique to the AENV model was that R_b was observed to be dominant in several instances in summer and autumn months.

NO_2

For NO_2, R_c dominated in every instance for the ENVC model for all ranges presented. In the AENV model, R_c was typically observed to dominate, but there were instances where R_a dominated. This difference suggests that AENV's approach for representing R_c values for NO_2 has a tendency to predict lower acid deposition velocities as compared to the ENVC approach. In this case, the AENV model would be a less conservative estimator of acid deposition. In spring and summer months, there was a greater occurrence of smaller total resistance values in the AENV model than in the ENVC model (Appendix E). This difference suggests that, again, AENV's approach for representing R_c values for NO_2 has a tendency to predict lower deposition velocities as compared to the ENVC approach spring and summer months. In this case, the AENV model would be a less conservative estimator of acid deposition.

HNO_3

For HNO_3, R_c dominated in most instances in the ENVC model, but there were instances in which R_a or R_b was more dominant (Appendix E). In the AENV model, R_b dominated most often, followed by R_a and then R_c (Appendix E).

The lowest total resistance range (10 to 100 s/m) was separated into smaller sections as shown in Appendix E to allow for a more detailed comparison of the two models. In the 15 to 25 s/m range, R_c was always the dominant resistance for both models, but there were far more occurrences when this was the case for the AENV model than for the ENVC model. In the 25 to 100 s/m range, R_b was the most common resistance factor that dominated in the AENV model; while R_c was the most common resistance factor that dominated in the ENVC model. These differences suggest that AENV's approach for representing R_c values for HNO_3 has a tendency to predict lower acid deposition velocities compared to the ENVC approach spring and summer months. In this case, the AENV model would be a less conservative estimator of acid deposition.

5.1.2.2 Sensitivity Testing of Resistance Factors

The other method to examine the relative importance of the three resistances was to check the influence of increasing and decreasing of magnitude of each of the resistances on monthly summed deposition flux. The original purpose of this analysis was to generally determine the effect of errors in the tabular values used for determining the resistances.

Percent Change in R_a

The influence of a ten and fifty percent change (increase and decrease) in R_a on monthly summed deposition flux (kg H^+/ha) is shown in Figure 38. The months that were most influenced by the change in R_a were January, April, October, and December. The most important species that were responsible for these changes were HNO_2 (December) and HNO_3 (January, April, and October). Details of deposition quantities for these two species are tabulated in Appendix F.

Percent Change in R_b

The influence of a ten and fifty percent change (increase and decrease) in R_b on monthly summed deposition flux is shown in Figure 39. The months that were most influenced by the change in R_b were January, February, March, July, and November. A change in R_b values has more impact on total deposition than does an equivalent percent change in R_a, but not necessarily in the same months. The most important species that were responsible for changes were HNO_3 (January and October), SO_4^{2-} (March), NH_4^+ (March), and Ca^{2+} (July and November). The changes observed in February were caused by an absence of the neutralizing effect of calcium. Details of the deposition quantities for these species are tabulated in Appendix F.

Percent Change in R_c

The influence of a ten and fifty percent change (increase and decrease) in R_c on monthly summed deposition flux is shown in Figure 40. Figure 40, when compared with Figures 38 and 39 shows that similar step changes in the magnitude of R_c are much more important in influencing total deposition than step changes in either R_a or R_b. The

influence of changes in R_c is independent of month of the year although April and August had the greatest changes. The increased deposition flux associated with the reduced R_c indicates that R_a and R_b are unable to dominate the sum of resistances. The most important species that were responsible for changes were SO_2 (April, July, and August) and NO_2 (April, August, and December). Details of the deposition quantities for these two species are tabulated in Appendix F.

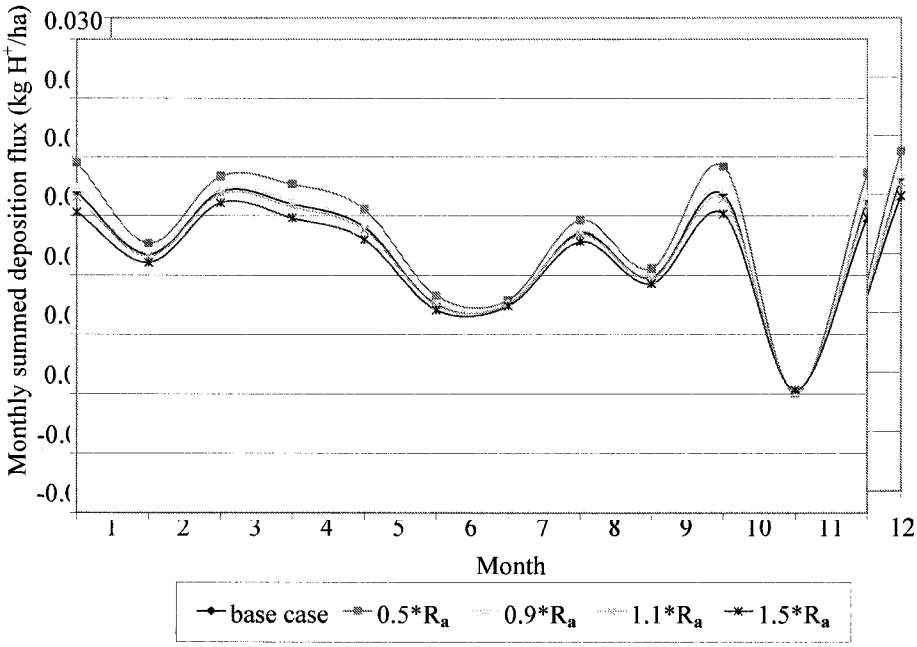

Figure 38 Monthly summed deposition flux for 11 species using AENV model showing influence of step changes in R_a for a coniferous forest cover.

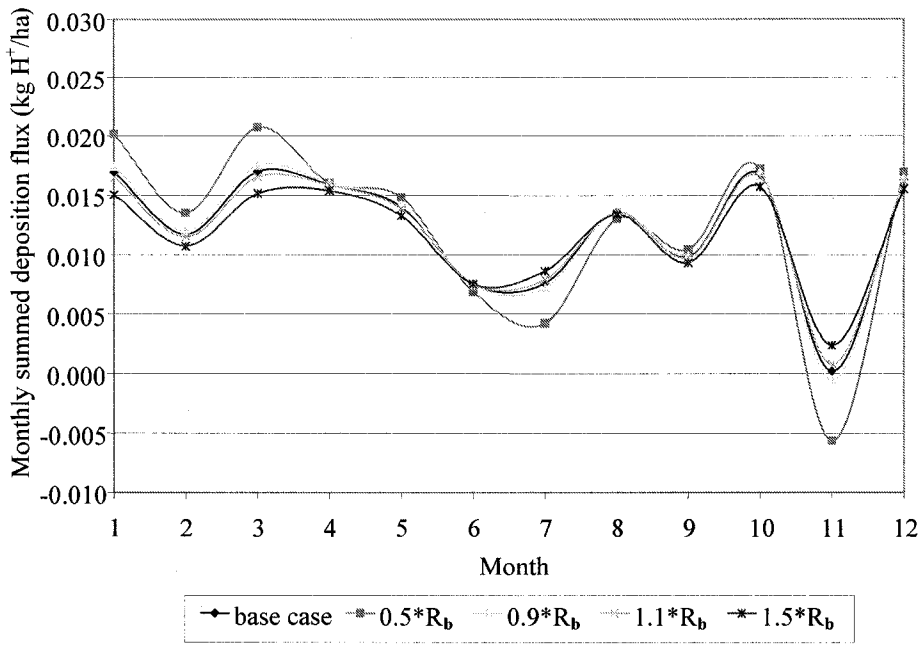

Figure 39 Monthly summed deposition flux for 11 species using AENV model showing influence of step changes in R_b for a coniferous forest cover.

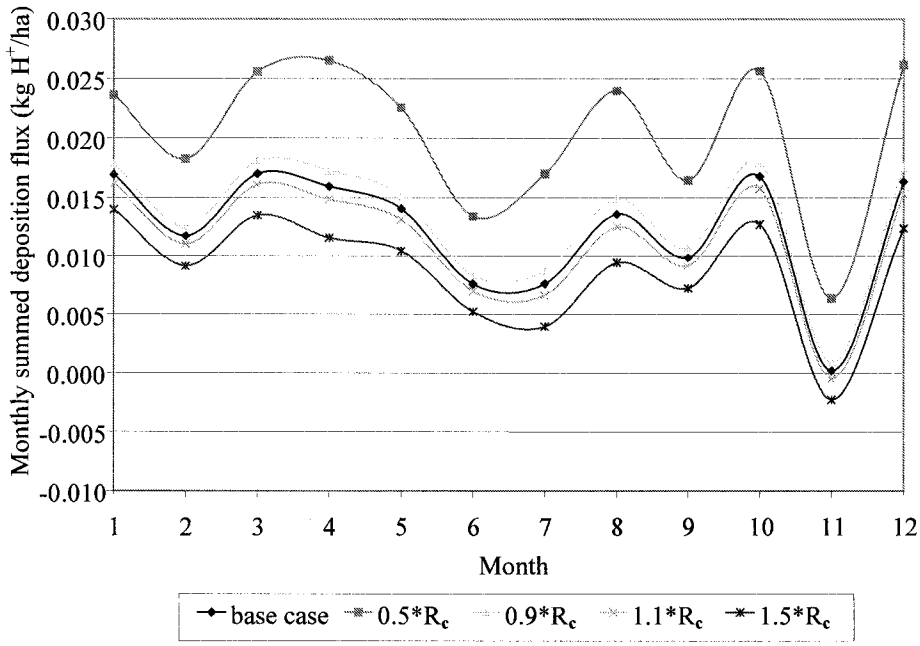

Figure 40 Monthly summed deposition flux for 11 species using AENV model showing influence of step changes in R_c for a coniferous forest cover.

5.1.2.3 Performance Indicators for AENV Model

Results discussed in the previous sections suggest that AENV model performance is closely related to deposition velocity modeling for NO_2 and SO_2, particularly with respect to the selection of surface (canopy) resistance (R_c) values used to parameterize NO_2 and SO_2 deposition. Relative to the performance of the ENVC model, there are indications that values used for parameterizing R_c in the AENV model may predict lower deposition velocity values for SO_2 in winter and spring while predicting higher acid deposition values in summer and autumn. For NO_2, R_c values used for parameterizing R_c in the AENV model may predict lower deposition velocities in the autumn and winter and higher deposition velocities in the spring and summer as compared with those of the ENVC model. For HNO_3, deposition in the AENV model is driven by R_b.

5.2 Parameter Boundary Conditions

One of the recommendations put forward by WBK (2006) was that performance of the AENV model may be improved relative to performance of the ENVC model by adopting some of the boundary conditions used for specific parameters in the ENVC model and including them in the AENV model. Specific boundary conditions in the ENVC model that are currently not used in the AENV model include the following:

- A defined range limit for R_a (minimum of 5; maximum of 1000 s/m (2000 s/m over water).
- A defined range limit for the Monin-Obukhov length (L) used as a measure of instability (L = -5 if -5 < L < 0 and L = 5 if 0 < L < 5, as specified in the ENVC model, Appendix A).
- Establishing a minimum wind speed of 1 m/s for wind speeds recorded below this level.

5.2.1 Evaluation Methods

The AENV model was run several times, each time with a modification to include a separate boundary condition used by the ENVC model using a coniferous forest cover

and hourly pollutant concentration and meteorological data from the Fort MacKay air monitoring station for 11 species. Results were compared to original AENV model results for the base case in terms of the monthly summed deposition flux for all 11 species.

5.2.2 Results

5.2.2.1 Aerodynamic Resistance

Minimum of 5 s/m for R_a

In the ENVC model, aerodynamic resistance (R_a) is limited to a minimum of 5 and a maximum of 1000 s/m for all land use categories except for water (which has an upper limit of 2000 s/m). R_a is an indication of the mixing conditions of atmosphere such that a very low R_a implies maximum mixing conditions. The purpose of using a minimum limit acknowledges that, inferentially, there is always some limit to mixing possible in a natural atmosphere. Because R_a is added to R_b and R_c in the determination of deposition velocity for a pollutant, a minimum R_a value will only have an important effect on deposition velocity if values for R_b and R_c for that hour are also small.

Using the AENV model (modified to include an allowable upper limit of 1000 s/m on R_a), the number of times hourly R_a values were within certain ranges were counted and summarized in Table 11. From Table 11, it can be seen that May is the month with the greatest number of hourly occurrences with the smallest computed R_a value (i.e, 0 to 10 s/m), which implies that it should be the month with the largest difference in the corresponding deposition flux.

The AENV model was modified and rerun using a minimum value of 5 s/m for R_a. Results were compared to the model run under base case conditions and to the ENVC model results and are presented in Table 12. As shown in Table 12, May did in fact demonstrate the largest change in deposition flux (0.06 g H^+/ha), although this difference only represented less than a 0.5% change in total deposition. This result indicates that the overall effect of setting this minimum limit on R_a in the AENV model is anticipated to be small.

Table 11 Counts of hourly R_a values within a maximum of 1000 s/m for the AENV model run with an allowable upper limit of 1000 s/m for a coniferous forest cover.

Ra (s/m)	≤ 10	≤ 20	≤ 30	≤ 40	≤ 50	≤ 60	≤ 70	≤ 80	≤ 90	≤ 100
Jan	58	105	58	28	16	9	7	4	8	8
Feb	72	150	55	18	11	8	4	2	6	2
Mar	209	113	35	10	8	4	5	3	2	2
Apr	102	221	82	41	25	15	0	6	2	2
May	293	91	22	12	15	9	5	6	1	2
Jun	212	167	52	14	12	5	9	5	5	3
Jul	164	199	70	31	12	9	12	3	3	2
Aug	140	210	70	18	14	16	4	3	3	7
Sep	260	128	31	21	8	6	5	5	3	3
Oct	139	135	45	37	19	15	13	5	5	2
Nov	29	182	92	55	20	18	11	13	5	7
Dec	7	89	142	94	35	23	22	9	12	11

Ra (s/m)	≤ 200	≤ 300	≤ 400	≤ 500	≤ 600	≤ 700	≤ 800	≤ 900	≤ 1000
Jan	26	10	9	6	6	5	5	3	372
Feb	11	10	7	6	1	1	1	1	330
Mar	12	5	8	2	2	2	1	6	291
Apr	16	7	4	3	2	1	0	0	191
May	19	12	4	4	11	2	1	2	233
Jun	25	13	6	6	5	4	1	6	170
Jul	15	11	8	6	3	2	4	3	187
Aug	21	8	4	6	2	5	4	2	207
Sep	22	13	9	2	11	2	2	2	187
Oct	31	19	14	5	5	7	5	3	240
Nov	29	14	7	5	3	3	2	5	220
Dec	54	16	10	9	15	2	0	2	192

Note: Ranges presented include the following increments – ≤10 = 0 to 10 s/m, ≤20 = 10 to 20 s/m, etc.

Table 12 Comparison of monthly summed deposition flux (g H^+/ha) for AENV model with minimum R_a limit of 5 s/m to AENV base case model and ENVC model results for coniferous forest cover.

	AENV w limit	AENV w/out limit	ENVC	difference w/in AENV model	closer to ENVC model
Month 1	15.5	15.5	15.5	-0.02	+
Month 2	10.6	10.6	11.4	0.00	0
Month 3	16.1	16.1	16.2	-0.02	+
Month 4	15.5	15.5	17.0	0.00	0
Month 5	13.6	13.7	12.0	-0.06	+
Month 6	7.4	7.4	6.5	-0.02	+
Month 7	7.5	7.5	10.7	0.00	0
Month 8	13.4	13.4	12.9	0.00	0
Month 9	9.6	9.6	12.2	-0.02	-
Month 10	16.3	16.3	18.0	-0.03	-
Month 11	-0.2	-0.2	3.6	0.00	0
Month 12	15.6	15.6	16.8	0.00	0
total	140.9	141.0	152.8	-0.2	-

Maximum of 1000 s/m for R_a

Just as a very low R_a value would not necessarily offer a reasonable representation of natural conditions during daytime, neither would an extremely high R_a value. A very high R_a value would be associated with no mixing in the atmosphere (ideally stable night time conditions). From a practical point of view, very large aerodynamic resistances are not much different than moderately large aerodynamic resistances since deposition velocity involves the inverse of the sum of all three resistances ($R_a + R_b + R_c$). When hourly deposition values for a month are summed, it is the hourly conditions with small summed values for the three resistance factors (and hence the correspondingly large deposition velocity and deposition flux values) that are important and drive the overall monthly summed deposition flux. Very large or moderately large aerodynamic resistance values (and correspondingly very small or moderately small deposition velocity and deposition flux values) are unimportant.

An upper limit on R_a might be expected to have an effect where a monthly summed deposition flux results from the sum of a large number of small hourly deposition flux values (corresponding to a large number of large hourly deposition velocity values perhaps influenced by large R_a values). As can be seen from Table 11, January had a large number of high R_a values between 900 and 1000 s/m (372) and few small R_a values (58 between 0 and 10 s/m). This month is in contrast to the month of September which had a small number of high R_a values between 900 and 1000 s/m (187) and numerous small R_a values (290 between 0 and 10 s/m). It would be expected that the month of January would show a greater response to the presence of a maximum limit set on R_a compared with September.

The AENV model was modified and rerun using a maximum value of 1000 s/m for R_a. Resulting monthly summed deposition fluxes were compared to the model run under base case conditions and to the ENVC model results and are presented in Table 13. As predicted, January shows the greatest change relative to the base case conditions. In addition, the direction of change caused by using a maximum value of 1000 s/m for R_a was to bring AENV model results closer to ENVC model results. In comparison with the AENV base case, using a maximum value of 1000 s/m for R_a in the AENV model

resulted in an overall increase of 7 g H^+/ha in total annual deposition flux (*PAI*) which represents a 5% difference. Monthly deposition is shown graphically in Figure 41.

Table 13 Comparison of monthly summed deposition flux (g H^+/ha) for AENV model with maximum R_a limit of 1000 s/m to AENV base case conditions and ENVC model results for coniferous forest cover.

	AENV w limit	AENV w/out limit	ENVC	w/in AENV model	closer to ENVC model
Month 1	17.0	15.5	15.5	1.5	-
Month 2	11.3	10.6	11.4	0.7	+
Month 3	17.1	16.1	16.2	1.0	-
Month 4	16.0	15.5	17.0	0.5	+
Month 5	14.3	13.7	12.0	0.6	-
Month 6	7.7	7.4	6.5	0.2	-
Month 7	7.5	7.5	10.7	0.1	+
Month 8	13.7	13.4	12.9	0.3	-
Month 9	9.9	9.6	12.2	0.3	+
Month 10	17.0	16.3	18.0	0.7	+
Month 11	0.3	-0.2	3.6	0.5	+
Month 12	16.5	15.6	16.8	0.9	+
total	148.3	141.0	152.8	7.2	+

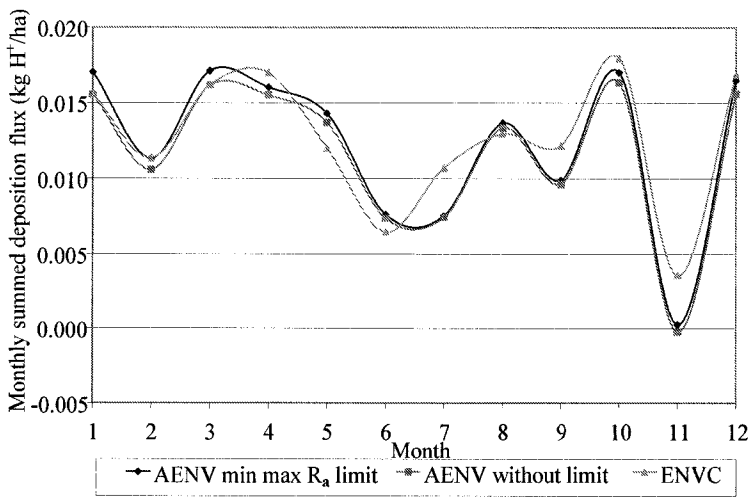

Figure 41 Monthly summed deposition flux for 11 species using AENV model showing changes with and without (base case) minimum 5 s/m and maximum 1000 s/m limits to hourly R_a values for a coniferous forest cover.

5.2.2.2 Monin-Obukhov Length

In the ENVC model, the Monin-Obukhov length (L) is limited to a maximum and minimum value of -5 and 5 for negative and positive values, respectively. L is used in the calculation of the stability function which is ultimately used in calculation of R_a. L represents the height above the surface in which convectively driven turbulence dominates over mechanically driven turbulence and it is indirectly a measure of the convective instability generated by the vertical heat flux through the surface layer. L is only meaningful in daytime convectively driven boundary layers.

A negative value for L represents atmospheric instability and a positive value represents stability. Small absolute values for L represent extremes which are not representative in nature. In general, as L approaches zero, R_a becomes larger and the corresponding deposition velocity is smaller.

The result of applying the limit to L is a slightly lower R_a and a slightly higher corresponding deposition velocity. Since it is the higher R_a values that are affected, the nature of the change should be similar to that of setting an upper limit on R_a. The effects of using limits to L are shown in Table 14 and Figure 42. Annual summed deposition flux is increased by 5 g H^+/ha which represents a 4% difference in total deposition. The direction of change caused by using limits to L is to bring AENV model results closer to ENVC model results (the same general effect caused by setting an upper limit or 1000 s/m to R_a).

Table 14 Monthly summed deposition flux (g H^+/ha) for 11 species showing changes with and without limits set on *L* with AENV base case conditions and ENVC model results for a coniferous forest cover.

	AENV w limit	AENV w/out limit	ENVC	difference w/in AENV model	closer to ENVC model
Month 1	16.4	15.5	15.5	0.9	-
Month 2	11.0	10.6	11.4	0.4	+
Month 3	16.6	16.1	16.2	0.4	-
Month 4	15.9	15.5	17.0	0.4	+
Month 5	14.4	13.7	12.0	0.7	-
Month 6	7.7	7.4	6.5	0.3	-
Month 7	7.6	7.5	10.7	0.1	+
Month 8	13.6	13.4	12.9	0.2	-
Month 9	9.8	9.6	12.2	0.2	+
Month 10	16.9	16.3	18.0	0.6	+
Month 11	0.3	-0.2	3.6	0.5	+
Month 12	16.1	15.6	16.8	0.5	+
total	146.2	141.0	152.8	5.1	+

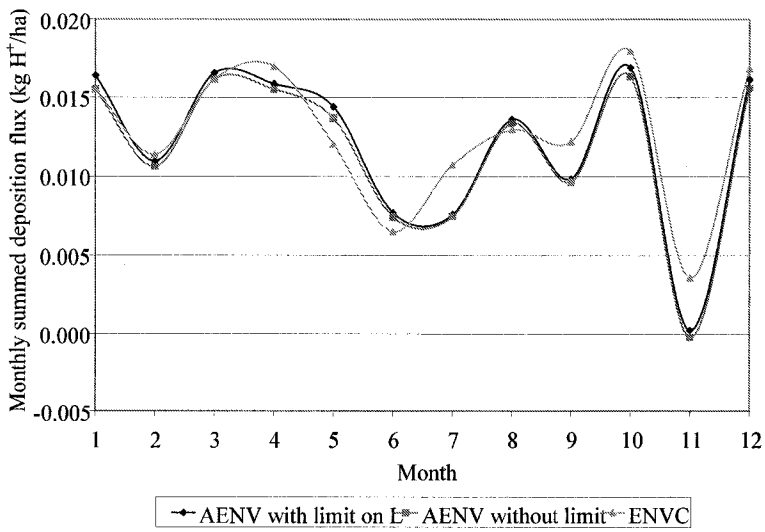

Figure 42 Monthly summed deposition flux for 11 species using AENV model showing influence with and without (base case) limits on *L* for a coniferous forest cover.

5.2.2.3 Minimum Wind Speed

Wind speed values in the AENV model are allowed to vary to a minimum of 0.09 m/s, below which they are assigned a value of 0 m/s. In the ENVC model, wind speed values are allowed to vary to a minimum of 1 m/s, below which they are assigned a value of 1 m/s. The effects of using a 1 m/s limit on wind speed in the ENVC model is shown in Table 15 and Figure 43. Annual deposition flux was increased by 6 g H^+/ha which represents a 4% difference in total deposition. The direction of change caused by using a 1 m/s limit to wind speed was to bring AENV model results closer to ENVC model results.

Table 15 Comparison of AENV total deposition for 1 m/s minimum limit on wind speed with AENV base case conditions and ENVC model results for a coniferous forest cover.

	AENV with 1 m/s wind speed limit	AENV without limit	ENVC	difference within AENV model	closer to ENVC model
Month 1	17.9	15.5	15.5	2.4	0
Month 2	11.2	10.6	11.4	0.6	+
Month 3	16.6	16.1	16.2	0.5	-
Month 4	15.6	15.5	17.0	0.1	+
Month 5	13.8	13.7	12.0	0.2	-
Month 6	7.5	7.4	6.5	0.1	-
Month 7	7.6	7.5	10.7	0.1	+
Month 8	13.7	13.4	12.9	0.3	-
Month 9	10.0	9.6	12.2	0.4	+
Month 10	16.9	16.3	18.0	0.6	+
Month 11	-0.3	-0.2	3.6	-0.1	-
Month 12	16.5	15.6	16.8	0.9	+
total	147.3	141.0	152.8	6.2	+

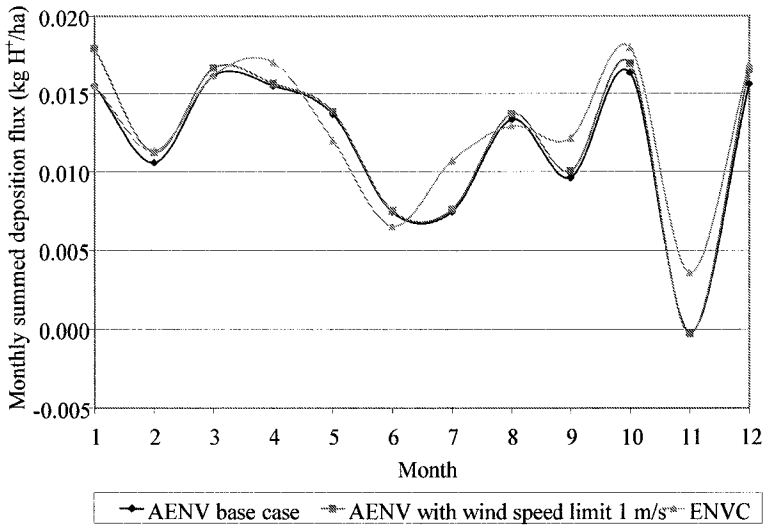

Figure 43 Monthly summed deposition flux for 11 species using AENV model showing the influence of with and without (base case) a 1 m/s minimum limit on wind speed for a coniferous forest cover.

Wind speed is involved in the calculation of both R_a (for gases and particulates) and R_b (for gases). Using a minimum wind speed limit would be expected to affect months that have a large number of low hourly wind speeds, resulting in low R_a and R_b. Similar to a maximum limit set for R_a, as discussed previously, January would be expected to show the largest difference. Table 15 indicates that January shows the greatest change relative to the base case conditions.

5.3 Non-Boundary Condition Components

Three non-boundary issues were examined during this study. In the AENV model, three issues that were further analyzed included the following:

i) calculation of surface roughness length (z_0),

ii) use of relative humidity (RH) as a surrogate parameter to define wetness conditions of a surface instead of a surface wetness measurement, and

iii) in the ENVC model, treatment of the particle distribution for particle deposition was examined.

5.3.1 Evaluation Methods of Non Boundary Condition Issues

5.3.1.1 Surface Roughness Length

One potential limitation of the AENV method is a requirement to calculate surface roughness length (z_0) as a monthly average using hourly data where the wind speed is greater than 6 m/s. The concern is that it is possible for there to be some months in which only a small number of hourly values exist in which the wind speed is greater than 6 m/s. This paucity of z_0 values used for the average results in greater uncertainty in the calculated average z_0 value. Upon the recommendations of Dr. Cheng of Alberta Environment (personal communitication), the procedure for generating a monthly z_0 value was modified to address situations in which the z_0 value would otherwise be generated from less than seven data points.

The following procedures are recommended for the calculation of z_0 for months that do not have at least seven qualifying hourly data points:

- if one consecutive month does not have at least seven hourly data points to be used in the calculation of the z_0 (e.g., November data in this case); then an average monthly z_0 computed from for the two adjacent months (October and December in this case) are to be used.
- if two or more consecutive months do not have at least seven hourly data points to be used in calculation of z_0 (e.g., February and March in this case); then an average annual value computed from z_0 values for all months that had at least seven hourly data points was used to represent these months. This could be applicable to surface cover characteristics that are not expected to undergo substantial change from season to season (e.g., a coniferous forest canopy). (Alternatively, if consecutive months have an insufficient number of observations for a surface cover whose characteristics are not expected to undergo substantial change within a season, then an average for the month within the season could be used for to represent these months.)

The AENV model was rerun using the modified criteria to establish representative values for z_0 based on a minimum requirement that at least seven hourly data points must

be used in the calculation of an average z_0 for that month. The resulting monthly summed deposition flux values were then compared with original results.

5.3.1.2 Surface Wetness and Relative Humidity

Wetness alters the characteristics of a surface to act a sink for depositing species (primarily gases). The AENV model requires an hourly measurement to represent the amount of wetness on a surface in determination of surface resistance (R_c). The model is designed to use field measurement data from surface wetness sensing equipment. Past experience has indicated that this field equipment does not provide reliable measurement data in an Alberta setting due to the wide temperature ranges experienced. Alternatively, the AENV model can use relative humidity (RH) as a surrogate criterion for surface wetness (Bates, 1996). The AENV method uses a lower limit for RH of 87.4% in classifying a surface as being wet for the full hour after Bates (1996).

The effect of using different limits for RH was examined. The original AENV model was modified to set the RH value as 80% for the cut-off in determination of a wet/dry condition for selection of the R_c value for SO_2 and NO_2 for each of land use category. Similarly, the original AENV model was modified to use a RH value of 92% as the cut-off. These cut-off values were selected as values being on each side of the value used in the model by enough to show some difference without being extremely different. Results in terms of monthly summed deposition flux for all 11 species were compared for the different RH cut-off values and the original results for each land use category.

5.3.1.3 Settling Properties of Large Particle Size Distributions

In the original design of the ENVC model, 40 aerodynamic sizes were used to represent an overall particle size distribution in the calculation of the deposition velocity for the species associated with the small particles. An aerodynamic size differs from the actual size in that the aerodynamic size standardizes the particle size as a perfect sphere based on the settling velocity and Stokes' law. When the ENVC model was modified to

include calculation of deposition velocity for species associated with the large particles (NO_3^-, Na^+, K^+, Ca^{2+}, and Mg^{2+}), the number of bin sizes remained at 40 so as to limit the largest particle size to that detected as PM_{10} (*i.e.*, 10 μm). The size distribution of sodium (Na^+) was used as a conservative representation for the distribution of all large particles (NO_3^-, Na^+, K^+, Ca^{2+}, and Mg^{2+}) in the ENVC model. A typical sodium particle distribution has a geometric mean of 0.5 μm and a standard deviation of 2.0 μm. Only 75.86% of this size distribution is encompassed within the first 40 bin sizes (which span from 0 to a diameter of 10 μm); therefore, greater than 24% of the particle sizes for this distribution are unaccounted for in the ENVC model.

Increasing the number of bins to capture larger particle sizes in the distribution (*i.e.*, greater than 10 μm) is typically not done because of uncertainty in extrapolation of the distribution and of the chemical concentrations in the atmosphere. Even if the particles greater than 10 μm and their buffering effects are completely ignored in the model, it is still necessary to adjust the formula for the fact that there is only 75.86% of the distribution under the curve for the portion of the curve to the left of the 10 μm cut-off. The best way to correct for this error is to divide the area under the curve for each bin or slice by 0.7586 to standardize the curve for the limit set on the size of particles measured. This adjustment was made and the corrected ENVC model results were compared with the uncorrected ENVC and the base case AENV results.

5.3.2 Results

5.3.2.1 Surface Roughness Length

One potential issue with the AENV model is the way surface roughness length (z_0) is calculated. In comparison, in the ENVC model, tabular values are used for the surface roughness lengths. The AENV model requires that hourly data to be used in calculation of z_0 during a particular month be initially based on a monthly average z_0 value using hourly data where the wind speed is greater than 6 m/s in that month (WBK, 2006). For the 2003 meteorological data used in this study, the month of February did not have a single hourly wind speed value greater than 6 m/s (shown in Table 16) such that it was necessary to use an average z_0 value of the two surrounding months. In

general, there was a lack of hourly values for several months (e.g., February, March, and November) for use in calculation of z_0, given the 6 m/s minimum wind speed cut-off value. The number of hourly values used for calculating each of the monthly average z_0 values ranged from 0 to 42 as shown in Table 16.

For months with too few hours from which to calculate z_0, it would perhaps be more suitable if monthly wind speed data from another meteorological year could be used to supplement the number of observations used in the initial calculation of a z_0 value for that that month at a site-specific location. Unfortunately, these data may not be available and would not be applicable for a location undergoing changes in the surrounding land use.

Table 16 Monthly average surface roughness length (z_0, m), standard deviation, and sample size (number of hourly values) in which wind speed greater than 6 m/s for calculation of monthly average surface roughness length for a coniferous forest cover.

Month	z_0	Standard Deviation	Sample Size
January	1.24	0.40	19
February			0
March	1.50	0.54	6
April	0.67	0.28	42
May	1.46	0.75	29
June	1.26	0.45	26
July	1.20	0.49	10
August	1.11	0.52	13
September	1.61	0.89	9
October	1.30	0.64	10
November	0.72	0.24	2
December	0.50	0.16	7
	1.12	Weighted Annual Average	

Surrogate values were generated for the months of February, March, and November because of the limited number of data values available for the calculation for the average monthly z_0 value as a result of the procedures outlined in section 5.3.1.1.

Following these procedures, the z_0 value used for November was taken as the average of October and December and the z_0 value used for February and March was taken as the annual average value (shown in Table 16). The results of these substitution is shown in Figure 44 as a comparison with the AENV base case which used the prior procedure which only required the generation of a surrogate value for February. Figure 44 shows that these substitutions result in slightly higher deposition fluxes in February and March, while the difference in November is negligible.

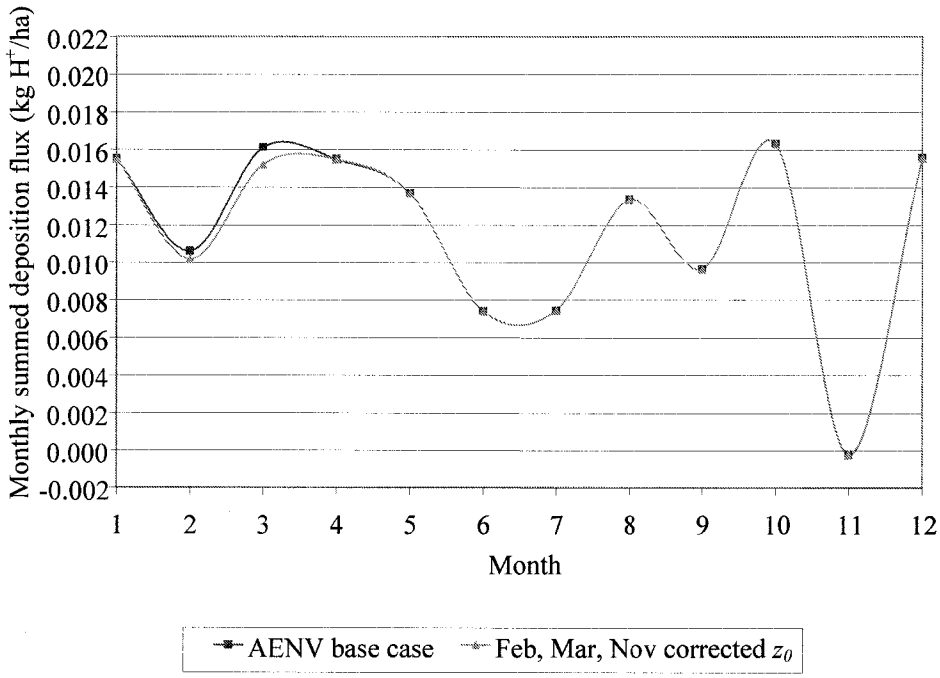

Figure 44 Monthly summed deposition flux for 11 species using AENV model showing influence resulting from corrected z_0 values for the months of February, March, and November for a coniferous forest cover.

Another potential issue with calculation of z_0 in the AENV model is that there was a wide variation computed for surface roughness lengths for different months across the year. In theory, a mature coniferous forest should have a similar friction coefficient across the year because the foliage does not change seasonally. The ENVC model (Appendix A) assumes that the friction length (z_0) for an evergreen needle leaf forest is

consistent throughout the year at a value of 0.9 m. In the AENV model in this study, z_0 ranged from 0.5 m in December to 1.6 meters in October (Table 16).

Even within a particular month, z_0 was variable as seen in standard deviations for the AENV model (shown in Table 16). It has been observed by others that values for z_0 can change for different wind speeds if the surface cover is such that it can bend with the wind, thereby reducing the friction length (Mahrt, 2001).

With respect to the dependence of z_0 upon wind speed, it was found that if the value of the wind speed criterion used to calculate a monthly value for z_0 was decreased from 6 m/s, the monthly re-calculated z_0 value and corresponding standard deviation increased. Values for z_0 and their standard deviations using different minimum wind speeds is shown in Table 17.

Table 17 Monthly average re-calculated surface roughness length (z_0) values (m), standard deviation, and sample size (number of hourly values) for different wind speed criteria used in the re-calculation for a coniferous forest cover.

Wind speed greater than or equal to	January			February			March			April			May			June		
(m/s)	Mean	St Dev	Sample Size	Mean	St Dev	Sample Size	Mean	St Dev	Sample Size	Mean	St Dev	Sample Size	Mean	St Dev	Sample Size	Mean	St Dev	Sample Size
1.5	1.76	1.26	347	1.84	1.27	350	1.93	1.25	517	1.89	1.34	578	2.32	1.26	601	2.37	1.17	573
2	1.49	1.09	210	1.68	1.21	215	1.80	1.19	394	1.77	1.27	476	2.28	1.19	506	2.41	1.09	447
2.5	1.18	0.95	133	1.59	1.10	124	1.66	1.15	287	1.69	1.25	374	2.20	1.08	398	2.35	1.02	354
3	1.05	0.85	95	1.66	1.04	68	1.60	1.11	211	1.45	1.20	286	2.10	1.01	309	2.17	0.96	259
3.5	1.19	0.84	64	1.69	1.01	37	1.48	1.06	161	1.30	1.13	227	2.10	0.96	236	2.11	0.93	178
4	1.27	0.74	44	1.47	0.99	16	1.25	0.95	108	1.00	0.91	169	2.05	0.96	183	1.99	0.89	122
4.5	1.42	0.71	36	2.15	0.94	6	1.03	0.75	58	0.85	0.71	137	1.97	0.92	125	1.80	0.85	78
5	1.45	0.66	27	2.00	1.39	2	0.96	0.67	29	0.70	0.40	96	1.99	0.93	84	1.59	0.70	54
5.5	1.46	0.64	25				1.26	0.54	14	0.68	0.30	66	1.65	0.91	51	1.45	0.63	38
6	1.24	0.40	19				1.50	0.54	6	0.67	0.28	42	1.46	0.75	30	1.26	0.45	25
7	1.20	0.41	14							0.61	0.23	16	0.97	0.43	10	1.03	0.30	16
8	1.13	0.14	7							0.50	0.13	4	0.75	0.11	6	0.95	0.22	10
9	1.22	0.19	3										0.77	0.12	3			

Wind speed greater than or equal to	July			August			September			October			November			December		
(m/s)	Mean	St Dev	Sample Size	Mean	St Dev	Sample Size	Mean	St Dev	Sample Size	Mean	St Dev	Sample Size	Mean	St Dev	Sample Size	Mean	St Dev	Sample Size
1.5	2.22	1.22	433	2.36	1.16	473	1.77	1.12	437	1.50	1.00	433	1.29	1.12	442	1.41	1.35	503
2	2.07	1.10	314	2.31	1.05	341	1.67	1.05	348	1.47	0.95	311	1.07	0.97	322	1.14	1.17	325
2.5	1.94	1.04	226	2.29	1.04	248	1.59	0.96	274	1.46	0.90	222	0.92	0.88	238	0.97	0.96	175
3	1.89	1.03	157	2.21	1.01	167	1.59	0.90	220	1.36	0.84	155	0.78	0.70	164	0.98	0.98	97
3.5	1.74	0.97	110	2.08	0.98	112	1.59	0.83	162	1.37	0.80	103	0.76	0.69	111	1.15	0.95	45
4	1.64	0.85	73	1.96	0.97	60	1.63	0.77	124	1.43	0.78	66	0.77	0.59	56	1.04	0.73	22
4.5	1.56	0.78	49	1.83	1.00	40	1.66	0.71	85	1.52	0.77	46	0.91	0.60	31	0.77	0.47	14
5	1.45	0.76	33	1.76	0.99	28	1.76	0.72	41	1.54	0.77	25	1.34	0.55	13	0.55	0.17	9
5.5	1.32	0.57	19	1.53	0.91	21	1.84	0.76	20	1.38	0.69	16	0.95	0.36	7	0.52	0.16	8
6	1.20	0.49	10	1.11	0.52	13	1.61	0.89	9	1.30	0.64	10	0.72	0.24	2	0.50	0.16	7
7	1.22	0.52	5	1.04	0.46	10										0.40	0.12	4
8				0.66	0.20	3												
9																		

Weighted annual average z_0 values were computed and plotted in Figure 45 showing one standard deviation for each wind speed criterion listed in Table 17. This figure shows a linear change in weighted annual average z_0 for different wind speeds cut-offs used. In comparison, the ENVC model uses the value of 0.9 for the surface roughness length for all seasons for an evergreen needleleaf trees land use category. If wind speeds are further separated into specific ranges and a corresponding z_0 value calculated for each range, as was done in Table 18, it is seen that z_0 values are highly variable among the ranges shown. Wind direction has also been found to affect calculation of z_0 as a result of differences in landscape features in different directions from a monitoring station (CEC, 1993).

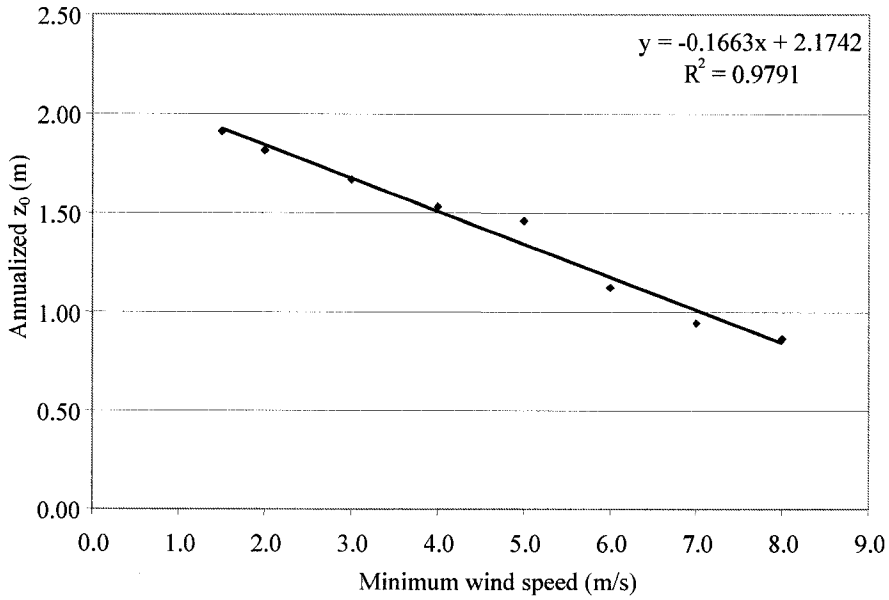

Figure 45 Annual average re-calculated surface roughness length (z_0) values (m) for different wind speed criteria used in the re-calculation for a coniferous forest cover.

Table 18 Monthly calculated surface roughness length (z_0) values (m) and standard deviation for different wind speed ranges for a coniferous forest cover.

Wind speed range	January		February		March		April		May		June	
(m/s)	Mean	St Dev	Mean	St Dev	Mean	St Dev	Mean	St Dev	Mean	St Dev	Mean	St Dev
$2 \leq u < 3$	1.85	1.14	1.69	1.29	2.02	1.25	2.25	1.24	2.56	1.39	2.73	1.18
$3 \leq u < 4$	0.86	0.90	1.72	1.06	1.97	1.15	2.10	1.26	2.17	1.08	2.34	0.99
$4 \leq u < 5$	0.99	0.80	1.40	0.97	1.35	1.01	1.38	1.20	2.09	0.99	2.30	0.90
$5 \leq u < 6$	1.96	0.88	2.00	1.39	0.82	0.64	0.73	0.48	2.28	0.89	1.87	0.76
$6 \leq u < 7$	1.36	0.36			1.50	0.54	0.70	0.30	1.71	0.76	1.67	0.38
$7 \leq u < 8$	1.27	0.58					0.64	0.25	1.30	0.54	1.16	0.38
$8 \leq u < 9$	1.07	0.07					0.50	0.13	0.74	0.13	0.95	0.22
$9 \leq u$	1.22	0.19							0.77	0.12		

Wind speed range	July		August		September		October		November		December	
(m/s)	Mean	St Dev	Mean	St Dev	Mean	St Dev	Mean	St Dev	Mean	St Dev	Mean	St Dev
$2 \leq u < 3$	2.24	1.15	2.41	1.08	1.79	1.26	1.57	1.03	1.36	1.12	1.21	1.23
$3 \leq u < 4$	2.12	1.11	2.35	1.01	1.54	1.04	1.31	0.88	0.79	0.75	0.97	1.05
$4 \leq u < 5$	1.79	0.90	2.14	0.92	1.57	0.79	1.36	0.79	0.60	0.49	1.38	0.78
$5 \leq u < 6$	1.55	0.83	2.33	0.96	1.81	0.68	1.70	0.83	1.45	0.51	0.71	0.08
$6 \leq u < 7$	1.19	0.53	1.32	0.76	1.61	0.89	1.30	0.64	0.72	0.24	0.62	0.13
$7 \leq u < 8$	1.22	0.52	1.21	0.45							0.40	0.12
$8 \leq u < 9$			0.66	0.20								
$9 \leq u$												

5.3.2.2 Surface Wetness and Relative Humidity

Surface wetness is difficult to measure and it is very difficult to generalize data from one area to an entire area (Panofsky, 1974). Surface wetness data are required for the AENV model; however experience has shown that these data are frequently unavailable due to problems with surface wetness sensing equipment in the field. Consequently, the AENV model allows a minimum relative humidity (RH) measurement cut-off (87%) to be used as an approximation to represent a surface as being wet. The selection of the RH value cut-off was further examined to assess the sensitivity of this AENV model criterion. The current cut-off in the model is 87% and two alternative values (80% and 92%) were assessed.

Wetness affects surface resistance (R_c) for SO_2 and NO_2 in the AENV model. Default values used to represent R_c in the AENV model for SO_2 are generally lower when a surface is considered wet as opposed to dry (refer to Appendix B) because wetness will enhance the contribution of SO_2 deposition to a surface. Default values used to represent R_c in the AENV model for NO_2 are generally higher when a surface is considered wet as opposed to dry (Appendix B) because wetness will decrease the contribution of NO_2 deposition to a surface.

The effects of changing the surface wetness cut-off for all the land use categories, (except Water) are shown in Figures 46 to 52 below. The Water *LUC* demonstrates no change in results from a change in the surface wetness cut-off condition because the values for the Water *LUC* are the same in wet and dry conditions as defined by relative humidity or surface wetness. The figures for the remaining seven *LUCs* show that there is very little change in the monthly summed deposition flux for 11 species caused by the use of a different RH cut-off (*i.e.*, 80%, 92% , or the base case of 87%) to represent a surface as being wet.

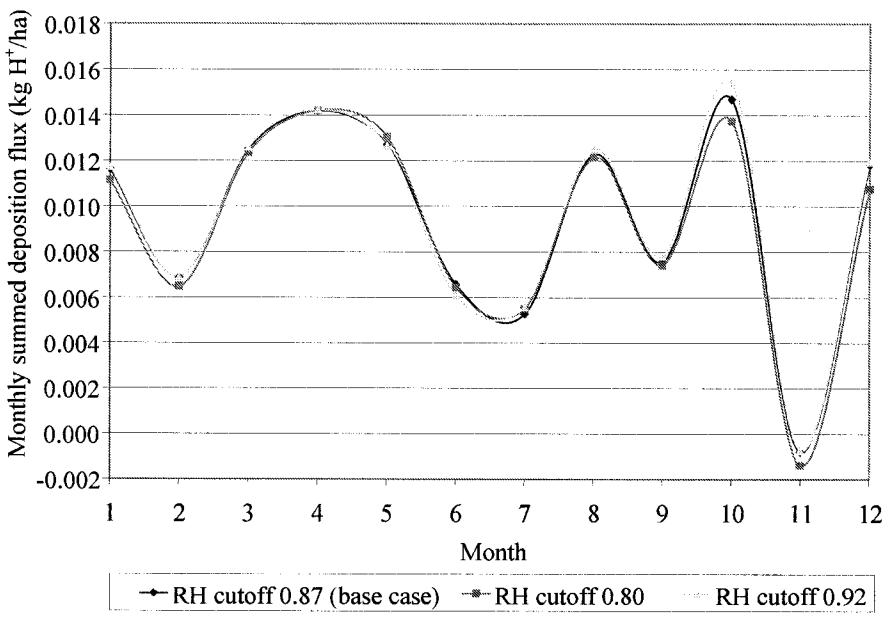

Figure 46 Monthly summed deposition flux for 11 species using AENV model showing influence of using a different RH cut-off for establishing a surface as wet (base case RH = 0.87) for deciduous forest cover.

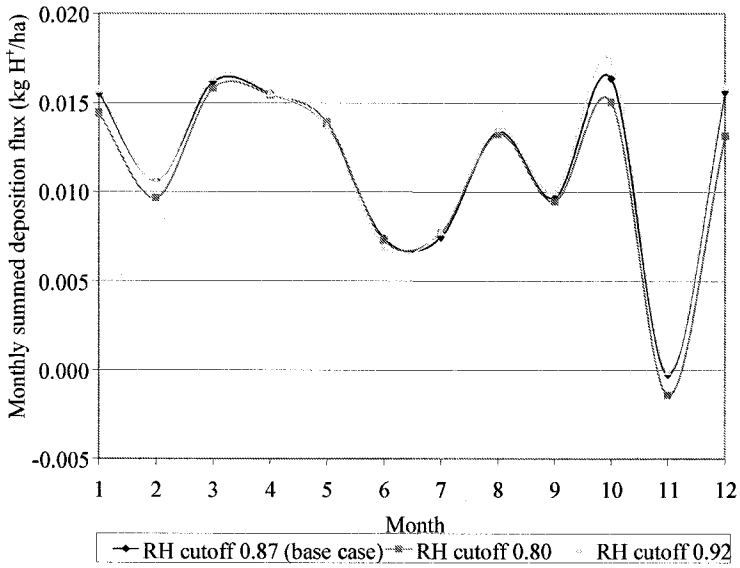

Figure 47 Monthly summed deposition flux for 11 species using AENV model showing influence of using a different RH cut-off for establishing a surface as wet (base case RH = 0.87) for a coniferous forest cover.

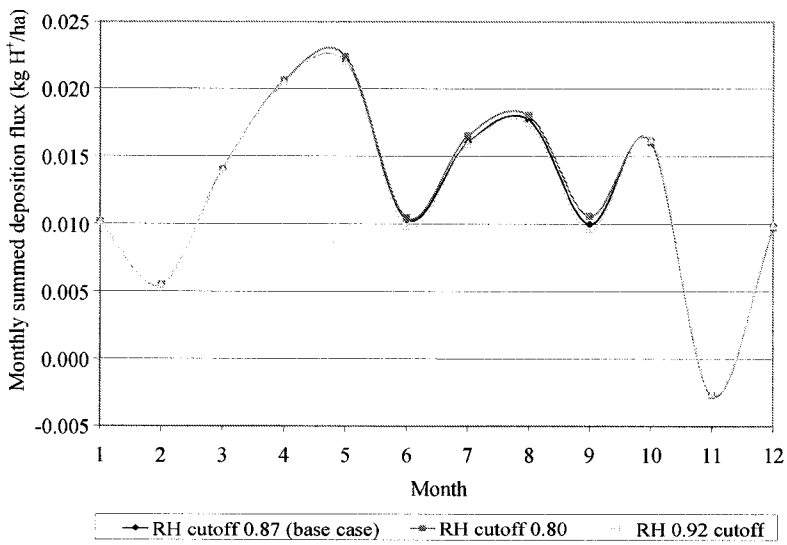

Figure 48 Monthly summed deposition flux for 11 species using AENV model showing influence of using a different RH cut-off for establishing a surface as wet (base case RH = 0.87) for wetland/swamp cover.

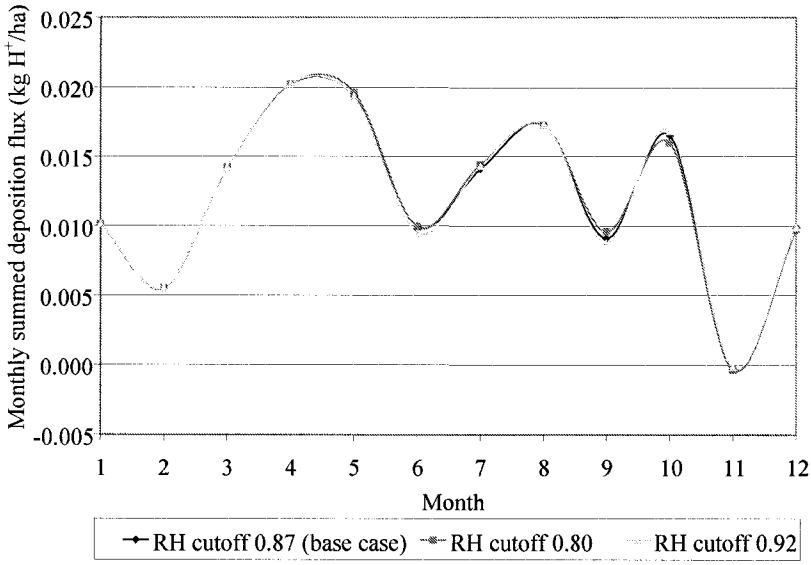

Figure 49 Monthly summed deposition flux for 11 species using AENV model showing influence of using a different RH cut-off for establishing a surface as wet (base case RH = 0.87) for grassland.

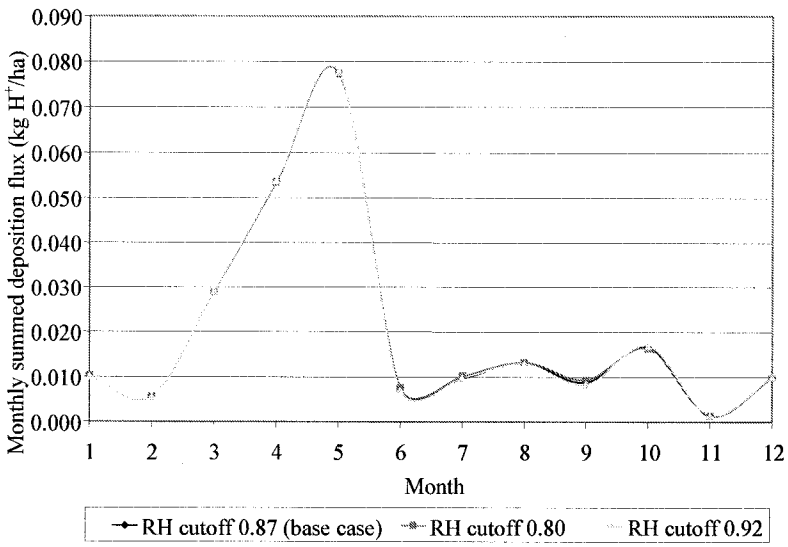

Figure 50 Monthly summed deposition flux for 11 species using AENV model showing influence of using a different RH cut-off for establishing a surface as wet (base case RH = 0.87) for cropland.

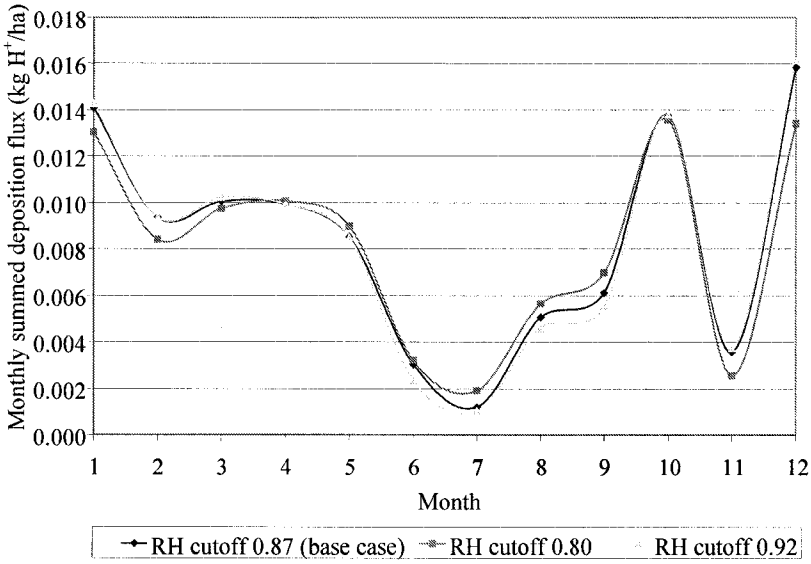

Figure 51 Monthly summed deposition flux for 11 species using AENV model showing influence of using a different RH cut-off for establishing a surface as wet (base case RH = 0.87) for urban cover.

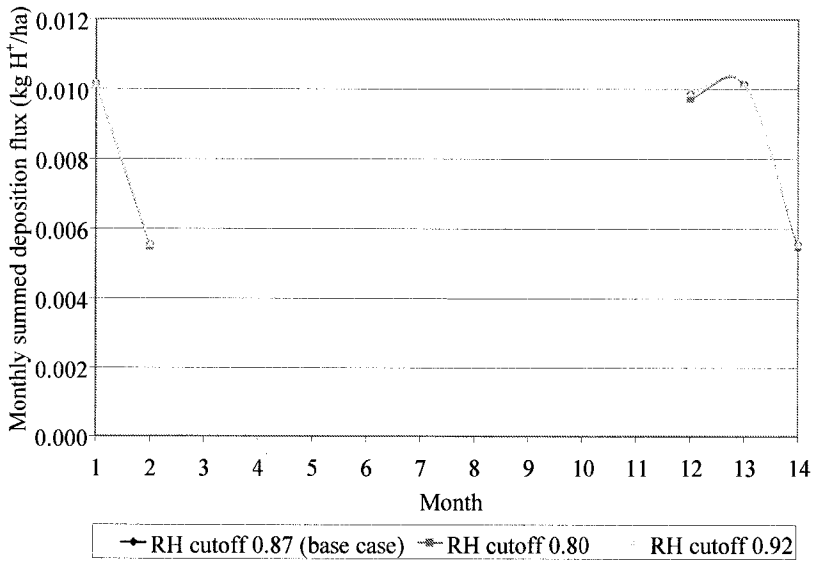

Figure 52 Monthly summed deposition flux for 11 species using AENV model showing influence of using a different RH cut-off for establishing a surface as wet (base case RH = 0.87) for snow/ice.

5.3.2.3 Particulate Size Distributions

In the AENV model, particle deposition is addressed by using literature values for the R_b. The effect of the particle size distribution for the specific particulate species is already within these literature values. The ENVC predicts the deposition of particles starting from an assumed particle size distribution.

In the original design of the ENVC model (which only addressed SO_4^{2-} and NH_4^+ deposition associated with small particles), 40 aerodynamic sizes (referred to as bin sizes by ENVC) were used to represent an overall particle size distribution in the calculation of the deposition velocity for the species associated with the small particles. The 40 slices that are generated are referred to as bins and contain the particles that are larger than those in the bin having the next smaller bin size up to the diameter that is used to describe the bin. The largest size bin encompasses particles up to 10 μm in diameter which matches the maximum size of particles classified as PM_{10}. This number of bin sizes (40) encompasses almost 100% of a typical small particle distribution having a geometric mean of 0.5 μm and a standard deviation of 2.0 μm.

When the ENVC model was modified to include calculation of deposition velocity for species associated with large particles (*i.e.*, NO_3^-, Na^+, K^+, Ca^{2+}, and Mg^{2+}), the number of bin sizes remained at 40 so as to limit the largest particle size to that detected as PM_{10} (*i.e.*, 10 μm). The size distribution of sodium (Na^+) was used as a conservative representation for the distribution of all large particles (NO_3^-, Na^+, K^+, Ca^{2+}, and Mg^{2+}) in the ENVC model. A typical sodium particle distribution has a geometric mean of 0.5 μm and a standard deviation of 2.0 μm. Only 75.86% of this size distribution is encompassed within the first 40 bin sizes (which span from 0 to a diameter of 10 μm); therefore, greater than 24% of the particle sizes for this distribution are unaccounted for in the ENVC model. These larger sized particles (greater than 10 μm in diameter), which include the base cation species, are functionally neglected in the model. Their larger size results in their having increased settling properties. The net results of taking larger sizes into account in the calculation would be a greater overall buffering effect, or more importantly, a net decrease in potential acid input.

Increasing the number of bins to capture larger particle sizes in the distribution (*i.e.*, greater than 10 μm) is typically not done because of uncertainty in extrapolation of

the distribution and of the chemical concentrations in the atmosphere. Little research has been done on the nature of the size distributions of larger particles in the atmosphere because they are generally less harmful to the environment. Current use of a truncated distribution for large particles in ENVC's model produces a conservative estimate of deposition flux when considering all species. Because a majority of base cations is associated with large particle deposition, underestimating deposition of large particles results in an underestimation of the neutralization capacity of base cations. This underestimation leads to an overestimation of total acid deposition and is therefore a more conservative approach to predicting tolerable levels of emissions gases in the atmosphere.

Even if the particles greater than 10 μm and their buffering effects are completely ignored in the model, it is still necessary to adjust the formula for the fact that there is only 75.86% of the distribution under the curve and not 100% when standardizing the curve to a log-normal distribution. If the error is corrected by dividing the area under the curve for each bin or slice by 0.7586 to standardize the curve for the size of particles measured, corrected ENVC model results (Figure 53) show much better agreement with AENV model results than previously presented.

The net difference in annual deposition flux for 11 species between the AENV model (base case) and corrected ENVC model was 1.2%, as opposed to a 7.7% difference without a correction (Table 2). As expected, the largest difference was observed in November. A breakdown of the influence of the ENVC model corrected for large particle size distribution on monthly summed deposition flux for NO_3^-, Na^+, K^+, Ca^{2+}, and Mg^{2+} for coniferous forest cover is provided in Appendix G.

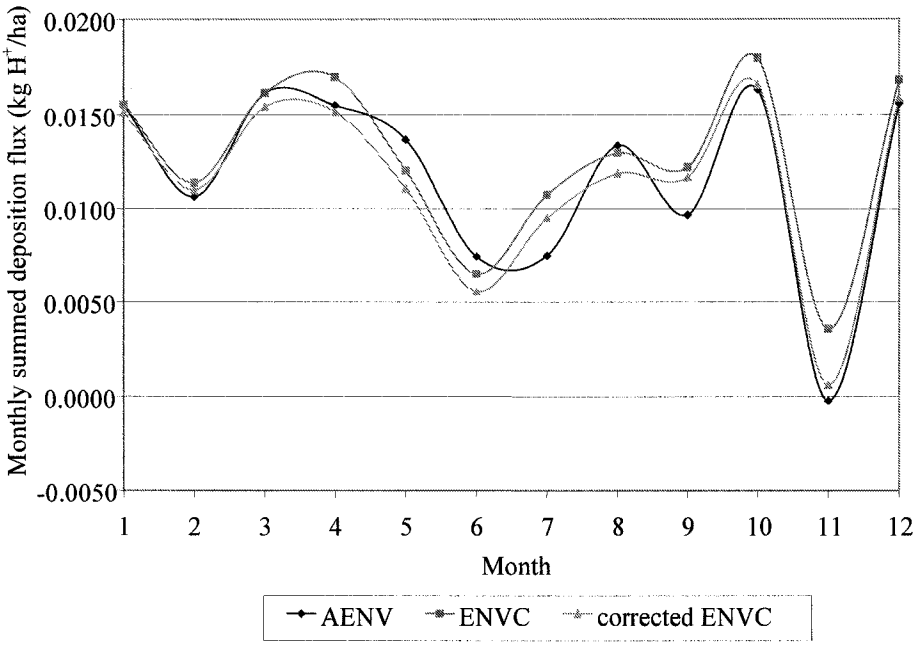

Figure 53 Monthly summed deposition flux for 11 species for AENV model base case, ENVC model, and ENVC model corrected for large particle size distribution for a coniferous forest cover.

6 Findings and Recommendations

An evaluation of the analytical basis of the Alberta Environment (AENV) and Environment Canada (ENVC) inference models for predicting dry deposition of 11 species was undertaken. These species included SO_2, NO_2, HNO_3, HNO_2, SO_4^{2-}, NH_4^+, NO_3^-, Na^+, K^+, Ca^{2+}, and Mg^{2+}. The important findings and recommends of this study include the following.

1. The three most important species contributing to potential acid input were SO_2, NO_2, and HNO_3.

2. Sensitivity testing of resistance factors R_a, R_b, and R_c used in AENV's model showed that step changes in the magnitude of R_c were much more important in influencing total deposition as compared to step changes in either R_a or R_b for all species examined. The influence of changes in R_c was independent of the month of the year.

3. AENV model performance in terms of overall deposition flux of 11 species was observed to be closely dependent on deposition velocity modeling for SO_2 and NO_2, particularly with respect to the selection of the R_c values used to parameterize these gases. Relative to performance of the ENVC model, values used to represent R_c in the AENV model resulted in lower deposition velocities for SO_2 in winter and spring and higher deposition velocities in summer and autumn. For NO_2, values used to represent R_c in the AENV model were resulted in lower deposition velocities in autumn and winter and higher deposition velocities in spring and summer. Because these are all acidic species, higher deposition velocities means over predicting the amount of acid deposited. For HNO_3, deposition in the AENV model was driven by R_b.

4. R_a is an indication of the mixing conditions in the atmosphere such that a very low R_a implies maximum mixing conditions experienced during daytime conditions. Setting a minimum value of 5 s/m for R_a in the AENV model had only a small positive change in model performance relative to the ENVC model. Although the effect of this change is small, it is recommended for future use in the AENV model. The purpose of a minimum limit for R_a acknowledges that, inferentially, there is always some limit to mixing possible in a natural atmosphere.

5. Setting a maximum value of 1000 s/m for R_a in the AENV model resulted in better agreement in overall deposition flux of 11 species relative to the ENVC model for the conditions tested. High R_a values would be associated with no mixing in the atmosphere (ideally stable night time conditions). An extremely high R_a value would not necessarily offer a reasonable representation of natural conditions. From a practical point of view, very large R_a values are not much different than moderately large values since deposition velocity involves the inverse of the sum of all three resistances ($R_a + R_b + R_c$). When hourly deposition values for a month are summed, hourly conditions with small summed values for the three resistance factors (and hence correspondingly large deposition velocity and deposition flux values) are most important and drive the overall monthly summed deposition flux. Hence very large or moderately large R_a values (and correspondingly very small or moderately small deposition velocity and deposition fluxes) are unimportant. This limit is recommended for future use in the AENV model.

6. The Monin-Obukhov length (L) is used in calculation of the stability function which is ultimately used to calculate R_a. This length represents the height above the surface at which convectively driven turbulence dominates over mechanically driven turbulence and it is indirectly a measure of the convective instability generated by the vertical heat flux through the surface layer. It is only meaningful in daytime convectively driven boundary layers. L is limited to a maximum and

minimum value of -5 and 5 m for negative and positive values, respectively, in the ENVC model. A negative value represents atmospheric instability and a positive value represents stability. In general, as L approaches zero, R_a becomes larger and corresponding deposition velocity is smaller. The result of applying these limits to L is a slightly lower R_a and a slightly higher corresponding deposition velocity. Since it is higher R_a values that are affected, the nature of the change is similar to that of setting an upper limit on R_a. The effect of using these limits to L was to bring AENV model results closer to ENVC model results (same general effect caused by setting an upper limit to R_a). These limits are recommended for future use in the AENV model as small absolute L values represent extremes which are not representative of nature.

7. Wind speed values in the AENV model are allowed to vary to a minimum of 0.09 m/s, below which they are assigned a value of 0 m/s. In the ENVC model, wind speed values are only allowed to vary to a minimum of 1 m/s, below which they are assigned a value of 1 m/s. The direction of change observed by using a 1 m/s limit to lowest wind speed values used in the AENV model was to bring model results in closer agreement to ENVC model results. This limit is recommended for future use in the AENV model.

8. One potential limitation of the AENV model is a requirement to calculate surface roughness length (z_0) as a monthly average using hourly data where the wind speed is greater than 6 m/s. The concern is when only a small number of hourly values exist during a month in which the wind speed is greater than 6 m/s such that the roughness length is calculated from a small number of values. Greater uncertainty exists in the calculated average z_0 value when computed from only a small number of hourly values. The following approach is recommended for future use in the AENV model to deal with this limitation in most cases –
   - Seven hourly observations is recommended as the minimum number of observations in which to use in a month for calculating z_0.

- The average z_0 value of two surrounding months can be used for any month in which an insufficient number of observations (*i.e.*, less than 7) exist.
- If two or more consecutive months have less than 7 observations for a surface cover whose characteristics are not expected to undergo substantial change from season to season (e.g., coniferous forest canopy), then an annual average z_0 value can be used to represent surface roughness length for these months.

9. Wetness alters the characteristics of a surface to act as a sink for depositing species (primarily gases). The AENV model requires an hourly measurement to represent the amount of wetness on a surface in determination of surface resistance (R_c). The model is designed to use field measurement data from surface wetness sensing equipment. However, past experience has indicated that this field equipment does not provide reliable measurement data in an Alberta setting due to the wide range of climatic conditions experienced. Alternatively, the model allows a relative humidity (RH) measurement cut-off (87%) to be used as a gross approximation to represent a surface as being wet. An evaluation of alternative RH cut-off values indicated little change in monthly summed deposition flux for 11 species. As a result, it is recommended that the current RH cut-off value be maintained in the model for future use.

10. A final issue that was examined related to performance of the ENVC model. The modified version of the ENVC model used in this study has an apparent limitation in the way it treats settling properties of species associated with large particles (NO_3^-, Na^+, K^+, Ca^{2+}, and Mg^{2+}). The model does not properly correct for the proportion of the particle size distribution which is greater than 10 μm. This omission results in the underestimation of the neutralization capacity offered by depositing particulates containing base cations; and overestimates total deposition flux to a surface when all depositing species are taken into account. Because the ENVC model tends to estimate higher total deposition fluxes compared to the AENV model, better agreement among these two models was achieved when corrections were made to the ENVC model to address this limitation.

11. Future research should involve comparing the modified AENV model with the ENVC model using data from another coniferous forest land cover in a different region of the province and then for a non-coniferous forest land cover.

Table 19 summarizes recommended changes to the AENV model for future use. Figure 54 shows the net effect of implementing recommended changes to the AENV model relative to ENVC model results for a coniferous forest cover for the conditions tested.

Table 19 Recommended changes to AENV acid deposition inference model.

Parameter	Original AENV model condition	Revised condition evaluated	Revised condition recommended for future use in AENV model
aerodynamic boundary resistance (R_a) [m]	upper limit on R_a is undefined	upper limit capped at 1000 s/m for all surface covers except water (2000 s/m for water)	yes
	lower limit on R_a is undefined	lower limit capped at 5 s/m for all surface covers	yes
Monin-Obukhov length (L) [m]	undefined limits	upper limit of -5 m on negative side and lower limit of +5 m on positive side	yes
wind speed minimum (u) [m/s]	set to 0 m/s if <0.09 m/s	set to 1 m/s if <1 m/s	yes
surface roughness length (z_0) [m]	computed as monthly average using hourly data where the wind speed >6 m/s	use seven hourly observations as minimum number of observations in a month to calculate z_0 and surrounding monthly average values for <7 observations	yes
surface wetness condition	uses relative humidity (RH) measurement cut-off of 87% as approximation to represent surface as being wet	uses alternative (higher/lower) relative humidity (RH) measurement cut-off as approximation to represent surface as being wet	no

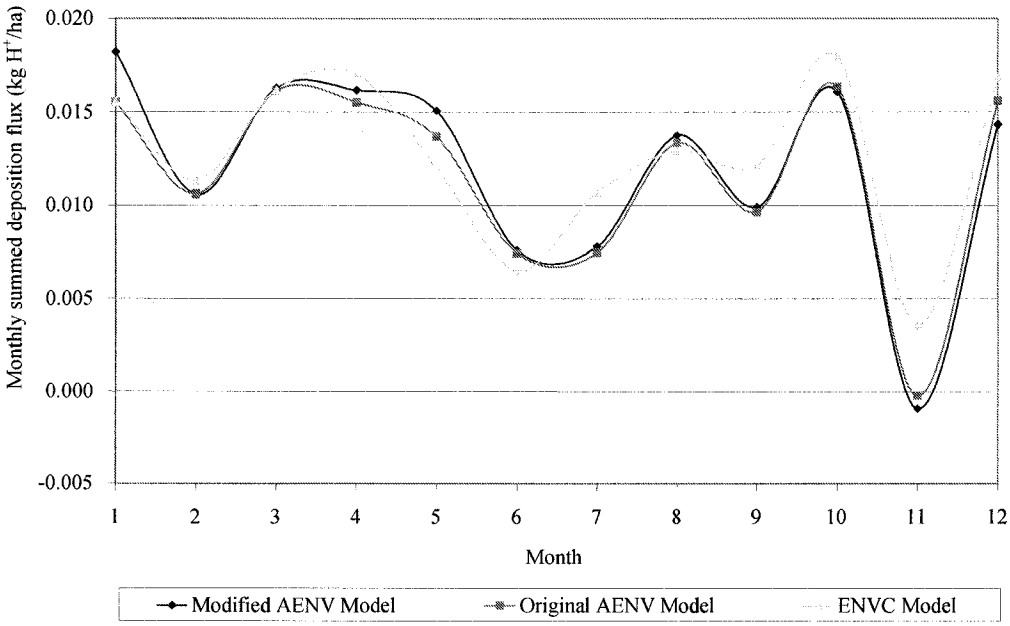

Figure 54 Monthly summed deposition flux for 11 species using modified AENV model compared to original AENV model and ENVC model for a coniferous forest cover.

7 References

Alberta Environment (AENV). 1999. "Application of Critical, Target, and Monitoring Loads for the Evaluation and Management of Acid Deposition." Alberta Environment Publications No. T/472. Environmental Service, Environmental Sciences Division, Edmonton, AB. November, 1999.

Arimoto, R., Ray, B. J., Lewis, N. F., Tomza, U., and Duce, R. A. (1997). "Mass-particle size distributions of atmospheric dust and the dry deposition of dust to the remote ocean." *J. Geophys. Res. - Atmospheres,* 102(D13), 15867-15874.

Bates, D.L., 1996. Calculation and Analysis of Dry Acidic Deposition at Royal Park. Alberta Environment, Air Issues and Monitoring Branch, Edmonton, AB. 42 pp.

Brook, J. R., Sirois, A., and Clarke, J. F. (1996). "Comparison of dry deposition velocities for SO2, HNO3, and SO42- estimated with two inferential models." *Atmos. Environ.,* 33(30), 5037-5051.

Brook, J. R., Zhang, L. M., Di-Giovanni, F., and Padro, J. (1999). "Description and evaluation of a model of deposition velocities for routine estimates of air pollutant dry deposition over North America. Part I: model development." *Atmos. Environ.,* 87(1-4), 205-218.

Businger, J. A. (1986). "Evaluation of the accuracy with which dry deposition can be measured with current micrometeorological techniques." *J. Climate Appl. Meteorol,,* 25(8), 1100-1124.

Cheng, L., Gates, D. L., and Myrick, B. (2001). "Acidic Deposition Monitoring and Calculations in Alberta, Draft 5." Alberta Environment, Edmonton, AB.

Concord Environmental Corporation (CEC) (1993). "Summary of Surface and Upper Air Data from the FSRIA Fort Saskatchewan Meteorological Station 1989 – 1992." Prepared for Alberta Environment, Environmental Quality Monitoring Branch in conjunction with Fort Saskatchewan Regional Industrial Association, CEC, Calgary, AB.

Draaijers, G. P. J., VanLeeuwen, E. P., DeJong, P. G. H., and Erisman, J. W. (1997). "Base cation deposition in Europe .1. Model description, results and uncertainties." *Atmos. Environ.,* 31(24), 4139-4157.

Dulac, F., Buatmenard, P., Arnold, M., Ezat, U., and Martin, D. (1987). "Atmospheric input of trace-metals to the western Mediterranean-Sea 1. Factors controlling the variability of atmospheric concentrations." *J. Geophys. Res. - Atmospheres,* 92(D7), 8437-8453.

Erisman, J. W., Draaijers, G., Duyzer, J., Hofschreuder, P., VanLeeuwen, N., Romer, F., Ruijgrok, W., Wyers, P., and Gallagher, M. (1997). "Particle deposition to forests - Summary of results and application." *Atmos. Environ.,* 31(3), 321-332.

Hedin, L. O., Granat, L., Likens, G. E., Buishand, T. A., Galloway, J. N., Butler, T. J., and Rodhe, H. (1994). "Steep declines in atmospheric base cations in regions of Europe and North-America." *Nature,* 367(6461), 351-354.

Hicks, B. B., Baldocchi, D. D., Meyers, T. P., Hosker, R. P., and Matt, D. R. (1987). "A preliminary multiple resitance routine for deriving dry deposition velocities from measured quantities." *Wat., Air, Soil Pollut.,* 36(3-4), 311-330.

Hoff, R. M., Leaitch, W. R., Fellin, P., and Barrie, L. A. (1983). "Mass size distributions of chemical-constituents of the winter Arctic aerosol." *J. Geophys. Res. - Oceans and Atmospheres,* 88(NC15), 947-956.

Holsen, T. M., and Noll, K. E. (1992). "Dry Deposition of Atmospheric Particles - Application of Current Models to Ambient Data." *Environ. Sci. Technol.,* 26(9), 1807-1815.

Lovett, G.M. (1994). "Atmospheric deposition of nutrients and pollutants in North America: an ecological perspective." *Ecol. Appl.*, 4, 629-650.

Mahrt, L., Vickers, D., Sun, J. L., Jensen, N. O., Jorgensen, H., Pardyjak, E., and Fernando, H. (2001). "Determination of the surface drag coefficient." *Bound.-Layer Meteorol.,* 99(2), 249-276.

Meyers, T. P., Finkelstein, P., Clarke, J., Ellestad, T. G., and Sims, P. F. (1998). "A multilayer model for inferring dry deposition using standard meteorological measurements." *J. Geophys. Res. - Atmospheres,* 103(D17), 22645-22661.

Meyers, T. P., Hall, M. E., Lindberg, S. E., and Kim, K. (1996). "Use of the modified Bowen-ratio technique to measure fluxes of trace gases." *Atmos. Environ.,* 30(19), 3321-3329.

Milford, J. B., and Davidson, C. I. (1985). "The Sizes of Particulate Trace-Elements in the Atmosphere - a Review." *J. Air Pollut. Control Assoc.,* 35(12), 1249-1260.

Niyogi, D. D. S., Alapaty, K., and Raman, S. (2003). "A photosynthesis-based dry deposition modeling approach." *Wat., Air, Soil Pollut.,* 144(1), 171-194.

Panofsky, H. A. (1974). "Atmospheric Boundary-Layer Below 150 Meters." *Annu. Rev. Fluid Mech.,* 6 147-177.

Peters, L. K., Berkowitz, C. M., Carmichael, G. R., Easter, R. C., Fairweather, G., Ghan, S. J., Hales, J. M., Leung, L. R., Pennell, W. R., Potra, F. A., Saylor, R. D., and Tsang, T. T. (1995). "The current state and future-direction of Eulerian models in simulating the

tropospheric chemistry and transport of trace species – a review." *Atmos. Environ.,* 29(2), 189-222.

Ruijgrok, W., Davidson, C. I., and Nicholson, K. W. (1995). "Dry deposition of particles – implications and recommendations for mapping of deposition over Europe." *Tellus Series B-Chem. Phys. Meteorol.,* 47(5), 587-601.

Ruijgrok, W., Tieben, H., and Eisinga, P. (1997). "The dry deposition of particles to a forest canopy: A comparison of model and experimental results." *Atmos. Environ.,* 31(3), 399-415.

Sehmel, G. A. (1980). "Particle and gas dry deposition – a review." *Atmos. Environ.,* 14(9), 983-1011.

Slinn, W. G. N. (1982). "Predictions for particle deposition to vegetative canopies." *Atmos. Environ.,* 16(7), 1785-1794.

Smith, R. I., Fowler, D., Sutton, M. A., Flechard, C., and Coyle, M. (2000). "Regional estimation of pollutant gas dry deposition in the UK: model description, sensitivity analyses and outputs." *Atmos. Environ.,* 34(22), 3757-3777.

Venkatram, A., Karamchandani, P. K., and Misra, P. K. (1988). "Testing a comprehensive acid deposition model." *Atmos. Environ.,* 22(4), 737-747.

Voldner, E. C., Barrie, L. A., and Sirois, A. (1986). "A Literature-Review of Dry Deposition of Oxides of Sulfur and Nitrogen with Emphasis on Long-Range Transport Modeling in North-America." *Atmos. Environ.,* 20(11), 2101-2123.

Walcek, C. J., Brost, R. A., Chang, J. S., and Wesely, M. L. (1986). "SO_2, Sulfate and HNO_3 Deposition Velocities Computed using Regional Land-use and Meteorological Data." *Atmos. Environ.,* 20(5), 949-964.

WBK and Associates Inc. (WBK). (2006). "Dry Deposition Monitoring Method In Alberta, Phase II." Prepared for Science and Standards Branch, Alberta Environment, Edmonton, AB. March 2006.

Wesely, M. L., and Hicks, B. B. (2000). "A review of the current status of knowledge on dry deposition." *Atmos. Environ.,* 34(12-14), 2261-2282.

Wesely, M. L., and Hicks, B. B. (1977). "Some Factors that Affect Deposition Rates of Sulfur-Dioxide and Similar Gases on Vegetation." *J. Air Pollut. Control Assoc.,* 27(11), 1110-1116.

Whitby, K. T. (1978). "Physical characteristics of sulfur aerosols." *Atmos. Environ.,* 12(1-3), 135-159.

Wiman, B. L. B., and Agren, G. I. (1985). "Aerosol depletions and deposition in forests – a model analysis." *Atmos. Environ.,* 19(2), 335-347.

Wolff, G. T. (1984). "On the nature of nitrate in coarse Continental aerosols." *Atmos. Environ.,* 18(5), 977-981.

Wyers, G. P., and Erisman, J. W. (1998). "Ammonia exchange over coniferous forest." *Atmos. Environ.,* 32(3), 441-451.

Zhang, L., Brook, J. R., and Vet, R. (2003). "A revised parameterization for gaseous dry deposition in air-quality models." *Atmos. Chem. Physics,* 3 2067-2082.

Zhang, L. M., Brook, J. R., and Vet, R. (2002a). "On ozone dry deposition - with emphasis on non-stomatal uptake and wet canopies." *Atmos. Environ.,* 36(30), 4787-4799.

Zhang, L., M. Moran, P. Makar, J. Brook, and S. Gong. (2002b). "Modelling gaseous dry deposition in AURAMS – A Unified Regional Air-quality Modelling System." *Atmos. Environ.*, 36, 537–560.

Zhang, L. M., Gong, S. L., Padro, J., and Barrie, L. (2001a). "A size-segregated particle dry deposition scheme for an atmospheric aerosol module." *Atmos. Environ.,* 35(3), 549-560.

Zhang, L. M., Moran, M. D., and Brook, J. R. (2001b). "A comparison of models to estimate in-canopy photosynthetically active radiation and their influence on canopy stomatal resistance." *Atmos. Environ.,* 35(26), 4463-4470.

Appendix A Environment Canada Calculation Methods for Gases and Particulates

(after Brook *et al.*, 1999; Zhang *et al.*, 2003, 2002a, 2002b, 2001a, and 2001b)

Parameters (for gases):

$cos\alpha$:	cosine of sun/leaf angle, set as 0.5
$cos\theta$:	cosine of solar zenith angle
D_{ENVC}:	water-vapour-pressure deficit
D_i:	molecular diffusivity
D_v:	water diffusivity
E:	ambient water vapour pressure (kPa)
$E^*(T)$:	saturation water vapour pressure (kPa) at air temperature T (°K)
$FCLD$:	fraction of cloud covering (%)
$f(D)$:	conductance-reducing effects of water-vapour-pressure deficit D
$f(T)$:	conductance-reducing effects of air temperature T (°C)
f_{snow}:	snow cover fraction
$f(\psi)$:	conductance-reducing effects of water stress ψ
g:	gravitational acceleration (9.81 m/s^2)
$G_s(PAR)$:	unstressed leaf stomatal conductance
H:	sensible heat flux
k:	von Karman constant (0.4)
L:	Monin-Obukhov length
LAI:	Leaf Area Index
LUC:	Land Use Category (26 *LUCs* in gas model)
MW:	Molecular Weight, $MW_{air} = 29$
P:	surface pressure (kPa)
PAR:	Photosynthetic Active Radiation
$Prec$:	precipitation (mm/hour)
R_a:	aerodynamic resistance (s/m)
R_{ac}:	in-canopy aerodynamic resistance (not chemical species-dependent)
R_b:	boundary-layer resistance (s/m)
R_B:	Bulk Richardson number
R_c:	surface resistance (s/m)
R_{cut}:	cuticle uptake resistance (scaled from SO_2 and O_3's R_{cut})
R_{cutd0}:	reference values of dry cuticle resistance, see Table A1

R_{cutw0}: reference values of wet cuticle resistance, see Table A1 for R_{cutw0} (O_3)

R_{cutw0}(SO_2): 50 s/m or 100 s/m for rain or dew conditions, respectively

R_g: ground resistance (scaled from SO_2 and O_3's R_g)

RH: relative humidity (%)

R_m: mesophyll resistance (dependent only on chemical species)

R_{st}: stomatal resistance

SC: Seasonal Category (5 in particulate model)

Sd: snow depth (cm)

Sd_{max}: maximum snow depth (cm)

SR: solar radiation (W/m^2)

T_{avg}: temperature average, $T_{avg} = (T_{2p} + T_s)/2$

T_d: temperature difference (°K)

T_s: surface temperature (°K)

$T_{2\,ENVC}$: temperature at reference height (°K)

T_{2p}: potential temperature at reference height (°K)

u: horizontal wind speed at reference height (m/s)

u^*: friction velocity (m/s)

V_d: deposition velocity (m/s)

V_i: thermal diffusivity

W_{st}: fraction of stomatal blocking under wet conditions

z: reference height (10m)

z_0: surface roughness length (m)

ψ_{c1} and ψ_{c2}: leaf-water-potential dependency

ψ_{ENVC}: water stress

ψ_H: stability function

Deposition Velocity:

$$V_d = \frac{1}{R_a + R_b + R_c}$$

Aerodynamic Resistance (R_a):

ENVC adapts the Acid Deposition and Oxidant Model (ADOM) formulated by Pleim et. al. (1984) as cited in Zhang *et al.* (2001b) and further investigated by Padro *et al.* (1990) as cited in Zhang *et al.* (2001b).

$R_a = \frac{1}{ku_*}[0.74\ln(z/z_0) - \psi_H]$, with a lower limit of 5 and an upper limit of 1000 (upper limit of 2000 if water or lake as land use)

Friction velocity:

$$u^* = \begin{cases} \dfrac{ku}{\ln\left(\frac{z}{z0}\right)(1+4.7Ri)} & \textit{Stable},\ Ri > 0 \\ \dfrac{ku}{\ln\left(\frac{z}{z0}\right)}\sqrt{1-\dfrac{9.4Ri}{1+7.4\left[k/\ln\left(\frac{z}{z0}\right)\right]^2\sqrt{|Ri|}}} & \textit{Unstable},\ Ri < 0 \end{cases}$$

Bulk Richardson number:

$R_B = \frac{gzT_d}{T_s u^2}$, with a fixed value of $1\text{x}10^{-15}$ if SR>0 and R_B>0

Temperature difference:

$T_d = T_{2p} - T_s$, with an upper limit of -10^{-10} for negative values and a lower limit of 10^{-10} for positive values

Stability function:

$$\psi_H = \begin{cases} -4.7\frac{z}{L} & \textit{stable},\ 0 < \frac{z}{L} < 1 \\ 0.74 \times 2\ln\left\{\dfrac{1+\sqrt{1-9\frac{z}{L}}}{2}\right\} & \textit{unstable},\ -1 < \frac{z}{L} < 0 \end{cases}$$

Monin-Obukhov length:

$L = \dfrac{T_{avg} u_*^3}{kHg}$, with an upper limit of -5 on the negative side and a lower limit of +5 on the positive side

Sensible heat flux:

$$H = \begin{cases} \left\{\dfrac{uT_d}{0.74}\right\}\left\{\dfrac{k}{\ln(z/z0)}\right\}^2\left\{\dfrac{1}{(1+4.7Ri)^2}\right\} & Stable,\ Ri > 0 \\ \left\{\dfrac{uT_d}{0.74}\right\}\left\{\dfrac{k}{\ln(z/z0)}\right\}^2\left\{1-\dfrac{9.4Ri}{1+5.3[k/\ln(z/z0)]^2\sqrt{|Ri|}}\right\} & Unstable,\ Ri < 0 \end{cases}$$

<u>Sub Layer Resistance (*Rb*)</u>:

$$R_b = \frac{5}{u_*}\left(\frac{Vi}{Di}\right)^{2/3}$$

Thermal diffusivity:

$$V_i = \frac{145.8\times10^{-4}T_{avg}^{3/2}}{T_{avg}+110.4}$$

Molecular diffusivity:

$$D_i = \frac{0.001T_s^{7/4}\sqrt{\dfrac{1}{MW_{gas}}+\dfrac{1}{MW_{air}}}}{(D_{air}^{1/3}+D_{gas}^{1/3})^2}$$

$$D_{gas} = 0.369MW_{gas} + 6.29$$
$$D_{air} = 0.369MW_{air} + 6.29$$

<u>Total Surface Resistance (*Rc*)</u>:

$\dfrac{1}{R_c} = \dfrac{1-W_{st}}{R_{st}+R_m} + \dfrac{1}{R_{ac}+R_g} + \dfrac{1}{R_{cut}}$, with a lower limit of 10 s/m

Fraction of stomatal blocking under wet conditions:

$$W_{st} = \begin{cases} 0 & SR \le 200 Wm^{-2} \\ (SR-200)/800 & 200 < SR \le 600 Wm^{-2} \\ 0.5 & SR > 600 Wm^{-2} \end{cases}$$

Stomatal resistance:

$$R_{st} = \frac{1}{G_s(PAR) f(T) f(D) f(\psi) D_i / D_v}$$

Water diffusivity:

$$D_v = \frac{0.001 T_s^{7/4} \sqrt{\frac{1}{MW_{water}} + \frac{1}{MW_{air}}}}{\left(D_{air}^{1/3} + D_{water}^{1/3}\right)^2}$$

Unstressed leaf stomatal conductance:

$$G_s(PAR) = F_{sun} / r_{st}(PAR_{sun}) + F_{shade} / r_{st}(PAR_{shade})$$

$$F_{sun} = 2\cos\theta\left[1 - e^{-0.5LAI/\cos\theta}\right]$$
$$F_{shade} = LAI - F_{sun}$$

$$r_{st}(PAR) = r_{st\min}(1 + b_{rs} / PAR)$$

$$PAR_{shade} = \begin{cases} R_{diff} e^{(-0.5LAI^{0.7})} + 0.07 R_{dir}(1.1 - 0.1LAI) e^{-\cos\theta} & LAI < 2.5 \quad or \quad SR < 200 wm^{-2} \\ R_{diff} e^{(-0.5LAI^{0.8})} + 0.07 R_{dir}(1.1 - 0.1LAI) e^{-\cos\theta} & LAI > 2.5 \quad and \quad SR > 200 wm^{-2} \end{cases}$$

$$PAR_{sun} = \begin{cases} R_{dir} \cos\alpha / \cos\theta + PAR_{shade} & LAI < 2.5 \quad or \quad SolarRad < 200 wm^{-2} \\ R_{dir}^{0.8} \cos\alpha / \cos\theta + PAR_{shade} & LAI > 2.5 \quad and \quad SolarRad > 200 wm^{-2} \end{cases}$$

Conductance-reducing effects of air temperature T:

$$f(T) = \frac{T - T_{\min}}{T_{opt} - T_{\min}} \left[\frac{T_{\max} - T}{T_{\max} - T_{opt}}\right]^{br} \qquad \text{where } br = \frac{T_{\max} - T_{opt}}{T_{opt} - T_{\min}}$$

Conductance-reducing effects of water-vapour-pressure deficit D:

$f(D) = 1 - b_{upd} D$, with a lower limit of 0.1 and a upper limit of 1

Water-vapour-pressure deficit:

$$D = E^*(T) - E$$

Saturation vapor pressure:

$E^*(T) = 0.6108e^{\frac{17.27(T-273.16)}{T-35.86}}$ (in units of mb in program code)

Ambient water vapour pressure:

$$E = E^*(T)RH$$

Conductance-reducing effects of water stress:

$$f(\psi_{ENVC}) = \begin{cases} (\psi_{ENVC} - \psi_{c2})/(\psi_{c1} - \psi_{c2}) & \psi_{ENVC} < \psi_{c1} \\ 1 & \psi_{ENVC} \geq \psi_{c1} \end{cases}$$

where $\psi_{ENVC} = -0.72 - 0.0013SR$, with a lower limit of 0.1 and upper limit of 1

Mesophyll resistance:

Values of R_m for all dry-depositing species in AURAMS gas-phase chemical mechanism listed in Table A1.

In-canopy aerodynamic resistance:

$$R_{ac} = \frac{R_{ac0} LAI^{1/4}}{u_*^2}$$ where

R_{ac0}: reference value for in-canopy aerodynamic resistance (Table 1)
LAI: Leaf area index (Table 1)

For some $LUCs$, a range of R_{ac0} values is given to reflect the change of canopy structure at different times of the growing season. R_{ac0} values for any day of the year based on minimum and maximum LAI values given as:

$$R_{ac0}(t) = R_{ac0}(\min) + \frac{LAI(t) - LAI(\min)}{LAI(Max) - LAI(\min)} \times \left[R_{ac0}(\max) - R_{ac0}(\min)\right]$$

Ground resistance:

$$\frac{1}{R_g(i)} = \frac{\alpha(i)}{R_g(SO_2)} + \frac{\beta(i)}{R_g(O_3)}$$

where

$$R_g(O_3) = \begin{cases} 2000\ s\ m^{-1} & LUC\ 1-3\ and\ Snow\ Surface \\ 200\ s\ m^{-1} & LUC\ 4-19,\ 25\ and\ 26 \\ 500\ s\ m^{-1} & LUC\ 20-24 \end{cases}$$

For snow surface, $R_g(O_3)$ adjusted by including a snow cover fraction(f_{snow}):

$$\frac{1}{R_g(O_3)} = \frac{1-2f_{snow}}{R_g(LUC)} + \frac{2f_{snow}}{R_{snow}}$$

where

$f_{snow} = \frac{sd}{sd_{\max}}$, note – both f_{snow} and $2f_{snow}$ have a lower limit of 0 and upper limit of 1

$R_{snow} = 2000$ s/m

$$R_g(SO_2) = \begin{cases} 20\ s\ m^{-1} & LUC\ 1\ and\ 3 \\ 70(2-T) & LUC\ 2,\ T\ as\ Surface\ Temperature\ (°C) \\ 50 & LUC\ 4-26,\ Rain \\ 100 & LUC\ 4-26,\ Dew \\ R_{gd},\ (Table\ 1) & LUC\ 4-26,\ Not\ Rain\ or\ Dew,\ T \geq -1°C \\ \min(2R_{gd}, R_{gd}e^{0.2(-1-T)}) & LUC\ 4-26,\ Not\ Rain\ or\ Dew,\ T < -1°C \end{cases}$$

with a lower limit of 100 s/m and upper limit of 500 s/m (limit only applies to *LUC* 2)

For snow surface, $R_g(SO_2)$ are adjusted by snow cover fraction(f_{snow}):

$$\frac{1}{R_g(SO_2)} = \frac{1-2f_{snow}}{R_g(LUC)} + \frac{2f_{snow}}{R_{snow}}$$

where

$f_{snow} = \frac{sd}{sd_{\max}}$, note – both f_{snow} and $2f_{snow}$ have a lower limit of 0 and upper limit of 1

$R_{snow} = 70(2-T)$, T as °C

Canopy cuticle resistance:

$$R_{cut} = \begin{cases} \frac{R_{cutw0}}{LAI^{1/2}u_*} & Rain\ or\ Dew \\ \frac{R_{cutd0}}{e^{0.03RH}LAI^{1/4}u_*} & Not\ Rain \\ \min(2R_{cut}, R_{cut}e^{0.2(-1-T)}) & T < -1°C \end{cases}$$

where

$R_{cutw0}(O_3)$ listed in Table 1.
$R_{cutw0}(SO_2)$ = 50 s/m or 100 s/m for rain or dew conditions, respectively.
R_{cutd0} listed in Table 1.

with a lower limit of 100 s/m and 20 s/m for SO_2 dry and wet conditions, respectively

For snow surface, R_{cut} are adjusted by including a snow cover fraction (f_{snow})

$$\frac{1}{R_{cut}} = \frac{1-f_{snow}}{R_{cut}} + \frac{f_{snow}}{R_{snow}}$$

where

$$R_{snow} = \begin{cases} 2000 & O_3 \\ 70(2-T) & SO_2 \end{cases}$$

Roughness length:

$$z_0(t) = z_0(\min) + \frac{LAI(t) - LAI(\min)}{LAI(Max) - LAI(\min)} \times [z_0(\max) - z_0(\min)]$$

Rain or Dew conditions:

$$Condition = \begin{cases} Rain & T > 273.15°K \ and \ \Pr ec. > 0.1mm/hr \\ Dew & T > 273.15°K \ and \ u^* > u^*_{\min} \end{cases}$$

where:

$$u^*_{\min} = \frac{1.5Coedew}{DQ}$$

where:

$$Coedew = \begin{cases} 0.3 & FCLD < 0.25 \\ 0.2 & 0.25 \le FCLD < 0.75 \\ 0.1 & 0.75 \le FCLD \le 1 \end{cases}$$

and

$DQ = 0.0622(1-RH)E^*(T_s)$, with a lower limit of 0.0001

Parameters (for particulates):

(Variables for computing R_a were not included)

C:	Cunningham slip correction factor
D_B:	Brownian diffusivity
dp:	particle diameter
E_B:	collection efficiency from Brownian diffusion
E_{IM}:	collection efficiency from impaction
E_{IN}:	collection efficiency from interception
g:	gravitational acceleration (9.81 m/s^2)
K:	Boltzmann constant ($g*cm^2/s^2/°K$)
LAI:	Leaf Area Index
LUC:	Land Use Category (15 *LUCs* in particle model)
P:	surface pressure (kPa)
R_a:	aerodynamic resistance (s/m)
R_1:	correction factor representing fraction of particles that sticks to surface
R_s:	surface resistance (s/m)
Sc:	Schmidt number
SC:	Season Category (5 SCs in particle model, listed in Table A5)
St:	Stokes number
$T_{2\,ENVC}$:	temperature at reference height (°K)
u:	horizontal wind speed at reference height (m/s)
u^*:	friction velocity (m/s)
V_d:	deposition velocity (m/s)
λ:	mean free path of air molecules
μ:	dynamic viscosity of air
ν:	kinematic viscosity of air
ρ:	density of particle

Deposition Velocity:

$$V_d = V_g + \frac{1}{R_a + R_s}$$

Assumes SO_4^{2-} and NH_4^+ have the same V_d; and NO_3^-, Ca^{2+}, Mg^{2+}, Na^+, and K^+ have the same V_d as described in Cheng *et al.* (2001).

Mass median diameter (MMD) and geometric standard deviation (GSD) for SO_4^{2-} chosen as 0.35 μm and 2.0 μm, respectively as reported in Wesely *et al.* (1985).

MMD and GSD for Na^+ are taken as 5.12 μm and 2.64 μm, respectively as reported in Ruijgrok *et al* (1997).

Gravitational settling velocity:

$$V_g = \frac{\rho d_p^2 g C}{18\mu}$$

Cunningham slip correction factor:

$$C = 1 + \frac{2\lambda}{d_p}(1.257 + 0.4e^{-0.55 d_p/\lambda})$$

Aerodynamic Resistance:

R_a is computed with the same approach as the gas model, but the parameters are adapted from Table 4.

Surface Resistance:

$$R_s = \frac{1}{\varepsilon_0 u_* (E_B + E_{IM} + E_{IN}) R_1}, \text{ with a lower limit of 5}$$

where ε_0 is an empirical constant chosen as 3 for all *LUCs*

Collection efficiency from Brownian diffusion:

$$E_B = Sc^{-\gamma}$$

where γ lies between $^1/_2$ and $^2/_3$ with larger values for rougher surfaces. (Table A4)

Schmidt number:

$$Sc = \nu / D$$

Collection efficiency from impaction:

$$E_{IM} = \left(\frac{St}{\alpha + St}\right)^{\beta}$$

where

α: constant varying with *LUC* (Table A4)
β: constant, chosen as 2

Stokes number:

$$St = \begin{cases} \dfrac{V_g u^{*2}}{\nu} & \textit{smooth surface, LUC 8, 9, 12, 13, and 14} \\ \dfrac{V_g u^{*} A}{g} & \textit{vegetated surface, LUCs other than above} \end{cases}$$

where A is the characteristic radius varying with *LUC* and season (Table A4)

Collection efficiency from interception:

$E_{IN} = \frac{1}{2}\left(\frac{d_p}{A}\right)^2$, with a upper limit of 0.6

where A is the characteristic radius varying with *LUC* and season (Table A4)

Correction factor representing fraction of particles that sticks to the surface:

$R_1 = \exp(-St^{1/2})$, with a low limit of 0.5

Mean free path of air molecules:

$$\lambda = 6.54 \times 10^{-8} \frac{\mu}{1.818 \times 10^{-5}} \frac{101.3}{P} \left(\frac{T_2}{293.15}\right)^{1/2}$$

Brownian diffusivity:

$$D_B = \frac{CKT_2}{3\pi d_p \mu}$$

Dynamic viscosity of air:

$$\mu = \frac{145.8 \times 10^{-8} T_2^{3/2}}{T_2 + 110.4}$$

Kinematic viscosity of air:

$$\nu = \frac{\mu}{\rho_{air}}$$

Bin division:

For I = 1 to 40,

$$binsize = 0.001 * I^{2.5}$$

Units required for input parameters to Visual Basic Program

hourly pollutant concentration:	$\mu g/m^3$
hourly cloud fraction:	tenths (converted to decimal within program)
hourly pressure:	kPa (converted to mb within program)
hourly snow depth:	cm
hourly precipitation:	mm
hourly solar radiation:	W/m^2
hourly relative humidity:	% (converted to decimal within program)
hourly wind speed:	km/hr (converted to m/s within program)
hourly temperature:	°C (converted to K within program)

Table A1 *LUC* and all related parameters (all resistances have units of s/m; na = not applicable; f(u) = function of wind speed).

LUC	R_{sc0}	$R_{cut\,d0}$ O_3	$R_{cut\,w0}$ O_3	$R_{cut\,d0}$ SO_2	R_{gd} SO_2	r_{smin} (s/m)	b_{rs} (Wm^{-2})	T_{min} (°C)	T_{max} (°C)	T_{opt} (°C)	b_{vpd} (kPa^{-1})	ψ_{c1} (Mpa)	ψ_{c2} (Mpa)	z_0 (m)	Sd_{max} (cm)
water	0	na	na	na	20	na	na	na	na	na	na	na	na	f(u)	na
ice	0	na	na	na	Eq. (8a)	na	na	na	na	na	na	na	na	0.01	1
inland lake	0	na	na	na	20	na	na	na	na	na	na	na	na	f(u)	na
evergreen needleleaf trees	100	4000	200	2000	200	250	44	−5	40	15	0.31	−2	−2.5	0.9	200
evergreen broadleaf trees	250	6000	400	2500	100	150	40	0	45	30	0.27	−1	−5.0	2.0	400
deciduous needleleaf trees	60–100	4000	200	2000	200	250	44	−5	40	15	0.31	−2	−2.5	0.4–0.9	200
deciduous broadleaf trees	100–250	6000	400	2500	200	150	43	0	45	27	0.36	−1.9	−2.5	0.4–1.0	200
tropical broadleaf trees	300	6000	400	2500	100	150	40	0	45	30	0.27	−1	−5.0	2.5	400
drought deciduous trees	100	8000	400	6000	300	250	44	0	45	25	0.31	−1	−4.0	0.6	200
evergreen broadleaf shrubs	60	6000	400	2000	200	150	40	0	45	30	0.27	−2	−4.0	0.2	50
deciduous shrubs	20–60	5000	300	2000	200	150	44	−5	40	15	0.27	−2	−4.0	0.05–0.2	50
thorn shrubs	40	5000	300	2000	200	250	44	0	45	25	0.27	−2	−3.5	0.2	50
short grass and forbs	20	4000	200	1000	200	150	50	5	40	30	0	−1.5	−2.5	0.04	5
long grass	10–40	4000	200	1000	200	100	20	5	45	25	0	−1.5	−2.5	0.02—0.1	20
crops	10–40	4000	200	1500	200	120	40	5	45	27	0	−1.5	−2.5	0.02–0.1	10
rice	10–40	4000	200	1500	50	120	40	5	45	27	0	−1.5	−2.5	0.02–0.1	10
sugar	10–40	4000	200	2000	200	120	50	5	45	25	0	−1.5	−2.5	0.02–0.1	10
maize	10–50	5000	300	2000	200	250	65	5	45	25	0	−1.5	−2.5	0.02–0.1	10
cotton	10–40	5000	300	2000	200	125	65	10	45	30	0	−1.5	−2.5	0.02–0.2	10
irrigated crops	20	4000	200	2000	50	150	40	5	45	25	0	−1.5	−2.5	0.05	10
urban	40	6000	400	4000	300	200	42	0	45	22	0.31	−1.5	−3	1.0	50
tundra	0	8000	400	2000	300	150	25	−5	40	20	0.24	0	−1.5	0.03	2
swamp	20	5000	300	1500	50	150	40	0	45	20	0.27	−1.5	−2.5	0.1	10
Desert	0	na	na	na	700	na	na	na	na	na	na	na	na	0.04	2
mixed wood forests	100	4000	200	2500	200	150	44	−3	42	21	0.34	−2	−2.5	0.6–0.9	200
Transitional forest	100	4000	200	2500	200	150	43	0	45	25	0.31	−2	−3	0.6–0.9	200

Table A2 LAI(i) values dependent upon Land Use Category (*LUC*) ("i" represents month number, "i=14" and "i=15" represent minimum and maximum value, respectively).

LUC	1	2	3	4	5	6	7	8	9	10	11	12	13	14	15
water	0	0	0	0	0	0	0	0	0	0	0	0	0	0	0
ice	0	0	0	0	0	0	0	0	0	0	0	0	0	0	0
inland lake	0	0	0	0	0	0	0	0	0	0	0	0	0	0	0
evergreen needleleaf trees	5	5	5	5	5	5	5	5	5	5	5	5	5	5	5
evergreen broadleaf trees	6	6	6	6	6	6	6	6	6	6	6	6	6	6	6
deciduous needleleaf trees	0.1	0.1	0.5	1.0	2.0	4.0	5.0	5.0	4.0	2.0	1.0	0.1	0.1	0.1	5.0
deciduous broadleaf trees	0.1	0.1	0.5	1.0	2.0	4.0	5.0	5.0	4.0	2.0	1.0	0.1	0.1	0.1	5.0
tropical broadleaf trees	6	6	6	6	6	6	6	6	6	6	6	6	6	6	6
drought deciduous trees	4	4	4	4	4	4	4	4	4	4	4	4	4	4	4
evergreen broadleaf shrubs	3	3	3	3	3	3	3	3	3	3	3	3	3	3	3
deciduous shrubs	0.5	0.5	1.0	1.0	1.5	2.0	3.0	3.0	2.0	1.5	1.0	0.5	0.5	0.5	3.0
thorn shrubs	3	3	3	3	3	3	3	3	3	3	3	3	3	3	3
short grass and forbs	1	1	1	1	1	1	1	1	1	1	1	1	1	1	1
long grass	0.5	0.5	0.5	0.5	0.5	0.5	1.0	2.0	2.0	1.5	1.0	1.0	0.5	0.5	2.0
crops	0.1	0.1	0.1	0.5	1.0	2.0	3.0	3.5	4.0	0.1	0.1	0.1	0.1	0.1	4.0
rice	0.1	0.1	0.1	0.5	1.0	2.5	4.0	5.0	6.0	0.1	0.1	0.1	0.1	0.1	6.0
sugar	0.1	0.1	0.1	0.5	1.0	3.0	4.0	4.5	5.0	0.1	0.1	0.1	0.1	0.1	5.0
maize	0.1	0.1	0.1	0.5	1.0	2.0	3.0	3.5	4.0	0.1	0.1	0.1	0.1	0.1	4.0
cotton	0.1	0.1	0.1	0.5	1.0	3.0	4.0	4.5	5.0	0.1	0.1	0.1	0.1	0.1	5.0
irrigated crops	1	1	1	1	1	1	1	1	1	1	1	1	1	1	1
urban	0.1	0.1	0.1	0.1	0.5	1.0	1.0	1.0	1.0	1.0	0.4	0.1	0.1	0.1	1.0
tundra	1.0	1.0	0.5	0.1	0.1	0.1	0.1	1.0	2.0	1.5	1.5	1.0	1.0	0.1	2.0
swamp	4	4	4	4	4	4	4	4	4	4	4	4	4	4	4
Desert	0	0	0	0	0	0	0	0	0	0	0	0	0	0	0
mixed wood forests	3.0	3.0	3.0	4.0	4.5	5.0	5.0	5.0	4.0	3.0	3.0	3.0	3.0	3.0	5.0
Transitional forest	3.0	3.0	3.0	4.0	4.5	5.0	5.0	5.0	4.0	3.0	3.0	3.0	3.0	3.0	5.0

Table A3 Species-specific chemical and physical parameters.[a]

No.	Symbol	Name	Depn Mmts	MW	H (M atm^{-1})	H* (M atm^{-1})	pe^0 (W)	Rm	a	b
1	SO_2	Sulphur dioxide	Yes	64	(1.1-1.5) x 10^0	2.65 x 10^5	75.5 to -7.6	0	1	0
2	H_2SO_4	Sulphuric acid	No	98	2.1 x 10^5	>2.1 x 10^5	4.9 to -4.3	0	1	1
F	NO	Nitric oxide	Yes	30	(1.4-1.9) x10^{-3}	H	27.8 to 3.0	Not considered		
3	NO_2	Nitrogen dioxide	Yes	46	(0.7-4.1) x 10^{-2}	H	28.4 to 8.2	0	0	0.8
4	O_3	Ozone	Yes	48	(0.9-1.3) x 10^{-2}	H	28.1 to 18.6	0	0	1
5	H_2O_2	Hydrogen peroxide	Yes	34	(0.7-1.4) x 10^5	H	24.8 to 9.7	0	1	1
6	HNO_3	Nitric acid	Yes	63	(0.1-2.6) x 10^6	3.2 x 1013	14.1 to 8.9	0	10	10
7	HONO	Nitrous acid	Yes	47	(3.7-5.0) x 10^1	2.6 x 105	17.5 to 14.8	0	2	2
8	HNO_4	Pernitric acid	No	79	(0.1-1) x 10^5	>1 x 107	No data	0	5	5
9	NH_3	Ammonia	Yes	17	(1.0-7.8) x 10^1	1.1 x 104	Not applicable	0	1	0
10	PAN	Peroxyacetylnitrate	Yes	121	(2.8-5.0) x 10^0	H	30.2 to -1.5	0	0	0.6
11	PPN	Peroxypropylnitrate	No	135	2.9 x 10^0	H	37.8 to -2.3	0	0	0.6
12	APAN	Aromatic acylnitrate	No	183	No data	5	46.9 to 11.2	0	0	0.8
13	MPAN	Peroxymethacrylic nitric anhydride	No	147	1.7 x 10^0	H	3.1	0	0	0.3
14	HCHO	Formaldehyde	Yes	30	(0.3-1.4) x 10^4	4.9 x 103	3.0 to -0.1	0	0.8	0.2
15	MCHO	Acetaldehyde	No	44	(1.0-1.7) x 10^1	≥15	-1.0 to -3.9	100	0	0.05
16	PALD	C3 carbonyls	No	58	(2.4-3.7) x 10^0	H	-1.3 to -1.8	100	0	0.05
17	C4A	C4–C5 carbonyls	No	72	(0.9-1.8) x 10^1	H	-1.3 to -1.8	100	0	0.05
18	C7A	C6–C8 carbonyls	No	128	(0.4-11) x 10^1	H	-1.5	100	0	0.05
19	ACHO	Aromatic carbonyls	No	106	(3.5-4.2) x 10^1	H	-1.0 to -2.5	100	0	0.05
20	MVK	Methyl-vinyl-ketone	No	70	(2.1-4.4) x 10^1	H	0.2	0	0	0.05
21	MACR	Methacrolein	No	70	(4.3-6.5) x 10^0	H	-1.2	100	0	0.05
22	MGLY	Methylgloxal	No	72	(0.4-3.2) x 10^4	H	-0.7	0	0.01	0
23	MOH	Methyl alcohol	No	32	(1.4-2.3) x 10^2	≥H	3.0	0	0.6	0.1
24	ETOH	Ethyl alcohol	No	46	(1.2-2.3) x 10^2	≥H	-1.3 to -2.9	0	0.6	0
25	POH	C3 alcohol	No	60	(0.9-1.7) x 10^2	≥H	-0.3	0	0.4	0
26	CRES	Cresol	No	104	8.3 x 10^2	H	-2.5	0	0.01	0
27	FORM	Formic acid	Yes	46	(0.9-8.9) x 10^3	9.8 x 10^6	1.9 to -6.4	0	2	0
28	ACAC	Acetic acid	Yes	60	(0.8-9.3) x 10^3	9.6 x 10^5	-3.1 to -9.6	0	1.5	0
29	ROOH	Organic peroxides	Yes	48	(0.1-3.1) x 10^2	H	4.2 to 3.6	0	0.1	0.8
30	ONIT	Organic nitrates	No	77	2.0 x 10^0	H	10.5 to -5.0	100	0	0.5
31	INIT	Isoprene nitrate	No	147	2.0 x 10^0	H	No data	100	0	0.5

[a] Values for Henry's Law constant (H) were obtained from Howard and Meylan (1997) and Sander (1999).

Table A4 Parameters related to *LUC* and SC in particle model.

NO.	Land use categories Description (LUC)	Z_0 (m)					A (mm)						
		SC 1	SC 2	SC 3	SC4	SC 5	SC 1	SC 2	SC 3	SC 4	SC 5		
1	Evergreen}needleleaf trees	0.8	0.9	0.9	0.9	0.8	2	2	2	2	2	1	0.56
2	Evergreen broadleaf trees	2.65	2.65	2.65	2.65	2.65	5	5	5	5	5	0.6	0.58
3	Deciduous needleleaf trees	0.85	0.85	0.8	0.55	0.6	2	2	5	5	2	1.1	0.56
4	Deciduous broadleaf trees	1.05	1.05	0.95	0.55	0.75	5	5	10	10	5	0.8	0.56
5	Mixed broadleleaf and needleaf trees	1.15	1.15	1.15	1.15	1.15	5	5	5	5	5	0.8	0.56
6	Grass	0.1	0.1	0.05	0.02	0.05	2	2	5	5	2	1.2	0.54
7	Crops, mixed farming	0.1	0.1	0.02	0.02	0.05	2	2	5	5	2	1.2	0.54
8	Desert	0.04	0.04	0.04	0.04	0.04	na	na	na	na	na	50	0.54
9	Tundra	0.03	0.03	0.03	0.03	0.03	na	na	na	na	na	50	0.54
10	Shrubs and interrupted wood-lands	0.1	0.1	0.1	0.1	0.1	10	10	10	10	10	1.3	0.54
11	Wet land with plants	0.03	0.03	0.02	0.02	0.03	10	10	10	10	10	2	0.54
12	Ice cap and glacier	0.01	0.01	0.01	0.01	0.01	na	na	na	na	na	50	0.54
13	Inland water	f (u)	f (u)	f(u)	f(u)	f (u)	na	na	na	na	na	100	0.5
14	Ocean	f (u)	f (u)	f(u)	f(u)	f (u)	na	na	na	na	na	100	0.5
15	Urban	1	1	1	1	1	10	10	10	10	10	1.5	0.56

Table A5 Latitude values applied for the determination of Seasonal categories (SC) used in particle model.

NO.	Seasonal categories (SC)	Month											
		12	1	2	3	4	5	6	7	8	9	10	11
1	Midsummer with lush vegetation.	<30			<35			<55	<70	<45	<35		
2	Autumn with cropland that has not been harvested.									45-80	35-65	35-45	35-40
3	Late autumn after frost, no snow.										65-80	45-65	40-50
4	Winter, snow on ground and sub-freezing.				>40	>45	>60	>70	>80			>65	>50
5	Transitional spring with partially green short annuals.	30-35			35-40	35-45	35-60	55-70	70-80				

Appendix B Alberta Environment Calculation Methods for Gases and Particulates

(after Cheng *et al.*, 2001 and WBK, 2006)

Parameters:

B	defined equation described herein
C	concentration ($\mu g/m^3$)
D_{AENV}	diffusion coefficient of the substance of interest (cm^2/s)
F	dry deposition flux ($\mu g/m^2/s$)
g	gravitational acceleration (9.81 m/s^2)
H	sensible heat flux (w/m^2)
k	von Karman constant (0.4)
L	Monin-Obukhov length scale
PAI	Potential Acid Input (kg H^+/ha/yr)
Pr	Prandtl number for air (0.72)
R_a	aerodynamic resistance (s/m)
R_b	boundary-layer resistance (s/m)
R_c	surface resistance (s/m)
R_B	Bulk Richardson number
RH	relative humidity
Sc	Schmidt number
SW	soil wetness
T_d	temperature difference between 10 and 2 m (T_{10} - $T_{2\,AENV}$)
$T_{2\,AENV}$	temperature at 2 m (Kelvin)
u	wind speed (m/s)
u^*	friction velocity (m/s)
V_d	deposition velocity (m/s)
$[X]$	concentration of X chemical species deposited (kg/ha/yr)
z	reference height (10 m)
z_0	surface roughness length (m)
η	dynamic viscosity of air (18.0×10^{-6} N-s/m^2 at 1 atm and 25°C)
ρ	density of air (1.18 kg/m^3 at 1 atm and 25°C)
σ_θ	standard deviation of wind direction (rad)
ψ_{AENV}	integrated stability correction term

Equations:

$$PAI_{dry} = \frac{[SO_2]}{64} + \frac{[NO_2]}{46} + \frac{[HNO_2]}{47} + \frac{[HNO_3]}{63} + 2\frac{[SO_4^{2-}]}{96} + \frac{[NO_3^-]}{62} + \frac{[NH_4^+]}{18} - \left(\frac{[K^+]}{39} + \frac{[Na^+]}{23} + 2\frac{[Ca^{2+}]}{40} + 2\frac{[Mg^{2+}]}{24}\right)$$

deposition concentrations units in kg/ha/yr

$$F = V_d C$$

$$V_d = \frac{1}{(R_a + R_b + R_c)}$$

Summary of Species Specific Deposition Velocity Formulae:

$$V_{d\,(SO_2)} = \frac{1}{R_a + R_{b\,(SO_2)} + R_{c\,(SO_2)}}$$

$$V_{d\,(NO_2)} = \frac{1}{R_a + R_{b\,(NO_2)} + R_{c\,(NO_X)}}$$

$$V_{d\,(HNO_3)} = \frac{1}{R_a + R_{b\,(SO_2)}}$$

$$V_{d\,(HNO_2)} = \frac{1}{R_a + R_{b\,(HNO_2)}}$$

R_c is treated as being negligible for nitric and nitrous acid.

$$V_{d\,(SO_4^{2-},\,NH_4^+)} = \frac{1}{R_a + R_{b(SO_4^{2-})}}$$

$$V_{d\,(NO_3^-,\,Ca^{2+},\,Mg^{2+},\,K^+,\,Na^+)} = \frac{1}{R_a + (0.5 \times R_{b(SO_4^{2-})})}$$

Aerodynamic Resistance (R_a):

$$R_a = \frac{1}{ku^*}\left\{\ln\frac{z}{z_0} - \psi\left(\frac{z}{L}\right)\right\}$$ (R_a is infinite and $V_d = 0$ when u and T_d are zero)

Friction velocity:

$u^* = \frac{u\sigma_\theta}{1.9}$ (this relationship is used as an initial estimate of u^* to calculate z_0, a more precise value of u^* is calculated after z_0 is obtained – refer to below)

$z_0 = z\, e^{-\left(\frac{0.4u}{u^*}\right)}$ (calculated as a monthly average using data where the wind speed is >6 m/s)

A more precise value of u^* calculated after z_0 is obtained (based on atmospheric conditions):

$$u^* = ku\left\{\ln\left(\frac{z}{z_0}\right)(1+4.7Ri)\right\}^{-1}$$ *Stable conditions* $R_B > 0$

$$u^* = \frac{ku}{\ln\left(\frac{z}{z_0}\right)\sqrt{1-\left\{\frac{9.4Ri}{1+(7.4B)}\right\}}}$$ *Unstable conditions* $R_B < 0$

$$u^* = \frac{ku}{\ln\left(\frac{z}{z_0}\right)}$$ *Neutral conditions* $R_B = 0$

Bulk Richardson number

$$R_B = \frac{gzT_d}{T_2u^2}$$

Stability function (based on atmospheric conditions):

$$\psi_{AENV} = -\frac{5z}{L} \qquad \textit{Stable conditions}$$

$$\psi_{AENV} = 2\ln\left\{\frac{1}{2}\left(1+\sqrt{1-\frac{15z}{L}}\right)\right\} \qquad \textit{Unstable conditions}$$

$$\psi_{AENV} = 0 \qquad \textit{Neutral conditions}$$

Monin-Obukhov length:

$$L = \frac{T_2 u^{*3}}{kHg}$$

Sensible heat flux (based on atmospheric conditions):

$$\boldsymbol{H} = \left\{\frac{uT_d}{0.74}\right\}\left\{\frac{k}{\ln\left(\frac{z}{z_0}\right)}\right\}^2\left\{\frac{1}{(1+4.7R_B)^2}\right\} \qquad \textit{Neutral and Stable conditions}$$

$$\boldsymbol{H} = \left\{\frac{uT_d}{0.74}\right\}\left\{\frac{k}{\ln\left(\frac{z}{z_0}\right)}\right\}^2\left\{1-\frac{9.4R_B}{(1+5.3B)}\right\} \qquad \textit{Unstable conditions}$$

Where $\boldsymbol{B} = 9.4\left[\frac{k}{\ln\left(z/z_0\right)}\right]^2\left[|R_B|\frac{z}{z_0}\right]^{1/2}$

Boundary Layer Resistance (R_b):

R_b (gases):

$$R_b = \frac{2}{ku_*}\left(\frac{\eta}{\rho D} \times \frac{1}{\mathrm{Pr}}\right)^{2/3}$$

$$R_b = \frac{7.22}{u^*} \quad \text{for } SO_2 \text{ and } HNO_3$$

$$R_b = \frac{6.18}{u^*} \quad \text{for } NO_2$$

$$R_b = \frac{6.09}{u^*} \quad \text{for } HNO_2$$

R_b (particulates):

R_b values for particulate sulphate are obtained from scientific literature for daytime and nighttime as a function of surface type and weighted according to average day length for each month at a mid-Alberta latitude location (54°N latitude) after Cheng and Angle (1993) as cited in Cheng *et al.* (2001).

Table B1 Boundary-Layer Resistance (s/cm) for Fine Particulate (SO_4^{2-}, $NH4^+$), Day Length Weighted Averages at 54°N Latitude for the Middle of Each Month.

Surface Type	Winter (Dec, Jan, Feb)		Spring (Mar, Apr, May)		Summer (Jun, Jul, Aug)		Autumn (Sep, Oct, Nov)	
	Dry	Wet	Dry	Wet	Dry	Wet	Dry	Wet
Deciduous Forest	16.9	0	5.4	0	1.3	0	3.2	0
Coniferous Forest	2.5	0	2.7	0	1.9	0	2.3	0
Wetland/Swamp*	20.4	0	3.8	0	2.6	0	3.2	0
Grassland*	20.4	0	5.6	0	3.9	0	4.7	0
Cropland*	20.4	0	9.0†	0	3.9	0	7.9‡	0
Urban§	33.9	0	10.9	0	2.6	0	6.3	0
Open Water	0	0	0	0	0	0	0	0
Snow/Ice	20.4	0	-	-	-	-	-	-

* in winter, wetland, grassland, and cropland treated as a snow surface. † bare soil and active growth.
‡ bare soil and senescent growth. § consists of a mixture of deciduous forest and buildings.

Table B2 Boundary-Layer Resistance (s/cm) for Coarse Particulate (NO_3^-, Na, K, Ca, Mg) Day Length Weighted Averages at 54°N Latitude for the Middle of Each Month.

Surface Type	Winter (Dec, Jan, Feb)		Spring (Mar, Apr, May)		Summer (Jun, July, Aug)		Autumn (Sep, Oct, Nov)	
	Dry	Wet	Dry	Wet	Dry	Wet	Dry	Wet
Deciduous Forest	8.45	0	2.7	0	0.65	0	1.6	0
Coniferous Forest	1.25	0	1.35	0	0.95	0	1.15	0
Wetland/Swamp*	10.2	0	1.9	0	1.3	0	1.6	0
Grassland*	10.2	0	2.8	0	1.95	0	2.35	0
Cropland*	10.2	0	4.5†	0	1.95	0	3.95‡	0
Urban§	16.95	0	5.45	0	1.3	0	3.15	0
Open Water	0	0	0	0	0	0	0	0
Snow/Ice	10.2	0	-	-	-	-	-	-

* in winter, wetland, grassland, and cropland treated as a snow surface. † bare soil and active growth.
‡ bare soil and senescent growth. § consists of a mixture of deciduous forest and buildings.

Day length Weighted Seasonal Average $R_b = \frac{day\ length}{24hrs}\left(R_{b\ day}\right)+\left(1-\frac{day\ length}{24hrs}\left(R_{b\ night}\right)\right)$

Day length $= 0.133\left\{\cos^{-1}\left(-\tan(55^\circ)\times\tan(Solar\ Declination)\right)\right\}$

Solar Declination $= 23.45\left\{\sin\left(\frac{360\times(284+Julian\ Day)}{365}\right)\right\}$

Surface Resistance (R_c):

Bulk surface resistance values are used from literature as a function of surface type, surface wetness, and incident radiation. Day length weighted average R_c values for SO_2 and NO_2 are used from Voldner *et al.* (1986), Arrit *et al.* (1987) and Walcek *et al.* (1986) as cited in Cheng *et al.* (2001):

Table B3 Day Length Weighted Averages Bulk Surface Resistance (s/cm) for Sulphur Dioxide (SO_2):

Surface Type	Winter (Dec, Jan, Feb)		Spring (Mar, Apr, May)		Summer (Jun, July, Aug)		Autumn (Sep, Oct, Nov)	
	Dry	Wet	Dry	Wet	Dry	Wet	Dry	Wet
Deciduous Forest	10	10	4.7	0	3.5	0	7.9	0.4
Coniferous Forest	5	5	4.1	0	3.5	0	4.9	0.2
Wetland/Swamp*	7	1	0.5	0	0.7	0	1	0.1
Grassland*	7	1	1	0	1.3	0	2	0.1
Cropland*	7	1	0†	0	2	0	2‡	0.1
Urban§	10	2	10	0	10	0	10	0.1
Open Water	0	0	0	0	0	0	0	0
Snow/Ice	7	1	-	-	-	-	-	-

* in winter, wetland, grassland, and cropland treated as a snow surface. † bare soil and active growth.
‡ bare soil and senescent growth. § consists of a mixture of deciduous forest and buildings.

Table B4 Day Length Weighted Averages Bulk Surface Resistance (s/cm) for Nitrogen Dioxide (NO_2):

Surface Type	Winter (Dec, Jan, Feb)		Spring (Mar, Apr, May)		Summer (Jun, July, Aug)		Autumn (Sep, Oct, Nov)	
	Dry	Wet	Dry	Wet	Dry	Wet	Dry	Wet
Deciduous Forest	20.0	70.0	3.3	70.0	2.2	70.0	4.7	70.0
Coniferous Forest	10.0	70.0	2.7	70.0	2.2	70.0	3.3	70.0
Wetland/Swamp*	50.0	70.0	12.1	70.0	11.5	70.0	12.9	70.0
Grassland*	50.0	70.0	3.3	70.0	3.3	70.0	6.6	70.0
Cropland*	50.0	70.0	3.3†	70.0	4.6	70.0	7.9‡	70.0
Urban§	10.0	70.0	10.0	70.0	10.0	70.0	10.0	70.0
Open Water	70.0	70.0	70.0	70.0	70.0	70.0	70.0	70.0
Snow/Ice	50.0	70.0	-	-	-	-	-	-

* in winter, wetland, grassland, and cropland treated as a snow surface. † bare soil and active growth.
‡ bare soil and senescent growth. § consists of a mixture of deciduous forest and buildings.

R_c (HNO_3): 10 s/m (for all seasons and all surfaces)
R_c (HNO_2): 10 s/m (for all seasons and all surfaces)
R_c (NH_3): 28 s/m (dry conditions)
9 s/m (wet conditions)
201 s/m (when T_2<0°C)
R_c (particulates): 0 s/m

R_c is calculated based on surface wetness criteria, such that it either represents a "total dry condition," "total wet condition," or "weighted wet condition" using the following flowchart, and relative humidity (RH) and surface wetness (SW) criteria:

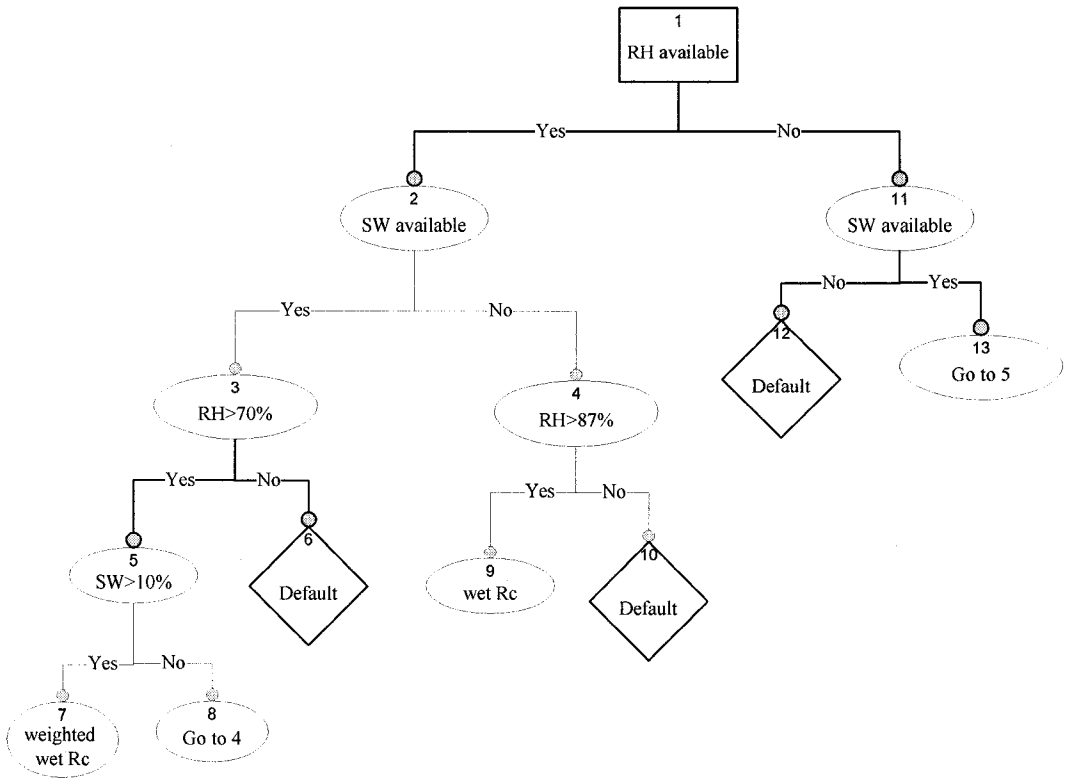

Figure B1 Flowchart for calculating *Rc* (Adapted from Bates (1996)

Default = R_c value for dry conditions
Wet R_c = R_c value for wet conditions
Weighted Wet R_c = Time weighted wet R_c

$$\textbf{Time weighted wet } R_c = \left(\frac{SW}{100} \times wet\ Rc\right) + \left[\left(1 - \frac{SW}{100}\right) \times dry\ Rc\right]$$

Calculation of V_d in the absence of meteorological data:

Missing hourly meteorological data are treated in the following manner:

- 1 hour of meteorological data missing → the average resistance of the hours before and after are used to represent the missing hour
- consecutive hours of meteorological data missing → each hour's calculated median resistance for the month is used to represent the missing hours

Units required for input parameters to Visual Basic Program

hourly pollutant concentration:	$\mu g/m^3$
hourly wind speed:	km/hr (converted to m/s within program)
hourly wind direction std. dev.:	degrees (converted to radians within program)
hourly temperature:	°C (converted to K in program)
hourly delta temperature:	°C
hourly relative humidity:	% (converted to decimal within program)
hourly surface wetness:	%

Appendix C Monthly Average Species Concentrations

Table C1 Monthly average chemical concentrations.

	gaseous chemicals			(μg/m^3)	particulate chemicals						(μg/m^3)
month	SO2	NO2	HNO2	HNO3	SO4	NH4	NO3	Na	K	Ca	Mg
Month 1	2.9	19.1	0.76	1.46	1.03	0.65	0.30	0.14	0.09	0.19	0.04
Month 2	3.7	18.6	0.14	0.62	1.01	0.46	0.15	0.10	0.01	0.26	0.04
Month 3	3.3	10.9	0.07	0.61	2.35	0.69	0.17	0.12	0.01	0.35	0.03
Month 4	4.3	9.4	0.11	0.74	0.95	0.49	0.14	0.07	0.03	0.81	0.04
Month 5	3.2	6.1	0.13	0.41	0.67	0.31	0.05	0.04	0.02	0.38	0.05
Month 6	2.3	3.7	0.01	0.19	0.53	0.25	0.04	0.02	0.03	0.47	0.04
Month 7	3.9	5.0	0.02	0.25	0.50	0.23	0.08	0.05	0.06	0.79	0.07
Month 8	4.2	7.0	0.06	0.31	0.70	0.34	0.07	0.05	0.04	0.61	0.07
Month 9	1.7	7.1	0.11	0.21	0.59	0.29	0.05	0.06	0.04	0.23	0.04
Month 10	2.6	10.7	0.27	1.24	0.97	0.43	0.07	0.05	0.04	0.88	0.06
Month 11	1.0	14.4	0.14	0.19	0.79	0.66	0.48	0.10	0.07	1.92	0.06
Month 12	4.9	21.7	0.80	0.34	0.68	0.34	0.38	0.10	0.09	0.55	0.05

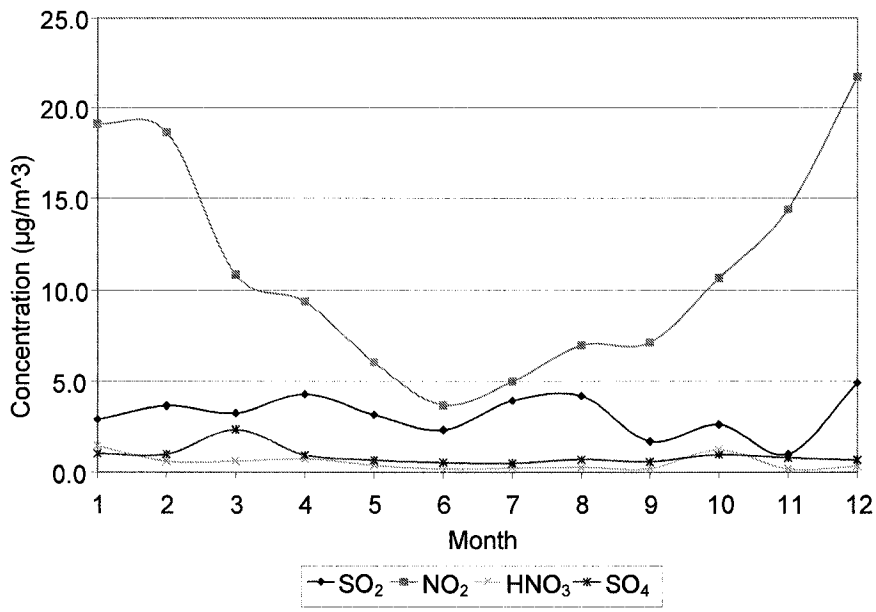

Figure C1 Monthly averaged chemical concentrations for the largest N and S contributors.

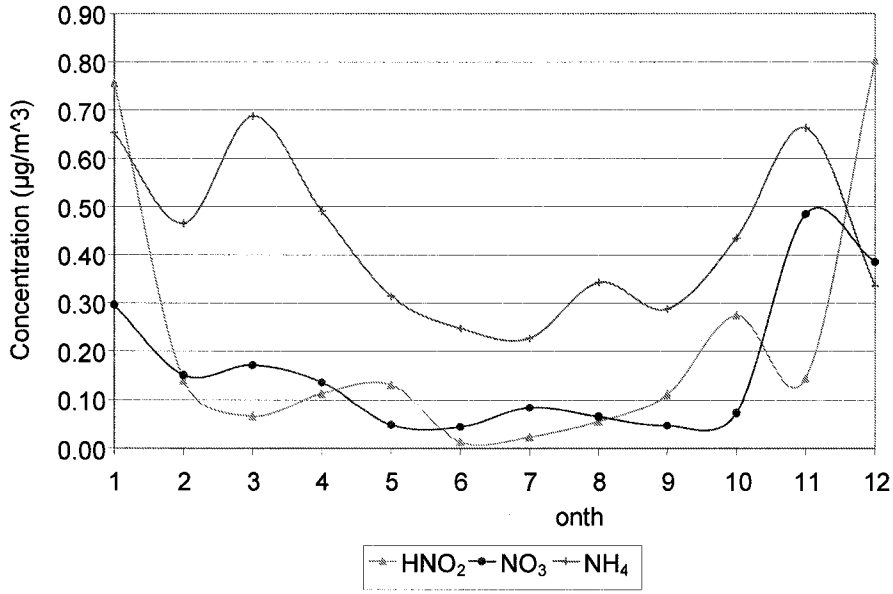

Figure C2 Monthly averaged chemical concentrations for remaining N species.

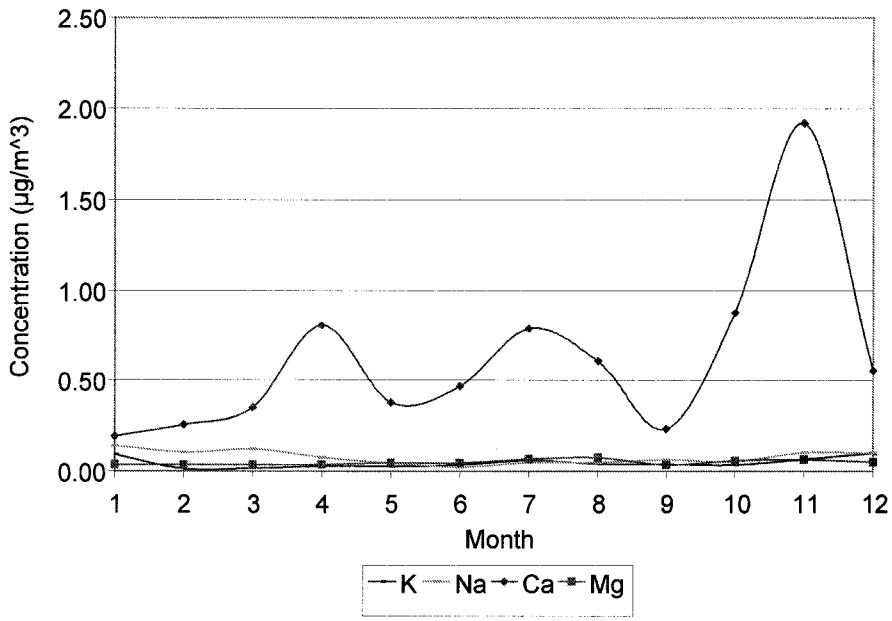

Figure C3 Monthly averaged chemical concentrations for base cations.

Appendix D Tables for Monthly Deposition Velocities of Component Chemicals

Table D1 Monthly average deposition velocities for SO_2 – coniferous forest (cm/s).

month	AENV	ENVC	difference
Month 1	0.09	0.14	-0.06
Month 2	0.10	0.12	-0.03
Month 3	0.13	0.23	-0.11
Month 4	0.17	0.34	-0.16
Month 5	0.25	0.37	-0.12
Month 6	0.49	0.36	0.13
Month 7	0.40	0.30	0.11
Month 8	0.35	0.29	0.06
Month 9	0.38	0.38	0.01
Month 10	0.36	0.35	0.01
Month 11	0.12	0.19	-0.07
Month 12	0.13	0.18	-0.05

Table D2 Monthly average deposition velocities for NO_2 – coniferous forest (cm/s).

month	AENV	ENVC	difference
Month 1	0.05	0.08	-0.04
Month 2	0.05	0.07	-0.02
Month 3	0.09	0.15	-0.06
Month 4	0.18	0.22	-0.04
Month 5	0.20	0.24	-0.04
Month 6	0.25	0.24	0.01
Month 7	0.24	0.20	0.04
Month 8	0.24	0.19	0.05
Month 9	0.15	0.23	-0.08
Month 10	0.11	0.20	-0.09
Month 11	0.08	0.11	-0.03
Month 12	0.07	0.10	-0.03

Table D3 Monthly average deposition velocities for HNO_2 – coniferous forest (cm/s).

month	AENV	ENVC	difference
Month 1	0.94	0.32	0.62
Month 2	1.15	0.27	0.87
Month 3	1.68	0.50	1.18
Month 4	1.78	0.68	1.10
Month 5	2.17	0.73	1.45
Month 6	2.04	0.69	1.35
Month 7	1.83	0.58	1.24
Month 8	1.73	0.57	1.17
Month 9	2.14	0.76	1.38
Month 10	1.51	0.69	0.82
Month 11	1.29	0.42	0.87
Month 12	1.07	0.39	0.67

Table D4 Monthly average deposition velocities for HNO_3 – coniferous forest (cm/s).

month	AENV	ENVC	difference
Month 1	0.88	0.86	0.02
Month 2	1.07	0.82	0.25
Month 3	1.57	1.25	0.32
Month 4	1.68	1.59	0.09
Month 5	2.05	1.58	0.47
Month 6	1.92	1.51	0.41
Month 7	1.71	1.33	0.38
Month 8	1.63	1.30	0.32
Month 9	2.01	1.59	0.42
Month 10	1.42	1.32	0.09
Month 11	1.21	1.11	0.10
Month 12	1.00	1.05	-0.04

Table D5 Monthly average deposition velocities for SO_4^{2-}/NH_4^+ – coniferous forest (cm/s).

month	AENV	ENVC	difference
Month 1	0.17	0.09	0.08
Month 2	0.19	0.09	0.10
Month 3	0.20	0.12	0.08
Month 4	0.25	0.15	0.10
Month 5	0.23	0.14	0.09
Month 6	0.35	0.13	0.22
Month 7	0.34	0.10	0.24
Month 8	0.33	0.10	0.23
Month 9	0.29	0.11	0.18
Month 10	0.25	0.10	0.16
Month 11	0.26	0.10	0.16
Month 12	0.24	0.09	0.15

Table D6 Monthly average deposition velocities for $NO_3^-/Na^+/K^+/Ca^{2+}/Mg^{2+}$ – coniferous forest (cm/s)

month	AENV	ENVC	difference
Month 1	0.30	0.30	0.00
Month 2	0.35	0.26	0.09
Month 3	0.38	0.38	-0.01
Month 4	0.46	0.51	-0.05
Month 5	0.44	0.48	-0.04
Month 6	0.64	0.41	0.23
Month 7	0.63	0.29	0.33
Month 8	0.60	0.32	0.28
Month 9	0.54	0.36	0.17
Month 10	0.45	0.30	0.16
Month 11	0.46	0.31	0.15
Month 12	0.42	0.28	0.15

Table D7 Small and large particle deposition velocities for AENV *LUCs*.

	deciduous forest	coniferous forest	wetland/swamp	grassland	cropland	urban	water	snow/ice
	small	small	small	small	small	small	small	small
Month 1	0.03	0.17	0.03	0.03	0.03	0.02	2.85	0.03
Month 2	0.03	0.19	0.03	0.03	0.03	0.02	3.49	0.03
Month 3	0.10	0.20	0.14	0.10	0.06	0.05	5.97	
Month 4	0.13	0.25	0.18	0.13	0.08	0.07	4.84	
Month 5	0.12	0.23	0.17	0.12	0.08	0.06	8.21	
Month 6	0.49	0.35	0.26	0.18	0.18	0.26	6.70	
Month 7	0.48	0.34	0.26	0.18	0.18	0.26	5.77	
Month 8	0.46	0.33	0.25	0.17	0.17	0.25	5.28	
Month 9	0.21	0.29	0.21	0.15	0.09	0.11	8.05	
Month 10	0.19	0.25	0.19	0.13	0.08	0.10	4.67	
Month 11	0.19	0.26	0.19	0.14	0.09	0.11	3.22	
Month 12	0.04	0.24	0.04	0.04	0.04	0.02	2.33	0.04
	large	large	large	large	large	large	large	large
Month 1	0.06	0.30	0.05	0.05	0.05	0.03	2.85	0.05
Month 2	0.06	0.35	0.05	0.05	0.05	0.03	3.49	0.05
Month 3	0.20	0.38	0.28	0.19	0.12	0.10	5.97	
Month 4	0.25	0.46	0.34	0.24	0.15	0.13	4.84	
Month 5	0.23	0.44	0.32	0.23	0.14	0.12	8.21	
Month 6	0.88	0.64	0.49	0.34	0.34	0.49	6.70	
Month 7	0.86	0.63	0.48	0.34	0.34	0.48	5.77	
Month 8	0.82	0.60	0.46	0.32	0.32	0.46	5.28	
Month 9	0.40	0.54	0.40	0.28	0.17	0.22	8.05	
Month 10	0.34	0.45	0.34	0.25	0.16	0.19	4.67	
Month 11	0.35	0.46	0.35	0.25	0.16	0.20	3.22	
Month 12	0.08	0.42	0.07	0.07	0.07	0.04	2.33	0.07

Appendix E Counts for Resistance Factors

Table E1 Number of times hourly calculated R_a, R_b, or R_c was the largest (dominant) resistance factor in AENV model for SO_2.

	value of total R (s/m)	<10	10-100	100-300	300-1000	>1000
	dep vel Vd (cm/s)	>10.0	1.0-10.0	0.3-1.0	0.1-0.3	<0.1
jan	total resistance	0	0	0	346	397
	Ra	0	0	0	0	194
	Rb	0	0	0	0	0
	Rc	0	0	0	346	6
feb	total resistance	0	0	0	351	321
	Ra	0	0	0	0	102
	Rb	0	0	0	0	0
	Rc	0	0	0	351	3
mar	total resistance	0	3	0	421	320
	Ra	0	0	0	0	123
	Rb	0	3	0	0	0
	Rc	0	0	0	421	2
apr	total resistance	0	6	1	520	193
	Ra	0	2	1	4	89
	Rb	0	4	0	0	0
	Rc	0	0	0	516	0
may	total resistance	0	16	1	479	248
	Ra	0	3	1	5	167
	Rb	0	13	0	0	0
	Rc	0	0	0	474	1
jun	total resistance	0	60	9	475	176
	Ra	0	10	9	22	157
	Rb	0	50	0	0	0
	Rc	0	0	0	453	0
jul	total resistance	0	66	27	457	194
	Ra	0	3	21	19	129
	Rb	0	63	6	0	0
	Rc	0	0	0	438	0
aug	total resistance	0	55	14	461	214
	Ra	0	13	14	18	165
	Rb	0	42	0	0	0
	Rc	0	0	0	443	0
sep	total resistance	0	81	31	414	194
	Ra	0	4	28	27	146
	Rb	0	30	3	0	0
	Rc	0	47	0	387	0
oct	total resistance	0	96	42	353	253
	Ra	0	20	42	25	233
	Rb	0	28	0	0	0
	Rc	0	48	0	328	0
nov	total resistance	0	0	0	483	237
	Ra	0	0	0	0	191
	Rb	0	0	0	0	0
	Rc	0	0	0	483	4
dec	total resistance	0	0	0	525	219
	Ra	0	0	0	0	161
	Rb	0	0	0	0	0
	Rc	0	0	0	525	8

Table E2 Number of times hourly calculated R_a, R_b, or R_c was the largest (dominant) resistance factor in ENVC model for SO_2.

	value of total R (s/m)	<10	10-100	100-300	300-1000	>1000
	dep vel Vd (cm/s)	>10.0	1.0-10.0	0.3-1.0	0.1-0.3	<0.1
jan	total resistance	0	3	68	300	372
	Ra	0	0	0	0	0
	Rb	0	0	0	0	0
	Rc	0	3	68	300	372
feb	total resistance	0	0	8	339	325
	Ra	0	0	0	0	0
	Rb	0	0	0	0	0
	Rc	0	0	8	339	325
mar	total resistance	0	8	157	359	220
	Ra	0	0	0	0	0
	Rb	0	0	0	0	0
	Rc	0	8	157	359	220
apr	total resistance	0	10	301	312	97
	Ra	0	0	0	0	0
	Rb	0	0	0	0	0
	Rc	0	10	301	312	97
may	total resistance	0	30	311	271	132
	Ra	0	0	0	0	0
	Rb	0	0	0	0	0
	Rc	0	30	311	271	132
jun	total resistance	0	19	299	306	96
	Ra	0	0	0	0	0
	Rb	0	0	0	0	0
	Rc	0	19	299	306	96
jul	total resistance	0	0	275	356	113
	Ra	0	0	0	0	0
	Rb	0	0	0	0	0
	Rc	0	0	275	356	113
aug	total resistance	0	5	258	342	139
	Ra	0	0	0	0	0
	Rb	0	0	0	0	0
	Rc	0	5	258	342	139
sep	total resistance	0	22	320	270	108
	Ra	0	0	0	0	0
	Rb	0	0	0	0	0
	Rc	0	22	320	270	108
oct	total resistance	0	12	317	264	151
	Ra	0	0	0	0	0
	Rb	0	0	0	0	0
	Rc	0	12	317	264	151
nov	total resistance	0	1	117	355	247
	Ra	0	0	0	0	0
	Rb	0	0	0	0	0
	Rc	0	1	117	355	247
dec	total resistance	0	1	89	385	269
	Ra	0	0	0	0	0
	Rb	0	0	0	0	0
	Rc	0	1	89	385	269

Table E3 Number of times hourly calculated R_a, R_b, or R_c was the largest (dominant) resistance factor in AENV model for NO_2.

	value of total R (s/m)	<10	10-100	100-300	300-1000	>1000
	dep vel Vd (cm/s)	>10.0	1.0-10.0	0.3-1.0	0.1-0.3	<0.1
jan	total resistance	0	0	0	0	743
	Ra	0	0	0	0	173
	Rb	0	0	0	0	0
	Rc	0	0	0	0	375
feb	total resistance	0	0	0	0	672
	Ra	0	0	0	0	98
	Rb	0	0	0	0	0
	Rc	0	0	0	0	361
mar	total resistance	0	0	75	33	636
	Ra	0	0	0	2	110
	Rb	0	0	0	0	0
	Rc	0	0	75	31	332
apr	total resistance	0	0	159	213	348
	Ra	0	0	0	13	87
	Rb	0	0	0	0	0
	Rc	0	0	159	200	157
may	total resistance	0	0	300	136	308
	Ra	0	0	0	16	157
	Rb	0	0	0	0	0
	Rc	0	0	300	120	71
jun	total resistance	0	0	397	70	253
	Ra	0	0	0	22	145
	Rb	0	0	0	0	0
	Rc	0	0	397	48	89
jul	total resistance	0	0	403	43	298
	Ra	0	0	0	17	120
	Rb	0	0	0	0	0
	Rc	0	0	403	26	115
aug	total resistance	0	0	395	59	290
	Ra	0	0	0	14	145
	Rb	0	0	0	0	0
	Rc	0	0	395	45	97
sep	total resistance	0	0	0	390	330
	Ra	0	0	0	7	120
	Rb	0	0	0	0	0
	Rc	0	0	0	383	163
oct	total resistance	0	0	0	271	473
	Ra	0	0	0	6	196
	Rb	0	0	0	0	0
	Rc	0	0	0	265	258
nov	total resistance	0	0	0	66	654
	Ra	0	0	0	2	173
	Rb	0	0	0	0	0
	Rc	0	0	0	64	440
dec	total resistance	0	0	0	0	744
	Ra	0	0	0	0	137
	Rb	0	0	0	0	0
	Rc	0	0	0	0	558

Table E4 Number of times hourly calculated R_a, R_b, or R_c was the largest (dominant) resistance factor in ENVC model for NO_2.

	value of total R (s/m)	<10	10-100	100-300	300-1000	>1000
	dep vel Vd (cm/s)	>10.0	1.0-10.0	0.3-1.0	0.1-0.3	<0.1
jan	total resistance	0	0	17	199	527
	Ra	0	0	0	0	0
	Rb	0	0	0	0	0
	Rc	0	0	17	199	527
feb	total resistance	0	0	2	184	486
	Ra	0	0	0	0	0
	Rb	0	0	0	0	0
	Rc	0	0	2	184	486
mar	total resistance	0	0	72	344	328
	Ra	0	0	0	0	0
	Rb	0	0	0	0	0
	Rc	0	0	72	344	328
apr	total resistance	0	0	161	390	169
	Ra	0	0	0	0	0
	Rb	0	0	0	0	0
	Rc	0	0	161	390	169
may	total resistance	0	0	197	364	183
	Ra	0	0	0	0	0
	Rb	0	0	0	0	0
	Rc	0	0	197	364	183
jun	total resistance	0	0	188	379	153
	Ra	0	0	0	0	0
	Rb	0	0	0	0	0
	Rc	0	0	188	379	153
jul	total resistance	0	0	97	463	184
	Ra	0	0	0	0	0
	Rb	0	0	0	0	0
	Rc	0	0	97	463	184
aug	total resistance	0	0	92	434	218
	Ra	0	0	0	0	0
	Rb	0	0	0	0	0
	Rc	0	0	92	434	218
sep	total resistance	0	0	170	383	167
	Ra	0	0	0	0	0
	Rb	0	0	0	0	0
	Rc	0	0	170	383	167
oct	total resistance	0	0	144	398	202
	Ra	0	0	0	0	0
	Rb	0	0	0	0	0
	Rc	0	0	144	398	202
nov	total resistance	0	0	29	302	389
	Ra	0	0	0	0	0
	Rb	0	0	0	0	0
	Rc	0	0	29	302	389
dec	total resistance	0	0	15	277	452
	Ra	0	0	0	0	0
	Rb	0	0	0	0	0
	Rc	0	0	15	277	452

Table E5 Number of times hourly calculated R_a, R_b, or R_c was the largest (dominant) resistance factor in AENV model for HNO_3.

	value of total R (s/m)	<10	10-100	100-300	300-1000	>1000
	dep vel Vd (cm/s)	>10.0	1.0-10.0	0.3-1.0	0.1-0.3	<0.1
jan	total resistance	0	257	73	41	372
	Ra	0	22	58	40	175
	Rb	0	210	15	1	0
	Rc	0	25	0	0	0
feb	total resistance	0	291	46	21	314
	Ra	0	8	29	21	98
	Rb	0	261	17	0	0
	Rc	0	22	0	0	0
mar	total resistance	0	383	29	24	308
	Ra	0	16	26	24	113
	Rb	0	267	3	0	0
	Rc	0	100	0	0	0
apr	total resistance	0	469	44	16	191
	Ra	0	35	36	16	87
	Rb	0	351	8	0	0
	Rc	0	83	0	0	0
may	total resistance	0	438	44	30	232
	Ra	0	48	43	30	152
	Rb	0	211	1	0	0
	Rc	0	179	0	0	0
jun	total resistance	0	461	54	37	168
	Ra	0	49	54	37	149
	Rb	0	319	0	0	0
	Rc	0	93	0	0	0
jul	total resistance	0	463	59	35	187
	Ra	0	7	35	35	122
	Rb	0	377	24	0	0
	Rc	0	79	0	0	0
aug	total resistance	0	447	63	27	207
	Ra	0	22	51	27	158
	Rb	0	374	12	0	0
	Rc	0	51	0	0	0
sep	total resistance	0	447	50	36	187
	Ra	0	18	46	36	139
	Rb	0	284	4	0	0
	Rc	0	145	0	0	0
oct	total resistance	0	377	77	51	239
	Ra	0	61	74	51	219
	Rb	0	252	3	0	0
	Rc	0	64	0	0	0
nov	total resistance	0	373	94	33	220
	Ra	0	57	87	33	178
	Rb	0	305	7	0	0
	Rc	0	11	0	0	0
dec	total resistance	0	367	139	47	191
	Ra	0	360	139	47	141
	Rb	0	0	0	0	0
	Rc	0	7	0	0	0

Table E6 Number of times hourly calculated R_a, R_b, or R_c was the largest (dominant) resistance factor in ENVC model for HNO_3.

	value of total R (s/m)	<10	10-100	100-300	300-1000	>1000
	dep vel Vd (cm/s)	>10.0	1.0-10.0	0.3-1.0	0.1-0.3	<0.1
jan	total resistance	0	237	299	116	91
	Ra	0	12	45	53	68
	Rb	0	3	0	0	0
	Rc	0	222	254	63	23
feb	total resistance	0	205	336	67	64
	Ra	0	3	4	39	42
	Rb	0	0	0	0	0
	Rc	0	202	332	28	22
mar	total resistance	0	400	198	80	66
	Ra	0	4	16	51	37
	Rb	0	37	0	0	0
	Rc	0	359	182	29	29
apr	total resistance	0	478	161	56	25
	Ra	0	22	35	50	25
	Rb	0	54	0	0	0
	Rc	0	402	126	6	0
may	total resistance	0	462	154	80	48
	Ra	0	43	65	64	47
	Rb	0	56	0	0	1
	Rc	0	363	89	16	0
jun	total resistance	0	433	202	69	16
	Ra	0	70	109	64	16
	Rb	0	16	0	0	0
	Rc	0	347	93	5	0
jul	total resistance	0	431	197	101	15
	Ra	0	54	89	101	15
	Rb	0	27	0	0	0
	Rc	0	350	108	0	0
aug	total resistance	0	437	160	135	12
	Ra	0	48	87	135	12
	Rb	0	19	0	0	0
	Rc	0	370	73	0	0
sep	total resistance	0	446	134	129	11
	Ra	0	62	103	129	11
	Rb	0	43	0	0	0
	Rc	0	341	31	0	0
oct	total resistance	0	380	199	117	48
	Ra	0	152	163	114	48
	Rb	0	19	0	0	0
	Rc	0	209	36	3	0
nov	total resistance	0	334	229	88	69
	Ra	0	13	62	80	69
	Rb	0	6	0	0	0
	Rc	0	315	167	8	0
dec	total resistance	0	339	288	75	42
	Ra	0	7	42	69	42
	Rb	0	9	0	0	0
	Rc	0	323	246	6	0

Table E7 Number of times hourly calculated R_a, R_b, or R_c was the largest (dominant) resistance factor in AENV model for HNO_3 for total resistance <100 s/m.

	value of total R (s/m)	<15	15-25	25-40	40-65	65-100
	dep vel Vd (cm/s)	>6.7	4.0-6.7	2.5-4.0	1.5-2.5	1.0-1.5
jan	total resistance	0	19	67	103	68
	Ra	0	0	0	3	19
	Rb	0	0	61	100	49
	Rc	0	19	6	0	0
feb	total resistance	0	7	111	121	52
	Ra	0	0	0	1	7
	Rb	0	0	96	120	45
	Rc	0	7	15	0	0
mar	total resistance	0	74	173	103	33
	Ra	0	0	0	3	13
	Rb	0	0	147	100	20
	Rc	0	74	26	0	0
apr	total resistance	0	29	197	162	81
	Ra	0	0	0	3	32
	Rb	0	0	143	159	49
	Rc	0	29	54	0	0
may	total resistance	0	146	189	69	34
	Ra	0	0	0	17	31
	Rb	0	0	156	52	3
	Rc	0	146	33	0	0
jun	total resistance	0	58	242	123	38
	Ra	0	0	4	17	28
	Rb	0	0	203	106	10
	Rc	0	58	35	0	0
jul	total resistance	0	51	183	171	58
	Ra	0	0	0	0	7
	Rb	0	0	155	171	51
	Rc	0	51	28	0	0
aug	total resistance	0	31	197	168	51
	Ra	0	0	0	2	20
	Rb	0	0	177	166	31
	Rc	0	31	20	0	0
sep	total resistance	0	124	179	105	39
	Ra	0	0	0	1	17
	Rb	0	0	158	104	22
	Rc	0	124	21	0	0
oct	total resistance	0	42	155	112	68
	Ra	0	0	0	12	49
	Rb	0	0	133	100	19
	Rc	0	42	22	0	0
nov	total resistance	0	1	121	164	87
	Ra	0	0	0	15	42
	Rb	0	0	111	149	45
	Rc	0	1	10	0	0
dec	total resistance	0	3	25	177	162
	Ra	0	0	21	177	162
	Rb	0	0	0	0	0
	Rc	0	3	4	0	0

Table E8 Number of times hourly calculated R_a, R_b, or R_c was the largest (dominant) resistance factor in ENVC model for HNO_3 for total resistance <100 s/m.

	value of total R (s/m)	<15	15-25	25-40	40-65	65-100
	dep vel Vd (cm/s)	>6.7	4.0-6.7	2.5-4.0	1.5-2.5	1.0-1.5
jan	total resistance	0	11	19	73	134
	Ra	0	0	0	4	8
	Rb	0	0	0	2	1
	Rc	0	11	19	67	125
feb	total resistance	0	0	1	75	129
	Ra	0	0	0	2	1
	Rb	0	0	0	0	0
	Rc	0	0	1	73	128
mar	total resistance	0	9	75	155	161
	Ra	0	0	0	0	4
	Rb	0	0	15	18	4
	Rc	0	9	60	137	153
apr	total resistance	0	15	138	170	155
	Ra	0	0	0	5	17
	Rb	0	0	34	15	5
	Rc	0	15	104	150	133
may	total resistance	0	27	138	166	131
	Ra	0	0	5	17	21
	Rb	0	0	38	13	5
	Rc	0	27	95	136	105
jun	total resistance	0	11	135	150	137
	Ra	0	0	18	22	30
	Rb	0	0	12	4	0
	Rc	0	11	105	124	107
jul	total resistance	0	9	78	186	158
	Ra	0	0	1	14	39
	Rb	0	0	6	11	10
	Rc	0	9	71	161	109
aug	total resistance	0	4	81	199	153
	Ra	0	0	0	17	31
	Rb	0	0	9	5	5
	Rc	0	4	72	177	117
sep	total resistance	0	35	132	162	117
	Ra	0	0	1	23	38
	Rb	0	0	15	14	14
	Rc	0	35	116	125	65
oct	total resistance	0	9	114	150	107
	Ra	0	0	17	76	59
	Rb	0	0	18	1	0
	Rc	0	9	79	73	48
nov	total resistance	0	0	58	145	131
	Ra	0	0	0	7	6
	Rb	0	0	5	1	0
	Rc	0	0	53	137	125
dec	total resistance	0	1	42	131	165
	Ra	0	0	0	5	2
	Rb	0	0	6	3	0
	Rc	0	1	36	123	163

Appendix F Breakdown of Chemicals Contributing to Differences in Deposition Caused by Percent Changes of Resistances (R_a, R_b, and R_c)

Table F1 Influence of ±10% and ±50% change in R_a on total deposition (in H^+ equivalents) as a result of sensitivity testing of AENV model.

	base case total	absolute difference from base case (g H+/ha)			
Ra		0.5	0.9	1.1	1.5
Month 1	16.9	2.6	0.4	-0.4	-1.7
Month 2	11.7	1.0	0.2	-0.2	-0.7
Month 3	17.0	1.3	0.2	-0.2	-0.9
Month 4	15.9	1.7	0.3	-0.3	-1.2
Month 5	14.0	1.5	0.2	-0.2	-1.0
Month 6	7.5	0.7	0.1	-0.1	-0.5
Month 7	7.6	0.3	0.0	0.0	-0.2
Month 8	13.6	1.1	0.2	-0.2	-0.7
Month 9	9.8	0.7	0.1	-0.1	-0.5
Month 10	16.8	2.4	0.4	-0.4	-1.6
Month 11	0.2	-0.1	0.0	0.0	0.1
Month 12	16.3	2.3	0.4	-0.3	-1.5

*Light yellow, gold, and orange highlighting in tables shown above indicate small, medium, and large differences in deposition (in H^+ equivalents), respectively.

Table F2 Influence of ±10% and ±50% change in R_a on HNO_2 deposition (in H^+ equivalents) as a result of sensitivity testing of AENV model.

	base case	absolute difference from base case (g H+/ha)			
month	(g H+/ha)	0.5	0.9	1.1	1.5
Month 1	3.2	0.8	0.1	-0.1	-0.5
Month 2	0.8	0.2	0.0	0.0	-0.1
Month 3	0.6	0.1	0.0	0.0	-0.1
Month 4	1.0	0.3	0.0	0.0	-0.2
Month 5	1.7	0.3	0.1	0.0	-0.2
Month 6	0.2	0.0	0.0	0.0	0.0
Month 7	0.3	0.1	0.0	0.0	0.0
Month 8	0.5	0.1	0.0	0.0	-0.1
Month 9	1.1	0.2	0.0	0.0	-0.1
Month 10	2.5	0.5	0.1	-0.1	-0.4
Month 11	1.2	0.3	0.1	0.0	-0.2
Month 12	4.8	1.5	0.2	-0.2	-0.9

*Light yellow, gold, and orange highlighting in tables shown above indicate small, medium, and large differences in deposition (in H^+ equivalents), respectively.

Table F3 Influence of ±10% and ±50% change in R_a on HNO_3 deposition (in H^+ equivalents) as a result of sensitivity testing of AENV model.

	base case	absolute difference from base case (g H+/ha)			
month	(g H+/ha)	0.5	0.9	1.1	1.5
Month 1	4.8	1.1	0.2	-0.2	-0.7
Month 2	2.5	0.5	0.1	-0.1	-0.3
Month 3	4.1	0.7	0.1	-0.1	-0.5
Month 4	4.6	1.0	0.2	-0.2	-0.7
Month 5	3.8	0.6	0.1	-0.1	-0.4
Month 6	1.7	0.3	0.1	0.0	-0.2
Month 7	1.9	0.4	0.1	-0.1	-0.3
Month 8	2.0	0.4	0.1	-0.1	-0.3
Month 9	1.4	0.2	0.0	0.0	-0.2
Month 10	8.3	1.5	0.3	-0.2	-1.1
Month 11	1.0	0.2	0.0	0.0	-0.2
Month 12	1.5	0.4	0.1	-0.1	-0.3

*Light yellow, gold, and orange highlighting in tables shown above indicate small, medium, and large differences in deposition (in H^+ equivalents), respectively.

Table F4 Influence of ±10% and ±50% change in R_b on total deposition (in H^+ equivalents) as a result of sensitivity testing of AENV model.

	base case total	absolute difference from base case (g H+/ha)			
Rb		0.5	0.9	1.1	1.5
Month 1	16.9	3.2	0.5	-0.4	-1.9
Month 2	11.7	1.8	0.3	-0.2	-1.0
Month 3	17.0	3.7	0.5	-0.4	-1.8
Month 4	15.9	0.1	0.1	-0.1	-0.6
Month 5	14.0	0.8	0.2	-0.2	-0.8
Month 6	7.5	-0.7	0.0	0.0	0.0
Month 7	7.6	-3.4	-0.4	0.3	1.0
Month 8	13.6	-0.6	0.0	0.0	-0.2
Month 9	9.8	0.6	0.1	-0.1	-0.5
Month 10	16.8	0.5	0.2	-0.2	-1.1
Month 11	0.2	-5.8	-0.7	0.6	2.2
Month 12	16.3	0.6	0.2	-0.2	-0.7

*Light yellow, gold, and orange highlighting in tables shown above indicate small, medium, and large differences in deposition (in H^+ equivalents), respectively.

Table F5 Influence of ±10% and ±50% change in R_b on HNO_3 deposition (in H^+ equivalents) as a result of sensitivity testing of AENV model.

	base case	absolute difference from base case (g H+/ha)			
month	(g H+/ha)	0.5	0.9	1.1	1.5
Month 1	4.8	1.3	0.2	-0.2	-0.8
Month 2	2.5	0.7	0.1	-0.1	-0.4
Month 3	4.1	1.0	0.2	-0.2	-0.7
Month 4	4.6	1.1	0.2	-0.2	-0.7
Month 5	3.8	0.8	0.1	-0.1	-0.6
Month 6	1.7	0.4	0.1	-0.1	-0.3
Month 7	1.9	0.5	0.1	-0.1	-0.3
Month 8	2.0	0.5	0.1	-0.1	-0.3
Month 9	1.4	0.3	0.1	-0.1	-0.2
Month 10	8.3	1.9	0.3	-0.3	-1.3
Month 11	1.0	0.2	0.0	0.0	-0.2
Month 12	1.5	0.4	0.1	-0.1	-0.2

*Light yellow, gold, and orange highlighting in tables shown above indicate small, medium, and large differences in deposition (in H^+ equivalents), respectively.

Table F6 Influence of ±10% and ±50% change in R_b on SO_4^{2-} deposition (in H^+ equivalents) as a result of sensitivity testing of AENV model.

	base case	absolute difference from base case (g H+/ha)			
month	(g H+/ha)	0.5	0.9	1.1	1.5
Month 1	1.0	0.7	0.1	-0.1	-0.3
Month 2	1.0	0.8	0.1	-0.1	-0.3
Month 3	2.9	2.4	0.3	-0.2	-0.9
Month 4	1.3	1.1	0.1	-0.1	-0.4
Month 5	0.9	0.8	0.1	-0.1	-0.3
Month 6	1.0	0.8	0.1	-0.1	-0.3
Month 7	1.0	0.8	0.1	-0.1	-0.3
Month 8	1.3	1.0	0.1	-0.1	-0.4
Month 9	0.9	0.8	0.1	-0.1	-0.3
Month 10	1.3	1.0	0.1	-0.1	-0.4
Month 11	1.2	0.9	0.1	-0.1	-0.3
Month 12	1.0	0.7	0.1	-0.1	-0.3

*Light yellow, gold, and orange highlighting in tables shown above indicate small, medium, and large differences in deposition (in H^+ equivalents), respectively.

Table F7 Influence of ±10% and ±50% change in R_b on NH_4^+ deposition (in H^+ equivalents) as a result of sensitivity testing of AENV model.

	base case	absolute difference from base case (g H+/ha)			
month	(g H+/ha)	0.5	0.9	1.1	1.5
Month 1	1.7	1.1	0.1	-0.1	-0.4
Month 2	1.3	1.0	0.1	-0.1	-0.4
Month 3	2.2	1.8	0.2	-0.2	-0.7
Month 4	1.8	1.5	0.2	-0.1	-0.5
Month 5	1.2	1.0	0.1	-0.1	-0.4
Month 6	1.2	1.0	0.1	-0.1	-0.4
Month 7	1.2	0.9	0.1	-0.1	-0.3
Month 8	1.7	1.3	0.2	-0.1	-0.5
Month 9	1.2	1.0	0.1	-0.1	-0.4
Month 10	1.5	1.2	0.1	-0.1	-0.4
Month 11	2.7	2.0	0.2	-0.2	-0.8
Month 12	1.2	0.9	0.1	-0.1	-0.3

*Light yellow, gold, and orange highlighting in tables shown above indicate small, medium, and large differences in deposition (in H^+ equivalents), respectively.

Table F8 Influence of ±10% and ±50% change in R_b on Ca^{2+} deposition (in H^+ equivalents) as a result of sensitivity testing of AENV model.

	base case	absolute difference from base case (g H+/ha)			
month	(g H+/ha)	0.5	0.9	1.1	1.5
Month 1	-1.3	-0.5	-0.1	0.1	0.2
Month 2	-2.0	-0.9	-0.1	0.1	0.3
Month 3	-3.3	-1.4	-0.2	0.1	0.5
Month 4	-8.5	-3.7	-0.4	0.4	1.4
Month 5	-4.2	-1.9	-0.2	0.2	0.7
Month 6	-6.6	-2.8	-0.3	0.3	1.1
Month 7	-12.0	-5.1	-0.6	0.5	2.0
Month 8	-8.5	-3.6	-0.4	0.4	1.4
Month 9	-3.1	-1.4	-0.2	0.1	0.5
Month 10	-9.0	-3.9	-0.5	0.4	1.5
Month 11	-22.0	-9.0	-1.1	1.0	3.7
Month 12	-5.5	-2.2	-0.3	0.2	0.9

*Light yellow, gold, and orange highlighting in tables shown above indicate small, medium, and large differences in deposition (in H^+ equivalents), respectively.

Table F9 Influence of ±10% and ±50% change in R_c on total deposition (in H^+ equivalents) as a result of sensitivity testing of AENV model.

	base case total	absolute difference from base case (g H+/ha)			
Rc		0.5	0.9	1.1	1.5
Month 1	16.9	6.7	0.9	-0.7	-2.9
Month 2	11.7	6.5	0.8	-0.7	-2.6
Month 3	17.0	8.6	1.1	-0.9	-3.5
Month 4	15.9	10.6	1.3	-1.1	-4.4
Month 5	14.0	8.5	1.1	-0.9	-3.6
Month 6	7.6	5.8	0.7	-0.6	-2.4
Month 7	7.6	9.4	1.1	-1.0	-3.6
Month 8	13.6	10.4	1.3	-1.1	-4.2
Month 9	9.8	6.6	0.8	-0.7	-2.6
Month 10	16.8	8.9	1.2	-1.0	-4.1
Month 11	0.2	6.2	0.8	-0.6	-2.4
Month 12	16.3	9.8	1.2	-1.0	-4.0

*Light yellow, gold, and orange highlighting in tables shown above indicate small, medium, and large differences in deposition (in H^+ equivalents), respectively.

Table F10 Influence of ±10% and ±50% change in R_c on SO_2 deposition (in H^+ equivalents) as a result of sensitivity testing of AENV model.

	base case	absolute difference from base case (g H+/ha)			
month		0.5	0.9	1.1	1.5
Month 1	1.2	0.9	0.1	-0.1	-0.3
Month 2	1.6	1.3	0.2	-0.1	-0.5
Month 3	2.2	1.8	0.2	-0.2	-0.6
Month 4	3.1	2.7	0.3	-0.3	-1.0
Month 5	2.6	2.3	0.3	-0.2	-0.8
Month 6	3.0	1.8	0.2	-0.2	-0.6
Month 7	4.5	3.6	0.4	-0.3	-1.3
Month 8	5.1	3.2	0.4	-0.3	-1.2
Month 9	2.1	1.3	0.2	-0.1	-0.5
Month 10	2.1	1.3	0.2	-0.1	-0.5
Month 11	0.6	0.5	0.1	-0.1	-0.2
Month 12	2.7	2.1	0.3	-0.2	-0.8

*Light yellow, gold, and orange highlighting in tables shown above indicate small, medium, and large differences in deposition (in H^+ equivalents), respectively.

Table F11 Influence of ±10% and ±50% change in R_c on NO_2 deposition (in H^+ equivalents) as a result of sensitivity testing of AENV model.

	base case	absolute difference from base case (g H+/ha)			
month	(g H+/ha)	0.5	0.9	1.1	1.5
Month 1	6.4	4.7	0.6	-0.5	-1.8
Month 2	6.1	4.8	0.6	-0.5	-1.8
Month 3	7.3	5.8	0.7	-0.6	-2.2
Month 4	9.5	7.0	0.9	-0.7	-2.7
Month 5	6.8	5.0	0.6	-0.5	-1.9
Month 6	5.1	3.7	0.5	-0.4	-1.5
Month 7	7.0	5.4	0.7	-0.5	-2.1
Month 8	9.2	6.8	0.8	-0.7	-2.7
Month 9	5.7	4.7	0.6	-0.5	-1.7
Month 10	7.0	5.4	0.7	-0.5	-2.0
Month 11	6.9	5.3	0.6	-0.5	-2.0
Month 12	8.9	7.1	0.8	-0.7	-2.6

*Light yellow, gold, and orange highlighting in tables shown above indicate small, medium, and large differences in deposition (in H^+ equivalents), respectively.

Appendix G Deposition Contributions for Species associated with Large Particles

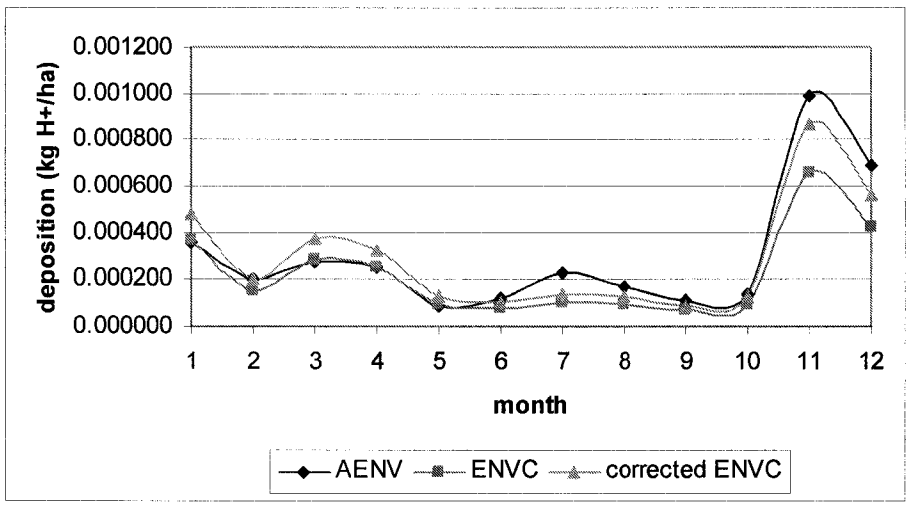

Figure G1 Monthly summed deposition flux for NO_3^- for AENV model base case, ENVC model, and ENVC model corrected for large particle size distribution for a coniferous forest cover.

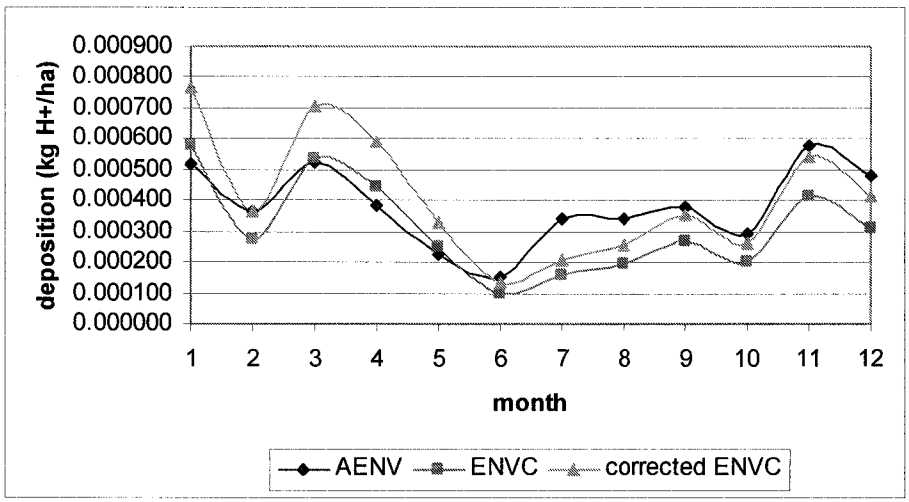

Figure G2 Monthly summed deposition flux for Na^+ for AENV model base case, ENVC model, and ENVC model corrected for large particle size distribution for a coniferous forest cover.

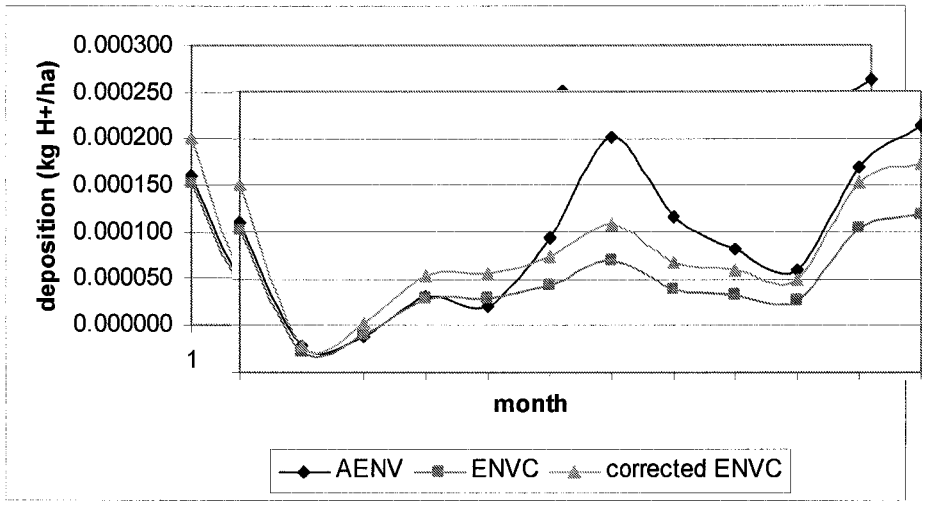

Figure G3 Monthly summed deposition flux for K^+ for AENV model base case, ENVC model, and ENVC model corrected for large particle size distribution for a coniferous forest cover.

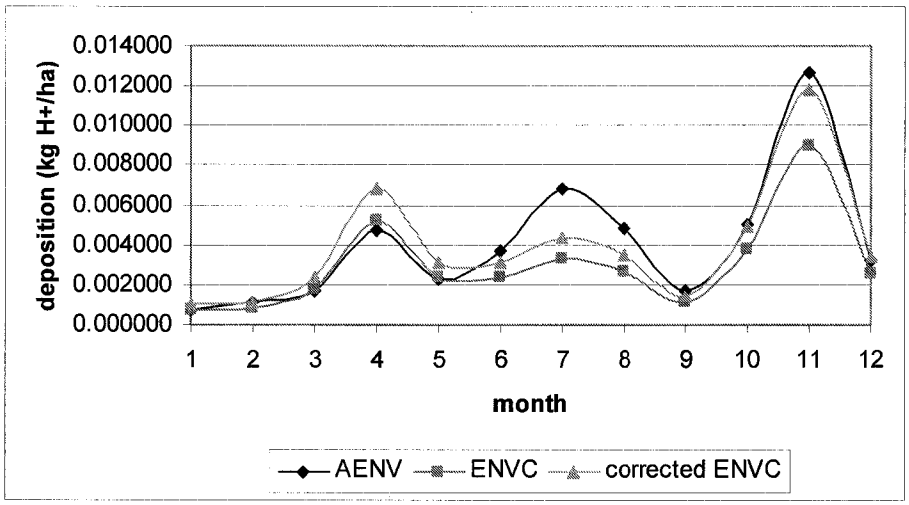

Figure G4 Monthly summed deposition flux for Ca^{2+} for AENV model base case, ENVC model, and ENVC model corrected for large particle size distribution for a coniferous forest cover.

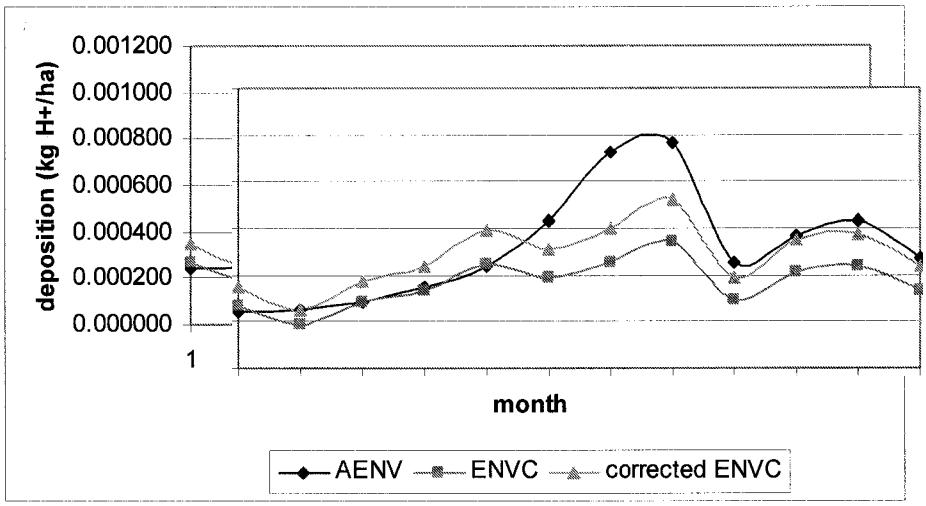

Figure G5 Monthly summed deposition flux for Mg^{2+} for AENV model base case, ENVC model, and ENVC model corrected for large particle size distribution for a coniferous forest cover.